FINAL REPORT

MAHLE Project#: 1528-01291

Award #: DE-FC26-07NT43275

Date: December 20, 2011

OPTIMALLY CONTROLLED FLEXIBLE FUEL POWERTRAIN SYSTEM

Partners:
MAHLE Powertrain LLC.
Michigan State University
Argonne National Lab
Visteon Corporation

Author: Duncan Sheppard
Principal Investigator: Duncan Sheppard
Prior PI's: Bruce Woodrow, Paul Kilmurray
Program Manager: Simon Thwaite

Distribution List:

Ralph Nine	Ralph.Nine@netl.doe.gov
Dr. Harold Schock	schock@egr.msu.edu
Dr. George Zhu	zhug@egr.msu.edu
Steve McConnell	smcconnell@anl.gov

DOE Project Officer: Ralph Nine

DISCLAIMER

Executive Summary

A multi phase program was undertaken with the stated goal of using advanced design and development tools to create a unique combination of existing technologies to create a powertrain system specification that allowed minimal increase of volumetric fuel consumption when operating on E85 relative to gasoline. Although on an energy basis gasoline / ethanol blends typically return similar fuel economy to straight gasoline, because of its lower energy density (gasoline ≈ 31.8MJ/l and ethanol ≈ 21.1MJ/l) the volume based fuel economy of gasoline / ethanol blends are typically considerably worse.

This project was able to define an initial engine specification envelope, develop specific hardware for the application, and test that hardware in both single and multi-cylinder test engines to verify the ability of the specified powertrain to deliver reduced E85 fuel consumption. Finally, the results from the engine testing were used in a vehicle drive cycle analysis tool to define a final vehicle level fuel economy result.

During the course of the project, it was identified that the technologies utilized to improve fuel economy on E85 also enabled improved fuel economy when operating on gasoline. However, the E85 fueled powertrain provided improved vehicle performance when compared to the gasoline fueled powertrain due to the improved high load performance of the E85 fuel. Relative to the baseline comparator engine and considering current market fuels, the volumetric fuel consumption penalty when running on E85 with the fully optimized project powertrain specification was reduced significantly. This result shows that alternative fuels can be utilized in high percentages while maintaining or improving vehicle performance and with minimal or positive impact on total cost of ownership to the end consumer.

The justification for this project was two-fold. In order to reduce the US dependence on crude oil, much of which is imported, the US Environmental Protection Agency (EPA) developed the Renewable Fuels Standard (RFS) under the Energy Policy Act of 2005. The RFS specifies targets for the amount of renewable fuel to be blended into petroleum based transportation fuels. The goal is to blend 36 billion gallons of renewable fuels into transportation fuels by 2022 (9 billion gallons were blended in 2008). The RFS also requires that the renewable fuels emit fewer greenhouse gasses than the petroleum fuels replaced. Thus the goal of the EPA is to have a more fuel efficient national fleet, less dependent on petroleum based fuels.

The limit to the implementation of certain technologies employed was the requirement to run the developed powertrain on gasoline with minimal performance degradation. The addition of ethanol to gasoline fuels improves the fuels octane rating and increases the fuels evaporative cooling. Both of these fuel property enhancements make gasoline / ethanol blends more suitable than straight gasoline for use in downsized engines or engines with increased compression ratio. The use of engine downsizing and high compression ratios as well as direct injection (DI), dual independent cam phasing, external EGR, and downspeeding were fundamental to the fuel economy improvements targeted in this project.

The developed powertrain specification utilized the MAHLE DI3 gasoline downsizing research engine. It was a turbocharged, intercooled, DI engine with dual independent cam phasing utilizing a compression ratio of 11.25 : 1 and a 15% reduction in final drive ratio. When compared to a gasoline fuelled 2.2L Ecotec engine in a Chevrolet HHR, vehicle drive cycle predictions indicate that the optimized powertrain operating on E85 would result in a reduced volume based drive cycle fuel economy penalty of 6% compared to an approximately 30% penalty for current technology engines.

Acknowledgements

This project has been completed with significant contributions by the following:

Dr Andrew Ickes, Argonne National Lab
Dr David Hung, Michigan State University
Paul Kilmurray, MAHLE Powertrain
Dr G Zhu, Michigan State University
Steve McConnell, Argonne National Lab
Dr. Harold Schock, Michigan State University
Simon Thwaite, MAHLE Powertrain
Dr Thomas Wallner, Argonne National Lab
Bruce Woodrow, MAHLE Powertrain

TABLE OF CONTENTS

LIST OF FIGURES

LIST OF TABLES

LIST OF ABBREVIATIONS AND ACRONYMS

A/D	Analog / Digital.
AFR	Air Fuel Ratio.
AIT	After Ignition Timing.
AMR	Adaptive Mesh Refinement.
ATDC	After Top Dead Center.
BDC	Bottom Dead Center.
BMEP	Brake Mean Effective Pressure.
BSFC	Brake Specific Fuel Consumption.
BTDC	Before Top Dead Center.
BTE	Brake Thermal Efficiency.
c_p	Specific Heat At Constant Pressure.
c_v	Specific Heat At Constant Volume.
CAD	Crank Angle Degrees.
CFD	Computational Fluid Dynamics.
CLCC	Closed Loop Combustion Control.
CMOS	Complementary Metal Oxide Semiconductor.
CO	Carbon Monoxide.
COV of IMEP	Coefficient Of Variation of Indicated Mean Effective Pressure.
CR	Compression Ratio.
Cyl	Cylinders.
DI	Direct Injection.
DISI	Direct Injected, Spark Ignited.
DI3	MAHLE Powertrain's downsized 1.2L, 3 cylinder SI engine.
DOE	US Department Of Energy.
E0	Fuel containing 100% gasoline, no ethanol.
E10	Fuel containing 10% ethanol and 90% gasoline.
E20	Fuel containing 20% ethanol and 80% gasoline.
E45	Fuel containing 45% ethanol and 55% gasoline.
E50	Fuel containing 50% ethanol and 50% gasoline.
E73.7	Fuel containing 73.7% ethanol and 26.3% gasoline.
E85	Fuel containing 85% ethanol and 15% gasoline.
ECU	Engine Control Unit.
EGR	Exhaust Gas Recirculation.
EMOP	Exhaust Valve Maximum Opening Point.
EPA	Environmental Protection Agency.
EUDC	EEC Extra Urban Driving Cycle.
EVO	Exhaust Valve Opening.
FD	Final Drive Ratio.
FFV	Flex Fuel Vehicles.
FTP	Federal Test Procedure – US City Drive Cycle.
FTP75	Federal Test Procedure – US City Drive Cycle.
GDI	Gasoline Direct Injection.
GUI	Graphical User Interface.
HDC	Highly Dilute Combustion.
HECCE	High Efficiency Clean Combustion E85.
HP	High Pressure.
HPDI	High Pressure Direct Injection.
HWFET	US Highway Fuel Economy Test Cycle.
HC	Hydrocarbon.

HIL	Hardware In the Loop.
I3	In Line Three Cylinder Engine.
I4	In Line Four Cylinder Engine.
I/O	Input / Output.
IMEP	Indicated Mean Effective Pressure.
IMOP	Intake Valve Maximum Opening Point.
ISFC	Indicated Specific Fuel Consumption.
IT	Ignition Timing.
IVC	Intake Valve Closing.
LP	Low Pressure.
LPDI	Low Pressure Direct Injection.
MAP	Manifold Absolute Pressure.
MBT	Minimum Spark Advance For Best Torque.
MFB	Mass Fraction Burned.
MPG	Miles Per Gallon.
NA	Naturally Aspirated.
NOx	Nitrous Oxides.
P & E	Performance and Emissions.
PID	Proportional Integral Derivative.
RFS	Renewable Fuels Standard.
RMS	Root Mean Squared.
RON	Research Octane Number.
SI	Spark Ignited.
SMD	Sauter Mean Diameter.
SOI	Start Of Injection.
T/C	Turbocharged.
TDC	Top Dead Center.
ULEV	Ultra Low Emissions Vehicle.
US	United States.
V6	Six Cylinder Engine – Cylinders In “V” Formation.
WOT	Wide Open Throttle.
γ	Specific Heat Ratio.
$\eta_{f,ig}$	Gross Fuel Conversion Efficiency
λ	Lambda.

1 Project Objectives

The key overall project objective was to develop, optimize and demonstrate using design analysis, computer modeling and a prototype engine, a pathway towards Flex Fuel Vehicles (FFV) that show a minimized fuel economy penalty when operating on any blend level of ethanol up to E85 as compared to a conventional gasoline fueled vehicle.

The developed FFV engine shall meet US Environmental Protection Agency and State emissions regulations (Ultra Low Emissions Vehicle (ULEV)).

The developed engine will be a new, commercially viable solution that, while optimized for E85, will operate with ethanol fuel blend from gasoline (E10) to E85 and offer the following characteristics:

- Show minimum economy impact of running E85 when compared to gasoline.
- Show no degradation in vehicle emissions running E85 when compared to gasoline.
- Allow the engine to run at various levels of ethanol fuel content up to 85 percent.
- Show minimal compromise of engine performance when running gasoline.
- Demonstrate superior performance by fully exploiting the properties of E85.
- Help DOE promote the economy and social benefits to the nation by using E85 fuel.

The research utilized MAHLE Powertrain's 'DI3' downsized 1.2L, 3 cylinder gasoline engine.

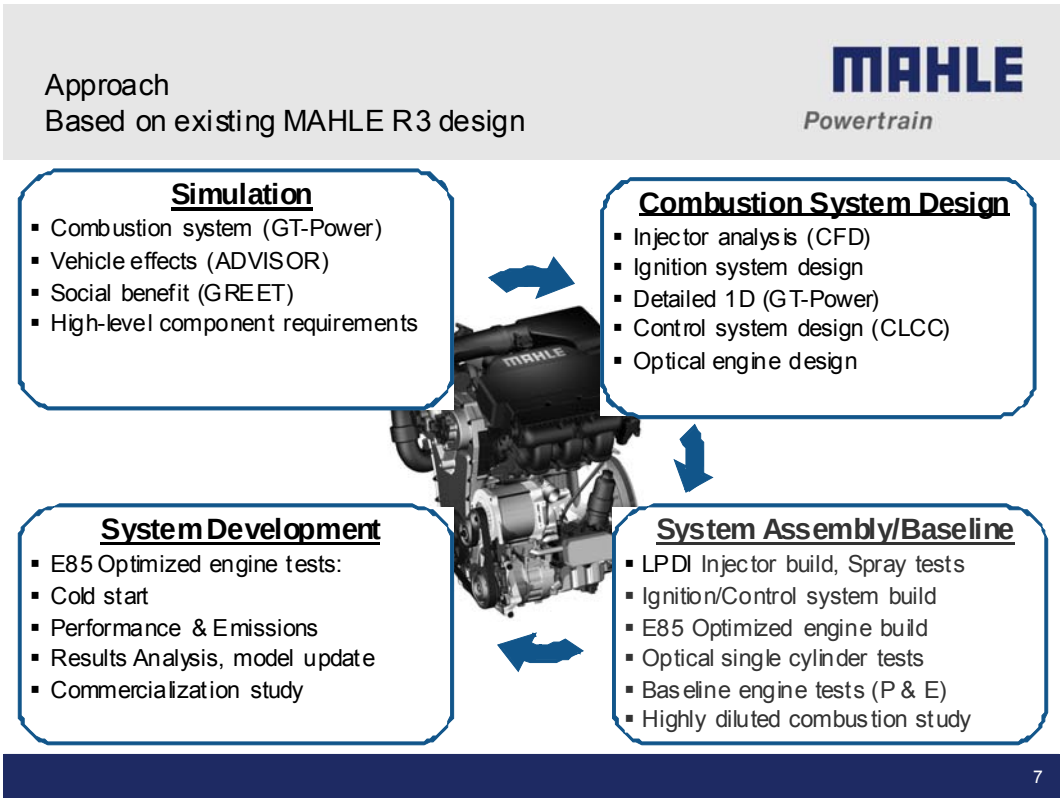

Figure 1:- Project Approach

2 PHASE 1 – APPLIED RESEARCH

Task 1.1 Confirmation of Engine Design and Specifications

'Perform initial design feasibility assessments of the factors requiring optimization for E85 fuelling (while maintaining gasoline FFV capability) and estimate potential benefits of the technology.'

This task was completed and a report titled 'Task 1.1', dated January 25th, 2008 was distributed.

It should be noted that, as indicated in the above-mentioned report, this entire program is based upon the modification and use of an existing MAHLE Powertrain engine design, intended for researching gasoline engine downsizing. As such, it is an ideal starting point for an E85 optimized flex fuel engine that can fully take advantage of the E85 fuel properties that allow high compression ratios to be utilized.

Figure 2:- MAHLE DI3 Engine

Task 1.2 Engine Simulations and Analysis

'Develop I3 and V6 engine and vehicle system simulation models. Use ADVISOR and GT-Power for vehicle-level benefit analysis. Complete an initial evaluation of the specifications for an E85 optimized combustion system that can meet performance and fuel economy targets within the potential for economic commercialization.'

Note: Following the submission of the original Statement of Project Objectives, it was decided that the primary baseline 'target' engine should be a 'state of the art', Direct Injection, 4 cylinder unit, instead of the stated port fuel injected V6. This decision significantly increases the challenge of achieving similar volumetric fuel economy, but provides a true comparison with the latest technology available in the US marketplace.

GT Power Analysis:

GT Power was used to perform engine analysis and optimization. The analysis and optimization resulted in a series of maps of fuel flow over the full engine speed / load envelope for the following model specifications:

Current Technology Comparator Engine

- 4 cylinder, 2.2L, NA, DI, Gasoline
- 4 cylinder, 2.2L, NA, DI, E85

Proposed Future Engine Technology

- 3 cylinder, 1.2L, T/C, DI, CR=9.25:1, Gasoline
- 3 cylinder, 1.2L, T/C, DI, CR=9.25:1, E85
- 3 cylinder, 1.2L, T/C, DI, CR=12.5:1, Gasoline
- 3 cylinder, 1.2L, T/C, DI, CR=12.5:1, E22
- 3 cylinder, 1.2L, T/C, DI, CR=12.5:1, E50
- 3 cylinder, 1.2L, T/C, DI, CR=12.5:1, E85

This data set allows for the separation of the effects of downsizing from optimization and provides a comparison of E85 use in a current technology DI engine vs. a next generation downsized, DI engine that has been partially E85 optimized.

ADVISOR Analysis:

In conjunction with the GT-Power results, ADVISOR software for vehicle fuel economy prediction used the fuel flow maps for each model specification considered, to provide a comparison of legislated drive cycle fuel consumption. To provide comparative results, all of the ADVISOR modeling was based on the same vehicle parameters taken from the 2008 Model Year Chevrolet Cobalt, which was selected as a suitably sized vehicle for the engines being studied. The only parameter that was changed between the two engine types (I3 and I4) was the transmission final drive ratio (FD). This was reduced for the I3 engine since it has significantly greater torque than the I4 engine and fuel economy could be gained without significant detriment to the vehicle performance.

ADVISOR also provides a prediction of vehicle performance as a 0 to 60 mph acceleration time. The fuel consumption and performance results for the MAHLE 1.2L and Ecotec 2.2L are shown in Table 1:

	Engine		FUEL	Ethanol Content	MPG				OVERALL EFFICIENCY (%)			0-60mph
	# Cyl	CR		%	FTP	HWFET	Combined FTP & HWFET	EUDC	FTP	HWFET	EUDC	Sec
Mahle with FD = 3.25	I3	9.25	E85	85%	23.4	29.9	25.9	26.0	9.5	18.2	15.8	6.8
			Gas	0%	35.5	45.6	39.4	40.1	9.8	19.0	16.6	6.9
	I3	12.50	E85	85%	**26.9**	**34.9**	**30.0**	29.9	10.9	21.2	18.1	6.6
			E50	50%	30.0	37.9	33.1	33.3	10.3	19.4	17.0	6.7
			E22	22%	34.1	43.4	37.7	38.2	10.2	19.4	17.1	6.7
			Gas	0%	37.4	47.8	41.5	42.0	10.4	19.8	17.4	6.7
Ecotec with FD=3.94	I4	12.00	E85	85%	20.9	25.7	22.8	22.5	8.5	15.6	13.6	8.3
			Gas	0%	**31.4**	**38.6**	**34.3**	33.8	8.7	16.0	14.0	8.3

Table 1:- Fuel Economy Predictions

Of particular interest are the figures in the shaded cells. These highlight the differences in fuel consumption and vehicle performance between the selected 'state-of-the-art', NA, DI engine, operating on gasoline and the proposed E85 optimized engine, operating on E85. It is important

to note that all of the gasoline modeling has been performed using 100% gasoline whereas, in reality, the lowest Ethanol / Gasoline mix generally commercially available is E10, at US fuel stations. The addition of 10% ethanol has the effect of decreasing fuel economy by approximately 3.5%.

After recalculating the figures to adjust for E10, a summary of the comparison is as shown in the following table:

	Engine		FUEL	Ethanol Content	MPG				0-60mph
	# Cyl	CR		%	FTP	HWFET	Combined FTP & HWFET	EUDC	Sec
MAHLE FD = **3.25**	I3	**12.50**	**E85**	**85%**	26.9	34.9	30.0	29.9	6.6
Ecotec FD=**3.94**	**I4**	**12.00**	**E10**	**10%**	30.3	37.2	33.1	32.6	8.3
			% Difference		-11.2	-6.3	-9.3	-8.3	20.5

Table 2:- Fuel Economy Predictions E10 and E85 Fuels

Although the objective of achieving equivalent fuel economy between the 2 engines / fuels (current technology engine running gasoline vs. the new engine running E85) has not been fully met, a significant improvement is predicted when compared with the typical 30% reduction in fuel economy seen in running with E85 fuel. The improvement shown is however, particularly impressive when the relative performance figures are taken into account – a 20.5% improvement in 0 to 60 mph acceleration is significant. This performance difference indicates that if a different compromise between performance and fuel economy were sought, with the emphasis more toward fuel economy (either by modifying the engine or by reducing the final drive ratio further) the fuel economy differences could be narrowed still further, without degrading 0 to 60mph acceleration below that seen with the Ecotec engine.

Task 1.2.1 Additional GT-Power / ADVISOR analysis

'Conduct further GT-Power / ADVISOR analysis, using Design of Experiments optimization techniques, to define the detailed requirements for compression ratio, turbocharger matching and boost system control methods for E85 optimization, maintaining FFV feasibility. This includes assessment of a range of fuel mixes between E85 and gasoline. Interrogate analytical models for peak cylinder pressures, fuel and air flow rates, etc. to assist in developing detailed component / sub-system requirement specifications.'

Optimization was performed on the following parameters:

Parameter	Lower Bound	Upper Bound
Compression ratio	9.0:1	19.0:1
Intake Maximum Opening Point (IMOP) [°ATDC]	80	120
Exhaust Maximum Opening Point (EMOP) [°ATDC]	-123	-83
EGR Quantity [%]	0	11.5

Table 3:- GT-Power Optimisation Parameters

From the Design of Experiment optimizations, a compromise compression ratio of 12.5:1 was selected to provide improved fuel economy without significantly degrading gasoline performance.

Task 1.3 Hardware Technical and Economic Viability

'Perform an initial assessment of the proposed component hardware's technical and economic viability.'

The technical viability of the primarily affected engine components were demonstrated, in the modeling results, through the adherence to the original design cylinder pressure limit of 140bar. This, combined with relatively low exhaust temperatures predicted for the ethanol blends (E22, E50 and E85), means that the proposed engine will be no less technically viable than the units already being used to successfully perform gasoline downsizing studies on dynamometer.

Economically there are no concerns, since all of the components can be produced using conventional, well-established methods and tools. The proposed engine represents a new combination of already proven and commercially viable technologies, included into a high strength, conventional, poppet valve, piston engine, including:

- 2 stage turbocharging (high boost level)
- Direct Injection
- Dual independent camshaft timing
- Exhaust Gas Recirculation (high flow and cooled)

It was acknowledged that the only technology not commercially proven, was the application of Closed Loop Combustion Control (CLCC). This technology had been developed and demonstrated on a port fuel injected application, however some tailoring to this advanced DI application using a modified ignition coil design and new software was expected. The economic impact was judged to be minimal.

Task 1.4 High Level Component Requirement Specifications

'Identify the detailed engineering specification requirements for all critically affected major engine components and sub-systems.'

The GT Power analysis of the proposed I3 1.2L engine demonstrated that a good performance compromise between gasoline and E85 with some fuel economy benefit for E85 can be achieved by increasing the 'geometric' compression ratio from the original 9.25:1, up to 12.5:1. Consequently, a compression ratio of 12.5:1 was selected as a lower bound, guiding the engine design and build program.

It was expected that further E85 fuel economy benefit would be achieved at higher compression ratios, but at the expense of gasoline performance due to the requirement to increasingly retard ignition in order to avoid knock.

It was proposed that 3 compression ratios were designed for, and tested, those being; 12.5:1, 13.5:1 and 14.5:1. Due to the uncertainty of knock effects in the modeling (as mentioned above), it was observed that only physical testing would allow a true comparison of these different specifications. The proposed compression ratios were to be achieved through changes in piston crown design without affecting other components.

Since there was to be no change made to the maximum cylinder pressure experienced by the major engine components, no design or specification changes were required. Further, the predicted reduction in exhaust gas temperatures, when operating on ethanol blends, was seen as being beneficial to those components contacted by the exhaust gas, such as; exhaust valves, exhaust manifold and turbocharger turbines, housings and wastegates. However this could be detrimental to turbocharger boost performance.

The requirements of the other components in the engine are unchanged from the original gasoline design, except that the cylinder head would require some redesign work depending on injector selection.

Task 1.5 Social Benefit Analyses

'Conduct analysis to determine potential fuel savings and emission reduction for the United States if proposed technology is successfully implemented. Includes GREET analysis - establishment of energy efficiencies through the various stages from oil well to the vehicle / engine.'

Analysis of the GT Power modeling results using GREET software to demonstrate the impact of the proposed E85 optimized flex fuel engine on greenhouse gas emissions was completed by Argonne National Lab.

GREET analysis predicted that the optimized flex fuel engine would reduce drive cycle greenhouse gas emissions by 32% in comparison with the default conventional gasoline engine. Again, it is worth emphasizing that this substantial reduction in greenhouse gas emissions is commensurate with a significant increase in vehicle performance.

3 PHASE 2 - Exploratory Development

Task 2.1 Optical Engine Design and Fabrication

'Two optical engine assemblies will be constructed. The first will feature a quartz cylinder along with a Bowditch style piston. This engine will be used to evaluate spray targeting with the low pressure direct injection system as well as generic fuel nozzle development. The second engine will be setup to operate over a range of speeds and loads. It will feature a sapphire insert for the Bowditch piston. Both engine assemblies will use MAHLE supplied heads from the three-cylinder prototype engine. The second engine will be configured to operate in both a metal and optically accessible configuration.'

The original plan to use the target (MAHLE DI3) three cylinder head to construct the single cylinder optical engine was changed for the following reasons. Fitting the three cylinder engine head onto the single cylinder with optical access hardware required machining off part of the MAHLE cylinder head area associated with cylinders 1 and 3 which could cause potential difficulties in sealing the exposed areas, leading to potential coolant and oil leaks. Also packaging the dual variable valve timing actuators in the confines of the single cylinder head would prove challenging.

Therefore, a unique single cylinder head was designed with the same characteristics as the target three cylinder head, while satisfying the integration requirements. Multiple engine heads have been fabricated, as shown in Figure 3.

Figure 3:- Optical Engine Cylinder Head Assembly

The cylinder head combustion chamber remained identical to the target engine head, see Figure 4. In order to be able to fit with multiple configurations of the DI injectors, the optical engine cylinder head was designed to be able to use both the Visteon low pressure DI injector and the Bosch Generation 2 DI injector.

Figure 4:- Optical Engine Combustion Chamber

The upper picture of Figure 5 shows the optical engine assembly including a quartz cylinder and part of the cylinder head; and the lower picture of Figure 5 shows the crankshaft and connecting rod assembly for the optical engine. An AVL crank case was used as the optical engine base. Assembly and integration of the optical engine was completed.

Figure 5:- Optical Engine Assembly Without Crankcase

Two different optical engine configurations were to be used for subsequent tests. The first featured a quartz cylinder. The second used a metal liner along with a Bowditch style piston, shown in Figure 6. The piston has a window mounted in the crown and an extension below with a 45° turning mirror near the bottom of the piston that provides access to the combustion chamber. This engine was used to evaluate spray targeting as well as generic fuel nozzle development. This setup was used to study the effect of injection timing, fuel pressure and injector nozzle on spray pattern, cylinder wall / piston wetting.

Figure 6:- Bowditch Piston

Task 2.2 In-cylinder CFD modeling for Injector Spray Specification

'Numerical simulations of the in-cylinder fuel air mixing process will be conducted using KIVA-4 and / or Fluent. This code will be used in conjunction with the spray experiments to access the mixing characteristics that will afford optimum mixing of the fuel-air-residual gas.'

In-Cylinder Engine Modeling Approach

Numerical simulations of in-cylinder fuel air mixing are intended to help define the specifications of the fuel injector such as fuel injector spray requirements, flow requirement, injector location, and injection strategy in order to optimize the fuel homogeneity in the combustion chamber. *KIVA-4* was originally chosen as the CFD code because it was an open source code and has been generalized to either structured or unstructured meshes. Specifically, this newer version was also capable of simulating in-cylinder engine flows with multi-component fuels.

Generally, in-cylinder fuel mixture and engine combustion simulations are considered very complex and computationally intensive due to the requirements of fine mesh density coupled with moving boundaries (motions of piston and valves) as the engine cycles progress. Therefore, in traditional in-cylinder simulation, a tremendous effort is devoted on mesh preparation in order to eliminate any problematic inverted cells. The structured mesh configuration was created using a mesh generator called *TrueGrid*. *TrueGrid* was selected

because of its ability to give both unstructured and structured meshes. Another advantage of using *TrueGrid* was that it provided output in *KIVA-4* format directly. However, due to the complex cylinder geometry with relatively large angles of the intake and exhaust valves, meshing density had to be increased in the areas surrounding the valve gaps. It created nearly 700,000 cells, divided into 183 blocks. The static mesh configuration was successfully generated, however when the moving meshes in the intake valves were tested, there were problems with a large number of inverted cells with negative volume and negative Jacobian. Despite a comprehensive effort in smoothing and relaxing the grids, the mesh problems in the vicinity of the valve skirt and the valve seat were not completely resolved to allow for the use of *KIVA-4* in a timely manner.

As a result a decision was made to switch from *KIVA-4* to another commercially available CFD code called *CONVERGE* which is developed by Convergent Science, Inc. In contrast to other codes which require fully moving meshes to be created for the entire run cycle, the meshing algorithm in *CONVERGE* is made at runtime automatically. A highly accurate numerical solver, coupled with its orthogonal and stationary mesh, fixed embedding, and adaptive mesh refinement, produces reliable results for in-cylinder flow modeling. Standard algorithms for modeling the droplet collision, coalescence, wall impingement and wall film formation are also included in the calculations.

Figure 7 and Figure 8 depict the engine geometry of the single cylinder configuration. The surface mesh is shown while the liner is hidden to show the details of the piston top shape. Specifically, a new piston geometry design of 13.5 : 1 geometrical compression ratio was used in the modeling, in accordance with the recommendations from Phase 1. The higher compression ratio should increase the engine combustion efficiency. For the CFD studies performed so far, approximately 300,000 cells were used in this analysis to balance between accuracy and computational speed.

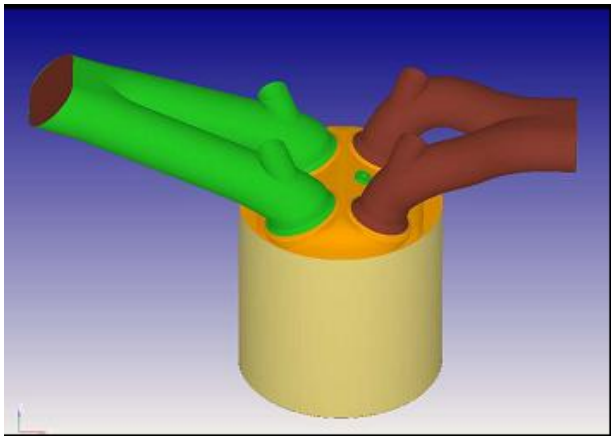

Figure 7:- Single Cylinder Configuration of the MAHLE DI3 Engine

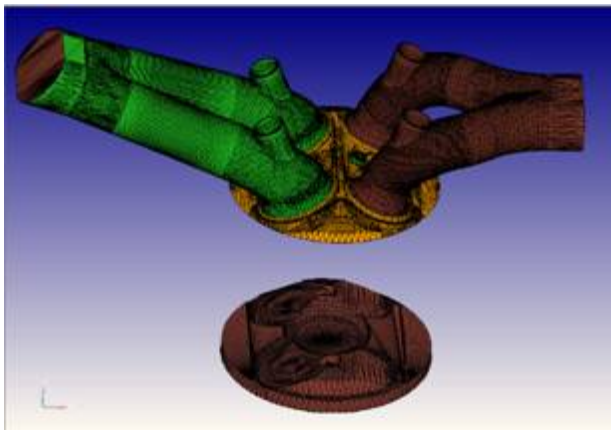

Figure 8:- Meshing Configuration in the Intake / Exhaust Ports and Piston Top Geometry

Fuel Injector Design Criteria and Functional Requirements

When developing combustion systems for DI gasoline engines, it is important to achieve optimal fuel-air mixture prior to ignition. Fuel spray design characteristics are a key consideration in avoiding major compromises and limitations. These characteristics are discussed with respect to the MAHLE I3 application.

Flow Characteristics

The key focus of this task was to define the injector specification and functional requirements. The first key design consideration was the sizing of the injector to deliver adequate fuel flow for the MAHLE I3 engine particularly at max engine speed and full load conditions. Given that the max engine power was rated at 132kW and a Brake Specific Fuel Consumption (BSFC) of 380g/kWhr (@ 6500rpm) was the engine efficiency target, it was estimated that at the rated fuel pressure, the injector static flow requirements were approximately 13.8g/sec for regular gasoline and 17.3g/sec for E85. The static flow requirements were set for the injector designs. A balance on designing the flow requirement in the low flow regime was also made to ensure that the injector would deliver consistent, controllable fuel metering at idle conditions.

At 6500rpm WOT, the injected fuel mass (for gasoline) would be about 60mg per cycle. At this max engine speed, it would take about 3.77ms to deliver the total amount if the static flow rate of the injector is at 16g/s. The following table shows the injection duration in terms of Crank Angle Degree (CAD):

Static Flow Rate (g/s)	Injection duration (ms)	Injection Duration (CAD)
10	6.03	235
12	5.03	196
14	4.31	168
16	3.77	147
18	3.35	131

The data above shows that the injection event at 6,500 rpm WOT can be accomplished prior to the piston reaching bottom dead center (BDC), which was the design goal for this stage of the project.

Injector Type Selection

The next step was to decide the most appropriate type of fuel injectors which would be used for this engine. Since the cylinder bore in this highly turbocharged engine is relatively small compared to other naturally aspirated engines of similar power output, the valves on both intake and exhaust became proportionally larger. This, coupled with the large tilted angles for the inlet and exhaust valves (21.5 degrees and 24.1 degrees, respectively) and the physical constraints of the engine cylinder head, constrain injector placement to ~12 degrees along the piston axis in the vicinity of the spark plug (i.e., a centrally-mounted injector configuration). A side-mounting installation cannot be implemented within the packaging constraints.

Two types of injector were considered:

- Conventional hollow cone swirl injector
- Multi-hole injectors

The selection criteria were based on the currently available GDI fuel injectors, as well as the engineering and manufacturability factors required to meet the project objective of potential implementation with a cost effective, production viable solution. For these reasons, solenoid injectors were preferred over the piezoelectric-actuated type.

Hollow cone swirl injectors were employed in many early production GDI vehicles. Swirl injectors typically provide well atomized spray structure, but are disadvantaged by their limitation in tailoring fuel droplet distributions uniformly throughout the cylinder due to the cone angle constraints of the swirler. To illustrate this observation, a 60-degree hollow cone spray from a swirl injector was simulated initially in the engine. As shown in Figure 9, when the injector was mounted at the specific location, spray droplets were found to impinge on the cylinder wall and the overall fuel droplet cloud was not well dispersed. The impingement was largely due to the spray cone angle and the orientation of the centrally-mounting injector on the cylinder head.

On the other hand, it has been shown that multi-hole fuel injectors offer advantages in spray pattern tailoring flexibility over other existing swirl or slit nozzle fuel injectors. This is because the hole pattern, hole orientation, internal flow cavity, and number of holes on a multi-hole nozzle can all be precisely designed to control individual spray plumes and the overall spray distribution. Therefore, multi-hole GDI injectors evolved as the leading candidate for this engine. The design and selection of multi-hole injector would be based on the hole plurality, hole pattern configuration, and overall spray pattern.

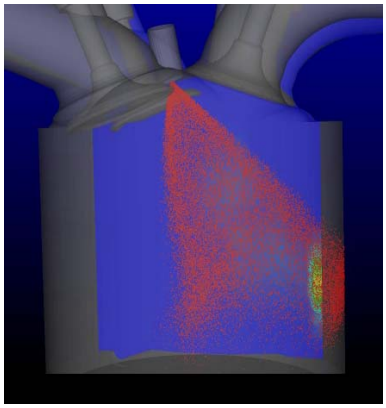

Figure 9:- Fuel Droplet Distribution From a 60-Degree Hollow Cone Swirl Injector

Simulations of Air-Fuel Mixture Formation

Two spray configurations from two different multi-hole GDI injectors were considered in the CFD simulation studies.

- Visteon's Low Pressure Direct Injection (LPDI) prototype 8-hole GDI injector with a spray angle of 80 degrees and a bent (gamma) angle of 10 degrees.
- A second injector spray configuration was created to mimic a 7 hole Bosch Generation 2 GDI injector commercially available in the market. This injector spray has a custom asymmetrical (ellipsoidal) spray pattern, a relatively large bent angle and roughly 70 degrees spray angle in one direction and 45 degrees spray angle in the perpendicular direction.

The engine operating point was set at 2500rpm full load. The initial drop size for the 8-hole injector was set to 30 microns Sauter Mean Diameter (SMD). The drop size was obtained from the measurements using Phase Doppler Particle Analyzer.

The operating point was chosen for the following reasons:

- Full load results show the critical fueling and droplet dispersion requirements in the cylinder.
- The results at this engine speed could be compared to the subsequent cold flow and firing tests to be done in optical engine where its max operating speed is also at about 2500rpm. Other speed and load conditions (for example, part load) may be evaluated as needed.

Figure 10 through Figure 13 show the air-fuel mixture formation of ethanol in the cylinder. Both iso-octane (to mimic regular gasoline) and ethanol were used as fuels in the numerical models. The tip of the injector is centrally located in the close vicinity of the spark plug. The fuel injection duration was calculated so that the lambda ratio was near unity. The injection pressure was set to 3MPa. Only the ethanol case is shown here for illustration. Images on the left depict a 7 hole injector spray and the right one is from an 8-hole injector. For illustrative purposes, the Start Of Injection (SOI) timing at 280^{o}BTDC and injection duration at 68 crank angle degrees are illustrated here. At this injection timing, there was very minimal fuel impingement on the piston top. In addition, there was also no apparent fuel deposited on the cylinder wall causing undesirable fuel films to be formed. Fuel impingement on the wall has been a major contributor to unburned HC emissions, smoke and particulate matter. At 240^{o}BTDC, it can be seen that while both injector sprays did not impinge very much on the cylinder wall, the 8-hole spray delivers more uniform fuel to the left side of the cylinder. This impingement location was found to be closely related to the geometrical mounting of the injector. A wider angle of fuel spray from the 8-hole injector produced a more homogeneous fuel-air mixture by dispersing the mixture formation more to the left region of the cylinder. At a later timing of 120^{o}BTDC, the fuel homogeneity from the 8-hole injector spray was found to be more uniform than the 7 hole injector spray. Similar difference in mixture homogeneity was found in two subsequent timings of 60^{o} and 20^{o}BTDC.

Based on the CFD simulation results, the Visteon 8-hole injector was at that time selected as the first candidate for this combustion system.

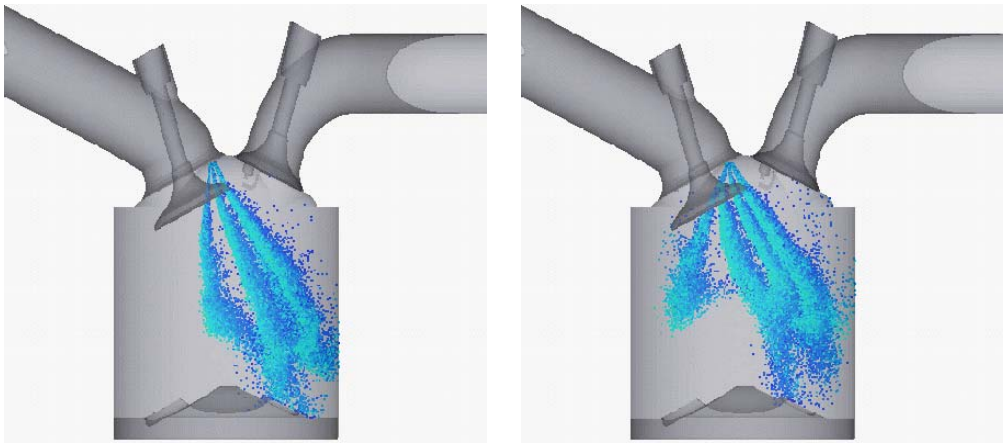

Figure 10:- In-Cylinder Fuel Mixture Formation (Ethanol) at 240°BTDC
(Left: 7 Hole Injector Spray; Right: 8 Hole Injector Spray)

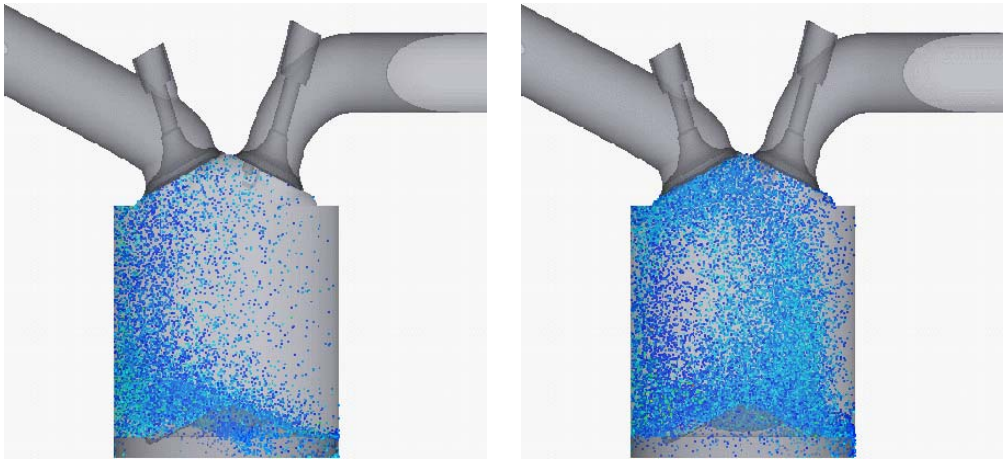

Figure 11:- In-Cylinder Fuel Mixture Formation (Ethanol) at 120°BTDC
(Left: 7 Hole Injector Spray; Right: 8 Hole Injector Spray)

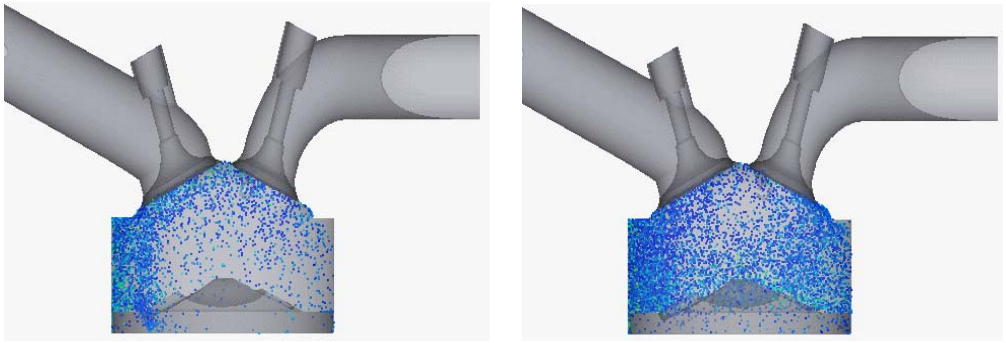

Figure 12:- In-Cylinder Fuel Mixture Formation (Ethanol) at 60°BTDC
(Left: 7 Hole Injector Spray; Right: 8 Hole Injector Spray)

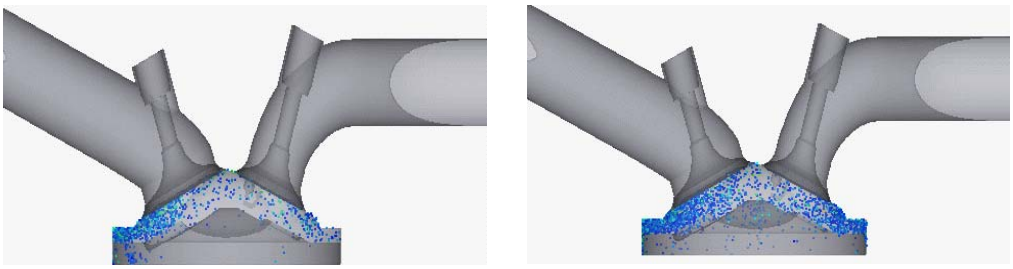

Figure 13:- In-Cylinder Fuel Mixture Formation (Ethanol) at 20°BTDC
(Left: 7 Hole Injector Spray; Right: 8 Hole Injector Spray)

Simulations of Spark Ignition

In addition to the fuel mixture analysis, a preliminary investigation of the spark ignition was also performed to reveal the effect of ignition on flame propagation in the cylinder, based on the fuel mixture formation in the vicinity of the spark plug. The purpose of this study was twofold:

(1) To reveal the ignition sequence which will serve as a basis for comparing the similar study in the optical engine.
(2) To examine the use of adaptive meshing refinement (AMR) processes surrounding the spark plug and flame boundaries where the use of finer meshes was advantageous for better accuracy.

Figure 14 depicts three sequential instances of the spark ignition event. Note that the meshes were made finer in those critical locations as mentioned. The spray mixture was formed from the 8-hole injector as a demonstration. The spark ignition was set at 15°BTDC. At 12°BTDC, the flame was initiated. At 6°BTDC, the flame propagated towards the intake side in the cylinder. Note that the meshes within flame and in the interface surrounding the flame were refined constantly to capture the flame propagation. At TDC, the flame nearly occupied the entire volume, except on the far sides near the cylinder wall. Overall, the simulated spark ignition events were within expectation.

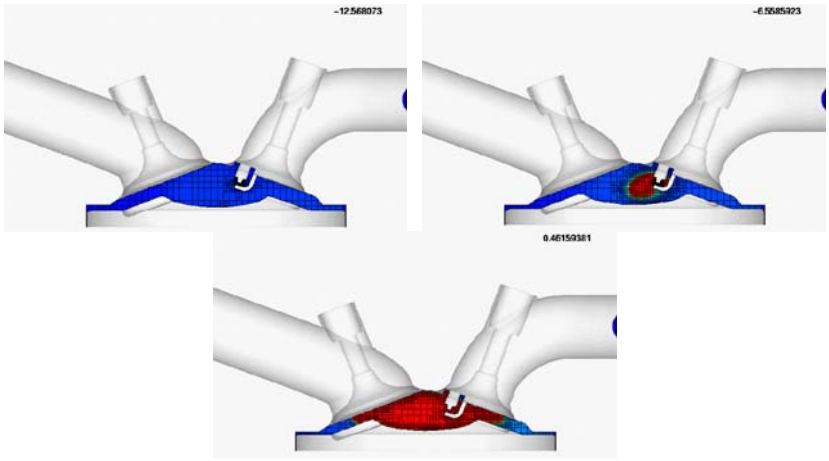

Figure 14:- Spark Ignition and Flame Propagation (Ignition at 15°BTDC)
(Left: 12°BTDC; Right: 6°BTDC; Lower: TDC)

Subtask 2.2.1 Fuel Injector Detailed Design Update

'Designs of electrical and mechanical components in the fuel injector will be optimized to accommodate the specific spray and flow requirements of E85 characteristics established in Task 2.2 as well as operate at the engine combustion pressures'.

Mechanical Design and Considerations

An injector flow dynamics model was created using *GT-Fuel* to optimize key injector design parameters, such as the performance of the solenoid, internal hydraulic resistance, spring force, nozzle hole number and geometry. While the majority of the mechanical design of the injector remained unchanged for use with E85 (except for the compatibility of o-ring in the injector inlet with ethanol-based fuels), particular attention was paid to designing the tip of the multi-hole nozzle configuration (metering plate) to meet the additional fuel flow requirement of E85.

Figure 15 shows a prototype sample of the 8-hole nozzle. The hole diameter was increased slightly to account for the additional fuel flow requirement of E85. The range of the hole diameter was expected to be between 200 and 300 microns. Consideration was also given to fuel pressure to achieve the required flow increase. The nominal fuel system pressure for the LPDI injector was 2MPa. It was confirmed that this pressure could be adjusted to as high as 3.5MPa without any degradation in the functionality of the injector. The increase of fuel system pressure should also increase the static flow rate of the injector to account for the higher flow requirement of E85.

Figure 15:- Typical 8-Hole Nozzle Plate Configuration (Looking From The Outside Of Injector Tip)

Electrical Design and Considerations

The operating voltage requirement for the injector was nominally 12V (min 6V and max 24V) but was modified to adjust the injector driver to account for the more robust injector opening and closing responses. Figure 16 shows the injector driving pulse and the current profile. Within each trigger pulse, the injector driver current profile consists of three phases: pre-charge, peak, and hold. Each phase of the current profile is responsible for controlling the opening, closing, main injection, and needle bounce (undesirable secondary injections). Both the electrical current and duration of each phase can be adjusted. Using the existing drawn current profile, the opening and closing times were at an acceptable range below 0.35ms, with no apparent injection bounces.

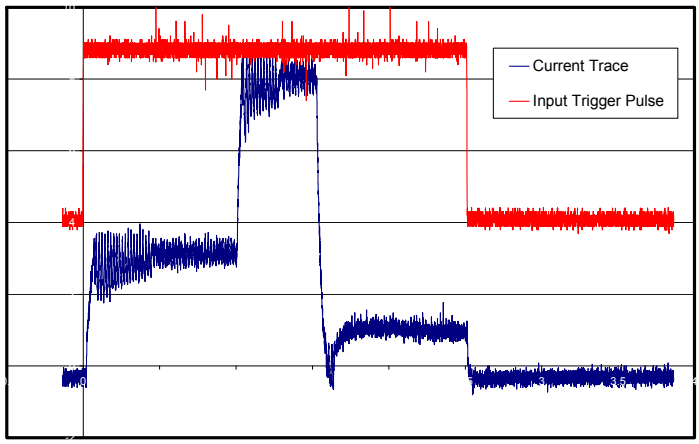

Figure 16:- Injector Trigger Input Pulse and Current Profile

It is also important to evaluate the functional performance of the fuel injector in terms of spray and flow characteristics. The measurements allow the use of more accurate calibration (such as fueling strategy) and other operating conditions of the injectors in the subsequent verification of the engine testing.

Task 2.3 Ionization Based Ignition System Design

'Design specifications of the ignition system will be established for operation at engine combustion pressures established in Subtask 1.2.1'.

The ionization detection system was seen as a key enabler for this project. Combustion produces ions and free electrons, and with a conventional spark plug and a modification of the ignition system, a current proportional to ions and free electrons produced during the combustion event can be measured. An ionization detection system uses a spark plug as a sensor to evaluate the in-cylinder combustion process when a bias voltage is applied between the spark plug center and ground electrodes [1 and 2].

Because the flame starts at the spark plug gap and gradually moves away, the ionization signal actually may provide more detailed information about in-cylinder combustion than an in-cylinder pressure signal. As the Ethanol content of fuel increases, the ionization signal strength also increases, allowing this characteristic to be utilized for detecting changing combustion characteristics with ethanol content.

Figure 17 shows a typical ionization signal versus crank angle and the corresponding in-cylinder pressure signal. Different from an in-cylinder pressure signal, an ionization signal actually shows more detailed information about the combustion process through its waveform. It shows when a flame kernel is formed and propagates away from the gap, when the combustion is accelerating rapidly, when the combustion reaches its peak burning rate, and when the combustion ends. A typical ionization signal usually consists of two peaks. The first peak of the ion signal represents the flame kernel growth and development, and the second peak is the re-ionization due to the in-cylinder temperature increase resulting from both pressure increase and flame development in the cylinder.

The ionization signal provides very useful information about engine combustion, such as misfire and partial burn [3, 4 and 5], inaudible and audible knock [3], combustion phasing [6, 7 and 8],

combustion stability [9], ethanol content, etc. Ionization based closed loop combustion control techniques have been developed for closed loop knock control, combustion phasing and combustion stability control [4, 6, 8 and 9].

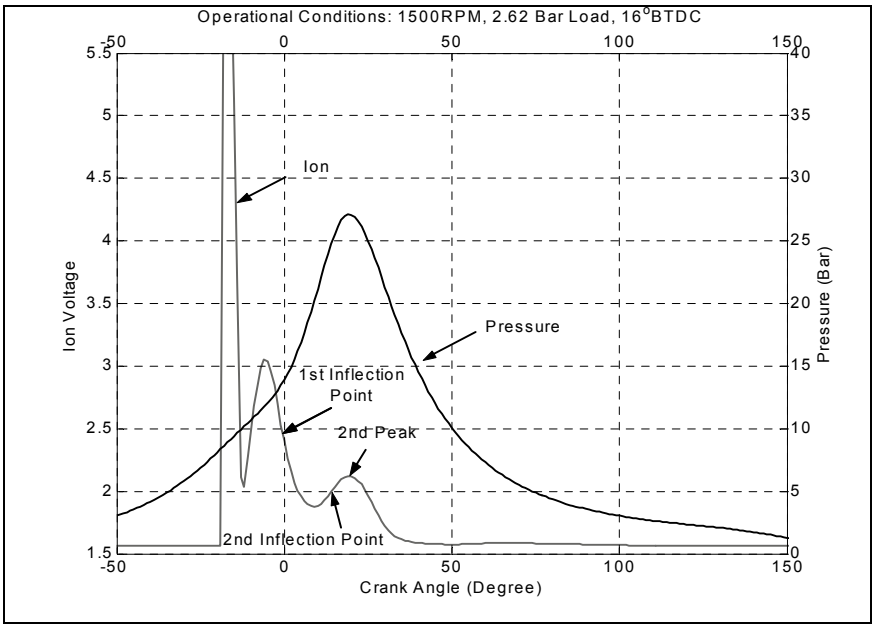

Figure 17:- A Typical Ionization Signal as a Function of Crank Angle

The main challenge of using ionization signals for combustion feedback was seen as making the ionization detection electronics function with the higher energy ignition system required for the turbocharged high compression-ratio DI3 engine. Design of the ionization detection circuit for high energy ignition systems was completed, see Figure 18 for the prototype circuit.

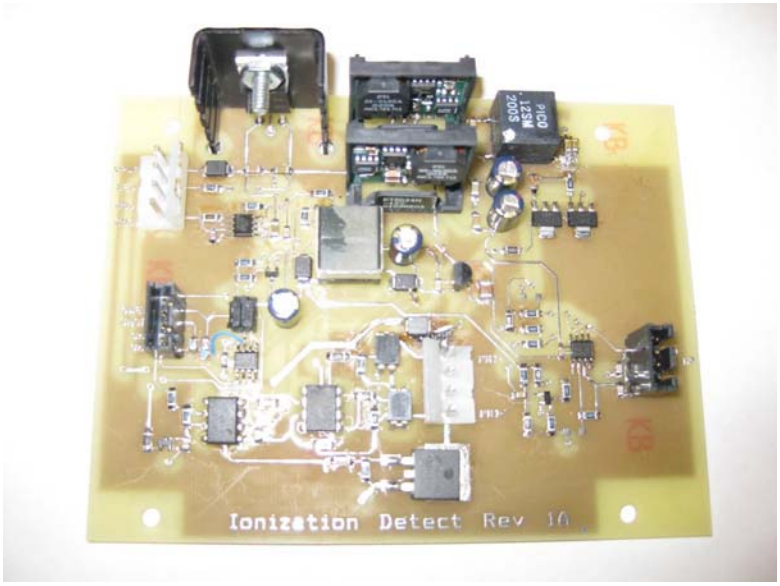

Figure 18:- High Energy Ionization Detection Prototype Circuit

Due to the target engine's higher compression ratio, gasoline direct injection, and compound

boosting, the in-cylinder compression pressures were high. The target ignition system was expected to provide at least 37kV (@25pF) and spark energy of 45mJ. A multi-strike technique (spark multiple times in one combustion cycle) was to be used to increase the ignition energy to over 80mJ. Figure 19 shows two target ignition coils with satisfactory ignition energy and voltage.

Figure 19:- Target High Energy Ignition Coils

As an alternative, a Delphi prototype DI ionization ignition system that meets minimal requirements for the ignition energy and voltage, (see Figure 20) was studied.

Figure 20:- Delphi Prototype Ionization Pencil Ignition Coil

In summary the ionization detection system for a high energy ignition system was designed for an ignition system specification providing at least 37kV (@ 25pF) and spark energy of 45mJ. It was intended to use a multi-strike technique to increase the ignition energy to over 80mJ.

Task 2.4 Detailed Engine Design Update and Procurement

Subtask 2.4.1 Detailed Engine Design Update

'Design the combustion system components including piston and combustion chamber adaptations for compression ratio and peak cylinder pressures, cylinder head for direct injector installation. Design supporting sub-systems including turbocharger impeller / compressor matching for revised boost control. Includes pro-rated portion of original engine design costs'.

Piston crown designs achieving geometric compression ratios of 12.5 : 1, 13.5 : 1 and 14.5 : 1 were completed, reference Figure 21, in accordance with the recommendations from Phase 1.

Figure 21:- Piston Designs To Support Compression Ratio Study (A) 12.5 : 1 (B) 13.5 : 1 (C) 14.5 : 1

Subtask 2.4.2 Procure Tooling and Major Components

'Ordering of Tooling changes to accommodate design update and ordering of all major engine components. Includes pro-rated portion of original tooling costs'.

The MAHLE DI3 engine was procured together with the major components and spares for both the single cylinder optical and metal engines.

Several sets of blank pistons were procured, in support of the proposed compression ratio investigations.

Task 2.5 Control System

Subtask 2.5.1 Mean Value Engine Model Development

'A mean value engine model will be developed for the purpose of Hardware In The Loop (HIL) simulation as a base for control system development.'

A mean value real-time engine model was developed in *Simulink* for the purpose of the HIL simulation to be used as a tool for control system development and to reduce development time. In order to develop the mean value real-time *Simulink* engine model, the *GT-Power* target engine model, developed in Phase 1, was refined first and used to study the engine behavior over the engine operational conditions. The *GT-Power* model was also used to generate the calibrations for the mean value real-time *Simulink* engine model.

a) GT-Power Modeling

Figure 22 shows the configuration of the downsized engine.

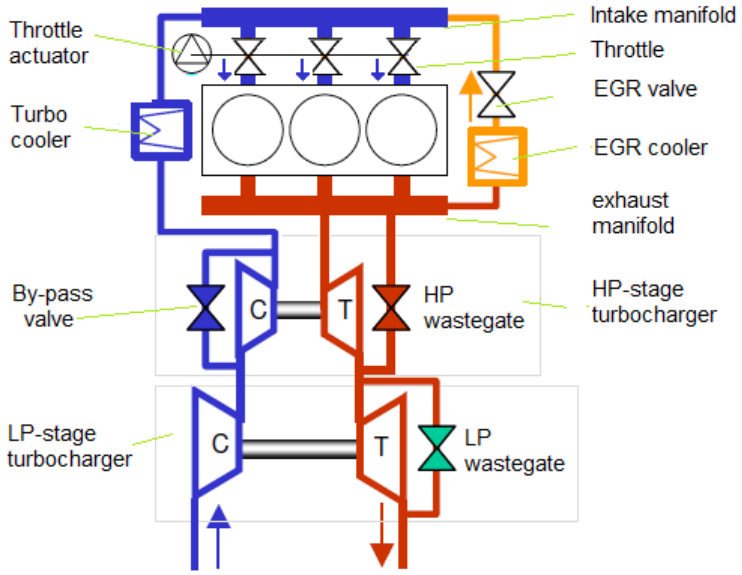

Figure 22:- Downsized Demonstrator Engine Configuration Diagram

The developed *GT-Power* model shown in Figure 23 is constructed according to the engine configuration shown in Figure 22. To simulate the engine operated at a given EGR rate, the EGR Mass Flow Rate and intake air mass flow rate are used as feedback signals to a PID controller to adjust the EGR valve position so that the desired exhaust gas flow is maintained in simulation. The engine combustion model was based on the Wiebe function.

The *GT-Power* model was also connected to a dynamometer model, which ensured that the engine was operating at the target speed and load, so that the simulation results can be compared with engine dynamometer test results.

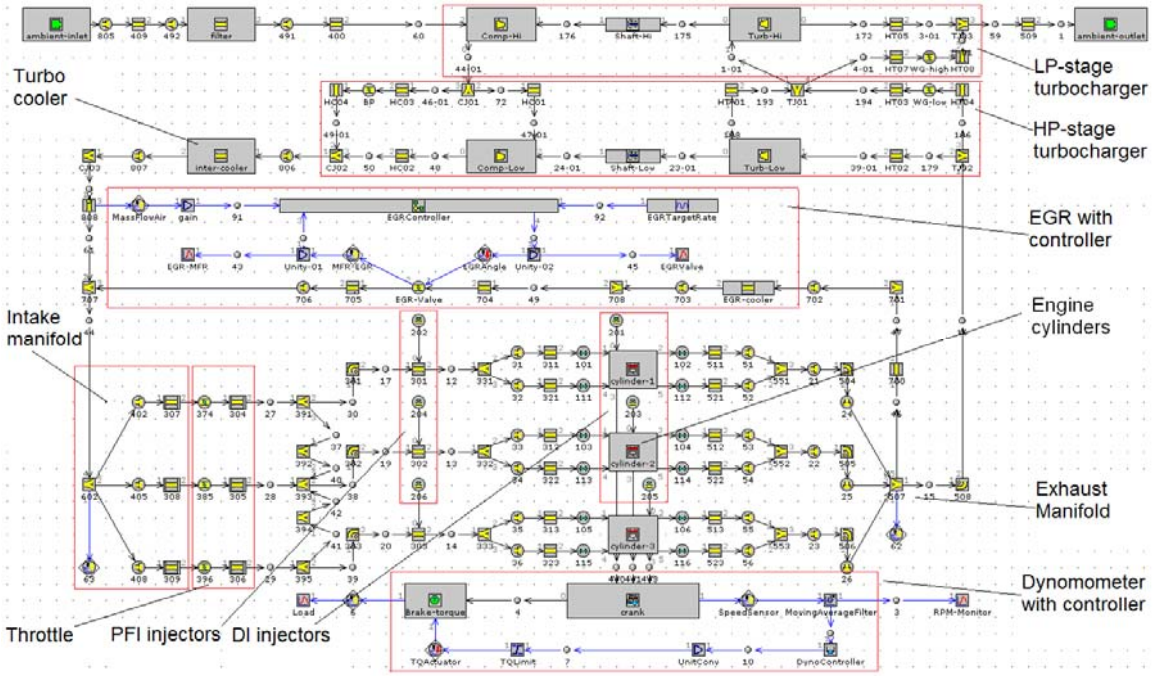

Figure 23:- GT-Power Engine Model Layout

Based upon the *GT-Power* simulation results of the developed dual-stage turbo engine model, it was found that a midsize single stage turbo (such as BorgWarner K03) could provide performance to match that of the baseline 2.2L Ecotec engine.

b) *Simulink* modeling

The mean valve real-time *Simulink* engine model was developed during this phase and parameterized to match *GT-Power* simulation results. The technical challenges were:

- The engine model had to be simple enough to be operated in real-time with a step size less than or equal to 1.5 milliseconds; while the basic engine dynamics shall be captured so that the real-time engine simulation will include all engine dynamics and be accurate for control strategy validation.
- The key challenge for developing this mean value real-time model was the additional dual-stage turbo-compressor loop of engine intake air flow, compared to naturally aspirated engine models. Iterative calculation technique for a given simulation step was used to improve the real-time simulation accuracy.

In order to ensure the model was capable of demonstrating closed loop combustion control, crank based in-cylinder pressure signals were also modeled, and implemented in the HIL simulation environment. Figure 24 shows the top level graphic program of the developed mean value *Simulink* engine model.

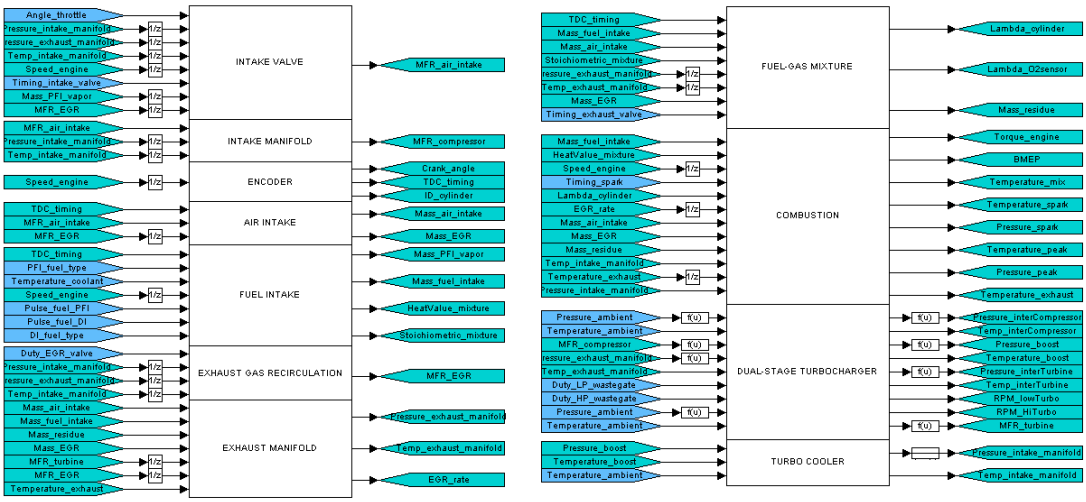

Figure 24:- Mean Value Real-Time Simulink Engine Model Layout

In order to test the transient performance of the model, a constant speed simulation at 2500rpm was performed. At the 10th second of the simulation shown in Figure 25, a step input was applied to the throttle, at the same time wastegates of both LP and HP turbochargers were adjusted.

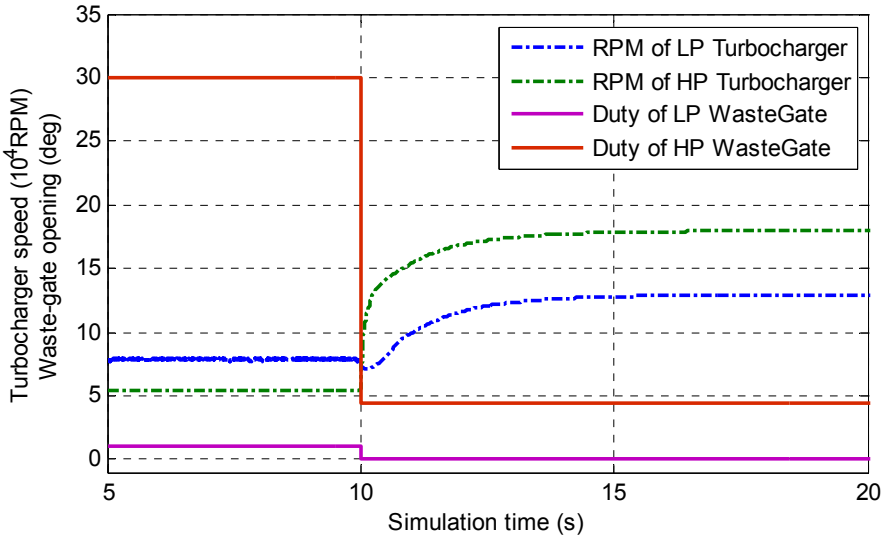

Figure 25:- Turbocharger Speed Response In Transient Process

Figure 25 also shows the turbocharger speed transient responses. As anticipated, the speed response of the smaller HP turbocharger is faster than that of the LP turbocharger, which can

be used to reduce turbo lag / delay in transient operation. Control strategies for reducing turbo lag were planned to be studied in the next phase of the project. One approach is to use the engine transient fueling schedule to reduce engine torque response time. As shown in Figure 26, the engine torque response time was reduced by more than half using the transient fueling schedule technique from the developed mean value real-time engine model.

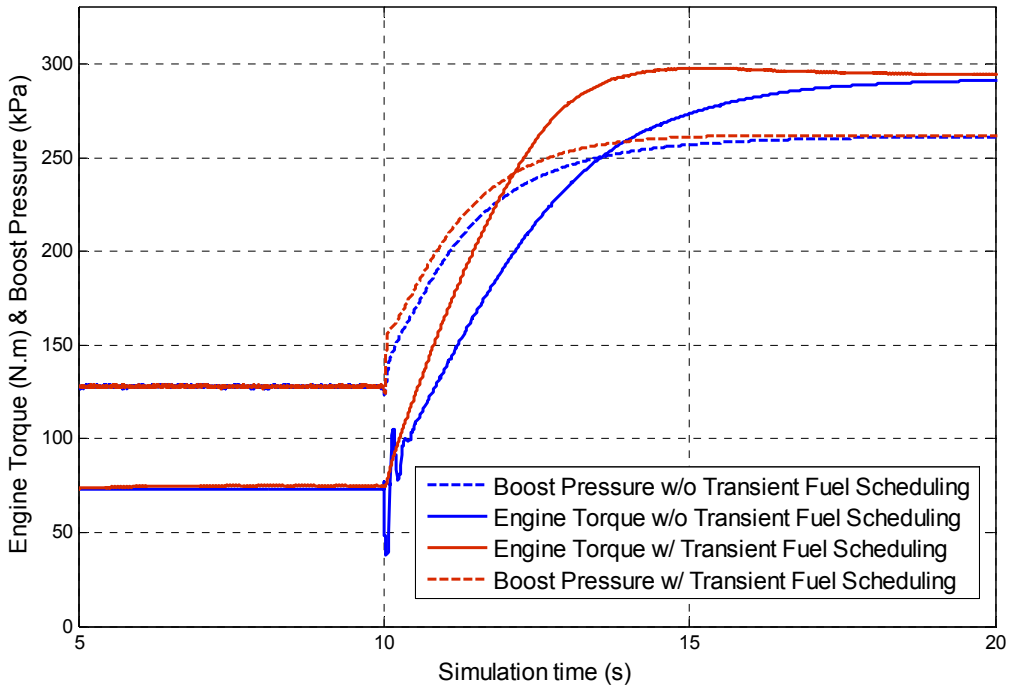

Figure 26:- Boost Pressure and Engine Torque Response With and Without Special Fuel Control

c) HIL simulation implementation

Interfaces to measure the control signals from the engine controller and to generate the engine sensor signals were added into the target HIL system (a *dSPACE* based simulator), see Figure 27.

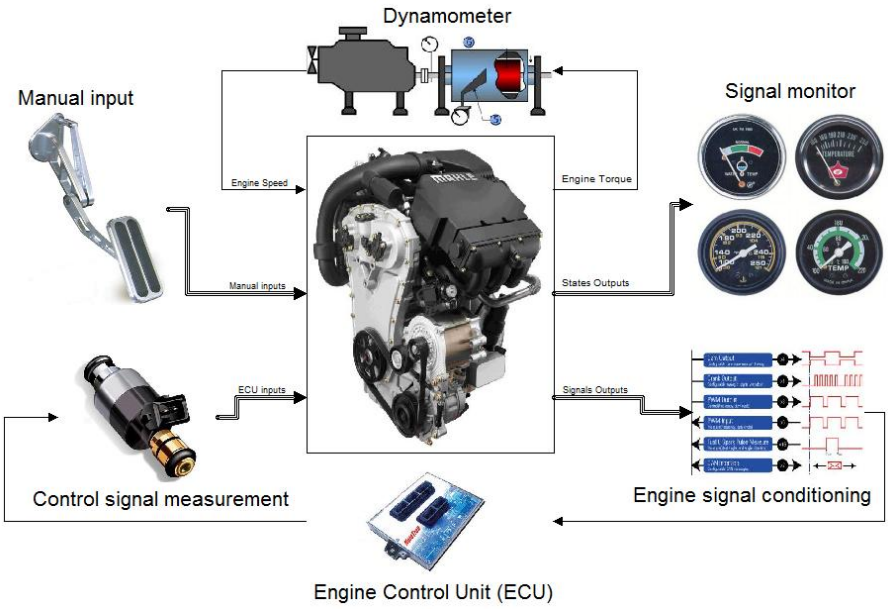

Figure 27:- System Diagram for HIL Simulation

After implementation of the Simulink model shown in Figure 24 into the *dSPACE* based HIL simulator, the engine model was calibrated using the *GT-Power* simulation results. The GUI interface of the *dSPACE* based HIL simulation is shown in Figure 28.

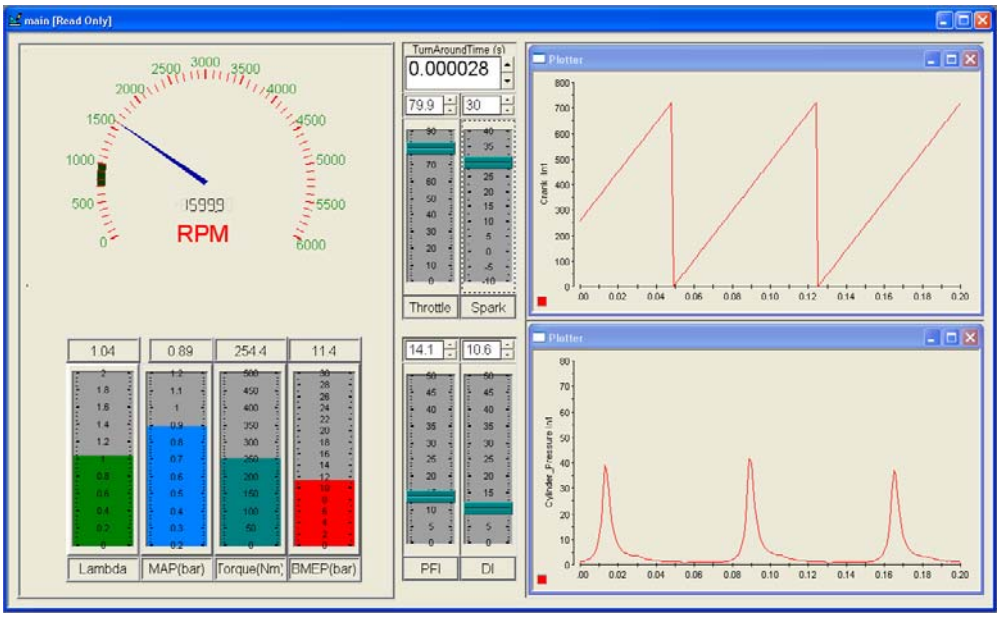

Figure 28:- GUI Interface of dSPACE HIL Simulator

Subtask 2.5.2 Control System Design

'The rapid prototype controller specifications will be developed including hardware input / output requirements and software throughput requirements. The basic control strategy will be developed and validated through HIL.'

Hardware configuration and procurement of the control system was completed. The two main components of the control system were the prototype engine controller (micro-controller) and its I/O box. The selected micro engine controller was an *Opal-RT* system due to its high real-time processor speed. The *Opal-RT* developed multi-core prototype engine controller, is shown in Figure 29. The developed *Opal-RT* engine controller is capable of crank based signal sampling at one degree resolution, which is critical for closed loop combustion control. The controller can also sample engine knock signal at 250kHz sample rate.

Figure 29:- Multi-Core Opal-RT Prototype Real-Time Controller

Figure 30 shows a block diagram of the prototype engine controller I/O box, which was constructed during the next phase of the project. The purpose of this box is two-fold:

a) Conditioning the engine sensor signals, such as ionization, in-cylinder pressure, and air fuel ratio (AFR), before they are sampled by the Opal-RT A/D channels.
b) Amplifying the engine control signals to make them suitable to drive ignition coil, fuel injector, turbo-waste gate, and EGR valve.

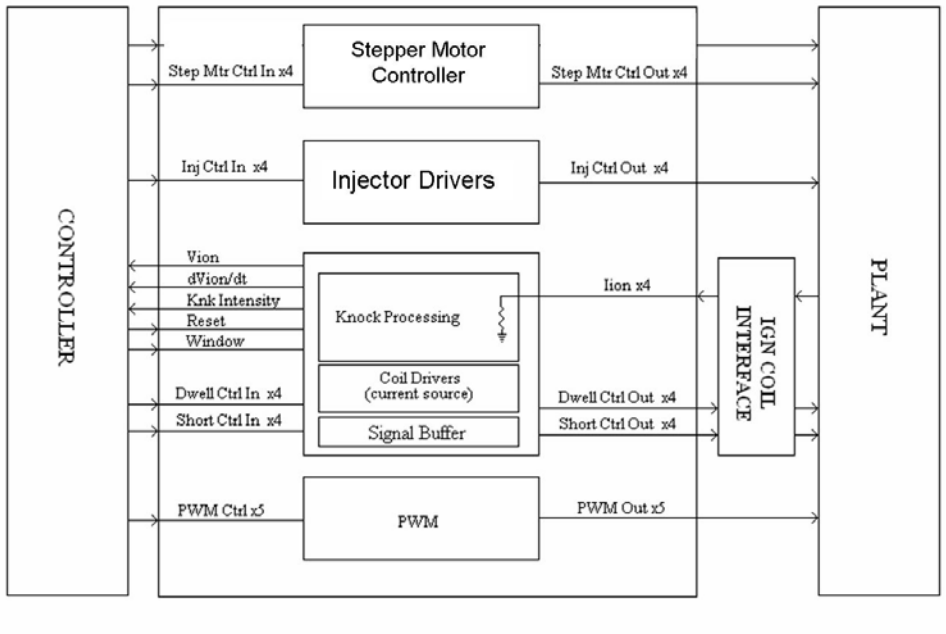

Figure 30:- Real-Time Controller Block Diagram

Figure 31 shows the initial *Simulink* graphic interface of the control diagram.

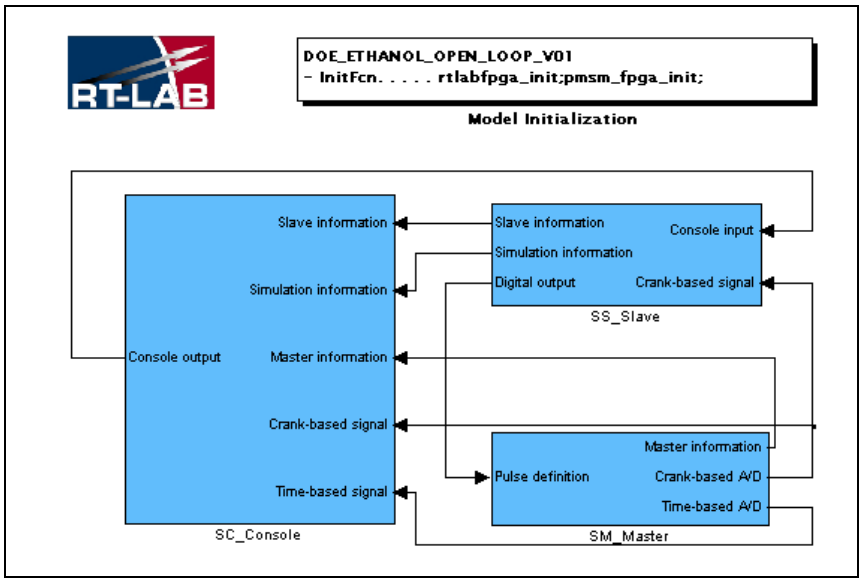

Figure 31:- Real-Time Control System Diagram for Opal-RT Controller

Task 2.6 Base Comparator Engine Procurement

'A state-of-the art direct injected spark ignited engine for the comparator engine will be procured. Along with the normal suite of thermocouples, the engine will be instrumented with in-cylinder pressure transducers and ionization sensors. The cylinder head will be modified by adding a port for the Visioscope to allow endoscopic spectroscopy. '

The 4 cylinder GM 2.2L Flex Fuel DI Ecotec selected as the conventional comparator engine for this project was procured, instrumented, fitted to into a dynamometer test cell at Argonne National Laboratories.

Figure 32:- Setup of the GM Ecotec Test Engine at Argonne National Laboratory.

It should be noted that the original Statement of Project Objectives proposed the use of a Visioscope to enable comparison of the ionization signal with combustion light intensity signals. Unfortunately, packaging restrictions of the 4 valve DI cylinder head precluded fitment of the Visioscope. Cylinder pressure transducers were fitted to each cylinder to derive combustion data such as heat release rates and phasing for subsequent validation of the ionization signals.

4 Phase 3 - Advanced Development

Task 3.1 Fabrication Of Injector Components

Fabricate / procure injectors and injection system hardware. A new generation of fine injector nozzles will be used in conjunction with the current injector design and hardware configuration. This should further improve the atomization quality and fuel vaporization characteristics of E85.'

The LPDI fuel injectors described in Phase 2 were fabricated. Additionally, current production HPDI injectors (Bosch Generation 2) were also procured.

Task 3.2 Fuel Injector Spray Characterization

'Particle sizes and spray patterns which emanate from the low pressure direct injector will be quantified. This work will be conducted in the Fuel Spray Laboratory and will make use of high speed photography systems, pulsed copper-vapor lasers and phase doppler anemometer. Spray characteristics inside and outside of the engine's combustion chamber will be quantified and compared with the results of the numerical simulations.'

Tests were completed for three different test injectors and three different test fuels, (gasoline, E50 and E85). The Bosch HDEV5 GDI injector was a late addition. Its inclusion was a substitution for the planned cold test work.

Injector spray imaging characterization tests

These tests were performed using MSU's Spray Imaging Bench. The testing involved visualization of spray structure using the Mie-scattered imaging method. Macroscopic spray characteristics such as the spray angle, bend angle, and spray tip penetration are analyzed and documented using custom designed image analysis and processing algorithms. An example of the results generated using the spray bench is shown in Figure 33.

Injector dynamic flow characterization tests

Dynamic flow measurement analysis is performed to evaluate the injection quantity per pulse at multiple pulse widths. The total injection amount is recorded based on a gravimetrical approach and the ensemble-average of the injected quantity at the corresponding pulse width is calculated. A flow curve is constructed and key flow data such as dynamic flow (injection quantity per injection count) and static flow rate at the rated pressure are obtained.

Injector drop sizing characterization tests

The line-of-sight spatially-integrated drop size characterizations were performed using a Spraytec / Malvern laser diffraction system. It is used to measure the drop size distributions and characteristic diameters. The representative drop diameters are SMD and Dv90. These two characteristic diameters are considered to be the mean drop diameter and the maximum drop diameter of the spray. The laser diffraction drop sizing measurement instrument consists of a 5mW, 10mm diameter laser transmitter with 623.8nm wavelength and a receiver with 36 detectors. Droplet sizes from 0.1 to 900 microns can be measured. The laser beam was positioned with the line of measurement centered at 50mm below the injector tip. To avoid vignetting and fuel spray onto the receiver, the injector was placed at a distance of 120mm from the receiver's Fourier lens. The injection frequency was set at 4Hz. All drop size measurements were performed under atmospheric conditions.

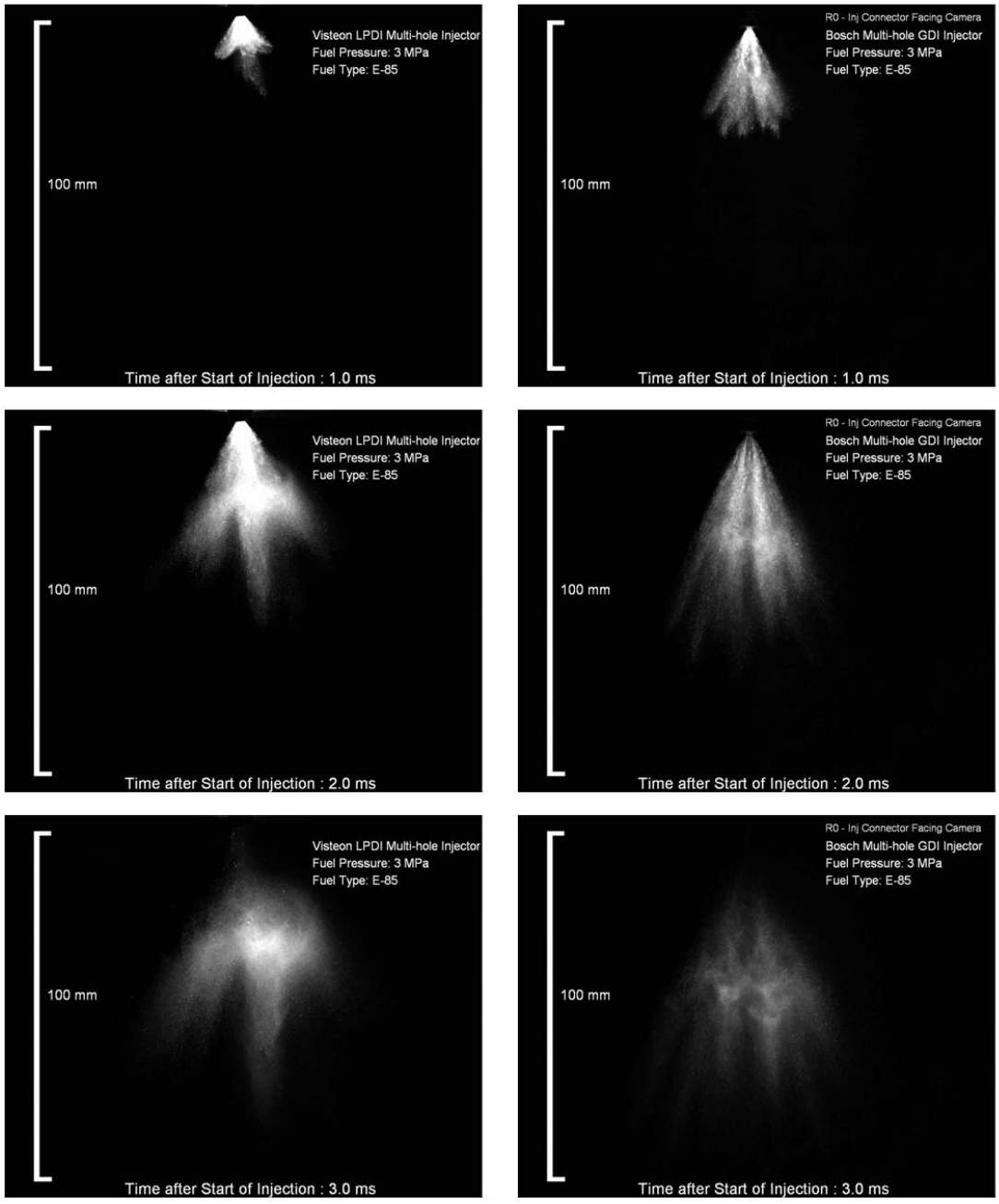

Figure 33:- Comparison of Injector Spray Performance using E85 Fuel @ 3MPa

Table 4**Error! Reference source not found.** shows a comparison of penetration, spray angle and bend angle.

Injector	Fuel	Pressure (MPa)	Penetration at 1.5 ms after SOI (mm)	Spray Angle at 1.5 ms after SOI (mm)	Bend Angle at 1.5 ms after SOI (mm)
Visteon LPDI Injector	n- heptane	3	41.0	71.2	n/a
	E85	3	41.6	72.4	n/a
Bosch Generation 2 GDI Injector	n- heptane	5	60.0	54.5	12.6
	n- heptane	10	71.5	51.5	13.0
	E85	3	52.7	52.8	12.3
	E85	5	58.2	54.8	10.9
	E85	10	70.0	56.5	11.8

Table 4:- Macroscopic Spray Imaging Characteristics Comparison

Table 5 lists the values of the representative diameters of the measured spray drop sizes.

Injector	Fuel	Pressure (MPa)	Dv10 (µm)	Dv50 (µm)	Dv90 (µm)	SMD (µm)	D43 (µm)
Visteon LPDI Injector	n-heptane	3	12.7	26.0	**44.0**	**20.1**	27.9
	E85	3	12.3	26.3	**49.2**	**20.8**	29.1
Bosch Generation 2 GDI Injector	n-heptane	3	10.4	23.6	**41.5**	**17.8**	25.2
	n-heptane	5	7.8	17.8	**29.0**	**13.3**	18.3
	n-heptane	10	5.3	12.3	**20.6**	**8.5**	12.8
	E85	3	11.5	24.9	**45.7**	**19.6**	27.3
	E85	5	8.7	20.1	**32.3**	**14.8**	20.5
	E85	10	6.1	15.3	**24.3**	**10.9**	15.4
Bosch HDEV5 GDI Injector	n-heptane	5	9.73	21.8	**48.39**	**16.88**	26.15
	n-heptane	10	6.63	14.61	**33.85**	**11.9**	17.38
	E85	5	10.92	25.45	**54.25**	**18.63**	29.6
	E85	10	7.06	14.67	**29.93**	**12.01**	16.98

Table 5:- Droplet Size Comparison

The level of atomization was found to be dependent upon many factors such as fluid properties, nozzle design, and most importantly, the injection pressure. The following observations were made:

- Droplet size decreased as fuel injection pressure increased. Higher injection pressure results in a larger inertia force to overcome the viscous effect of the fuel, leading to better atomization quality.
- Fuel property affects the fuel droplet size, which is consistent with test results for Task 3.2, especially with the low injection pressure. At 5MPa, the fuel droplet size of E85 is much larger than that of gasoline due to the higher viscosity of E85. However, when the pressure was increased to 10MPa, the difference was not as evident because under this condition, the pressure becomes the dominant factor. This is extremely important for selecting the injection pressure for the multi cylinder engine.
- Results indicated that little appreciable difference in spray characterization occurs when switching between the studied fuels (n-heptane & E85). Injection pressure being the most significant control factor.
- Higher injection pressures result in increased spray tip penetration, higher static flow rate, smaller droplet size and finer atomization, while spray- and bend-angle remain constant

Data supports selection of the Bosch HDEV5 injector in the Phase 4 multi cylinder DI3 engine tests.

Task 3.3 Ignition System Build

'Procure and fabricate ignition system hardware'.

Due to the DI3 engine's specification (high compression ratio, gasoline direct injection, and compound boosting), the in-cylinder compression pressure will be high. Therefore, an ignition system to provide higher spark ignition energy (for robust ignition) designed in the previous phase was constructed, providing 37kV (@ 25pF) and spark energy of 45mJ.

A feedback knock and combustion stability control system, using proprietary ionization circuitry provided a high quality ionization current signal. The closed-loop knock control is essential to support high compression ratio operation of the E85 optimized engine. The electronics on the circuit include an ignition driver and ionization signal conditioning to provide a feedback signal, dwell current, spark duration and combustion ionization information, see Figure 34.

Figure 34:- Engine Control Interface, Including Ion Sensing Ignition System and LPDI Injector Driver

Task 3.4 Single Cylinder Engine Tests

'The entire team will meet periodically to evaluate which experiments related to the injection of ethanol are deemed to be the most important. These experiments will be tailored to meet the goal of developing an E85 fueled engine which has the performance and fuel consumption equivalent on a per volume basis of the gasoline fueled version of the engine which it is replacing'.

Subtask 3.4.1 Optical Engine Tests

'The first set of experiments will be conducted in the engine assembly with full optical access (both cylinder liner and piston are transparent). When used in conjunction with numerical simulations under Task 2.2, we will be able to assess the quality of fuel targeting and the evaporation characteristics of the injector and combustion system. Optical engine experiments will be conducted with the heavy-duty optical engine assembly allowing one to operate at realistic speeds and loads'.

Subtask 3.4.1.1 & 3.4.1.2 Gasoline and E85 Tests

"Performance testing of the gasoline (and E85) version of the target engine will be conducted using the optical version of the single cylinder engine. High speed photography and pressure diagnostics will be used to quantify details of engine performance based on the critical points identified in the performance tests of the single cylinder metal engine."

An optical engine was utilized, in conjunction with a high-speed camera to perform in-cylinder observations of the fuel injectors characterized in task 3.2. The optical engine enables study of the spray pattern dynamics in the presence of representative airflow and fluctuating in-cylinder pressures (through mechanical compression). Optical testing was performed for both non-firing and firing (ignition and combustion) cases. Only short periods of firing testing can be achieved due to the physical limitations of the optical cylinder liner.

Initially non firing testing was conducted using the Visteon LPDI system operating at 3MPa pressure and the Bosch Generation 2 HPDI system at pressures of 5 & 10MPa, engine speeds of 1500 and 2000rpm, with Gasoline, E50 and E85 and a flat top piston. The flat top piston was fabricated and used due to delays with the availability of the pentroof quartz insert representative piston.

When the representative piston and the new Bosch HDEV5 injector became available, testing had already established that the Bosch Generation 2 HPDI injector outperformed the Visteon LPDI in non-firing testing. Therefore further testing explained later on in this section concentrated on comparing performance of the two Bosch injectors.

Non Firing Optical Testing

A key area of study has been the degree of fuel spray impingement on cylinder walls and piston crown, as this can have a significant effect on HC emissions and smoke. Observation of high-speed camera footage allows subjective comparison of different test conditions

The optical engine tests have also enabled an assessment to be made of the in-cylinder injector spray and mixture formulation CFD modeling completed in Phase 2. The results were encouraging, suggesting that the model offers reasonable fidelity. Figure 35 demonstrates the results achieved for each of the studied injectors.

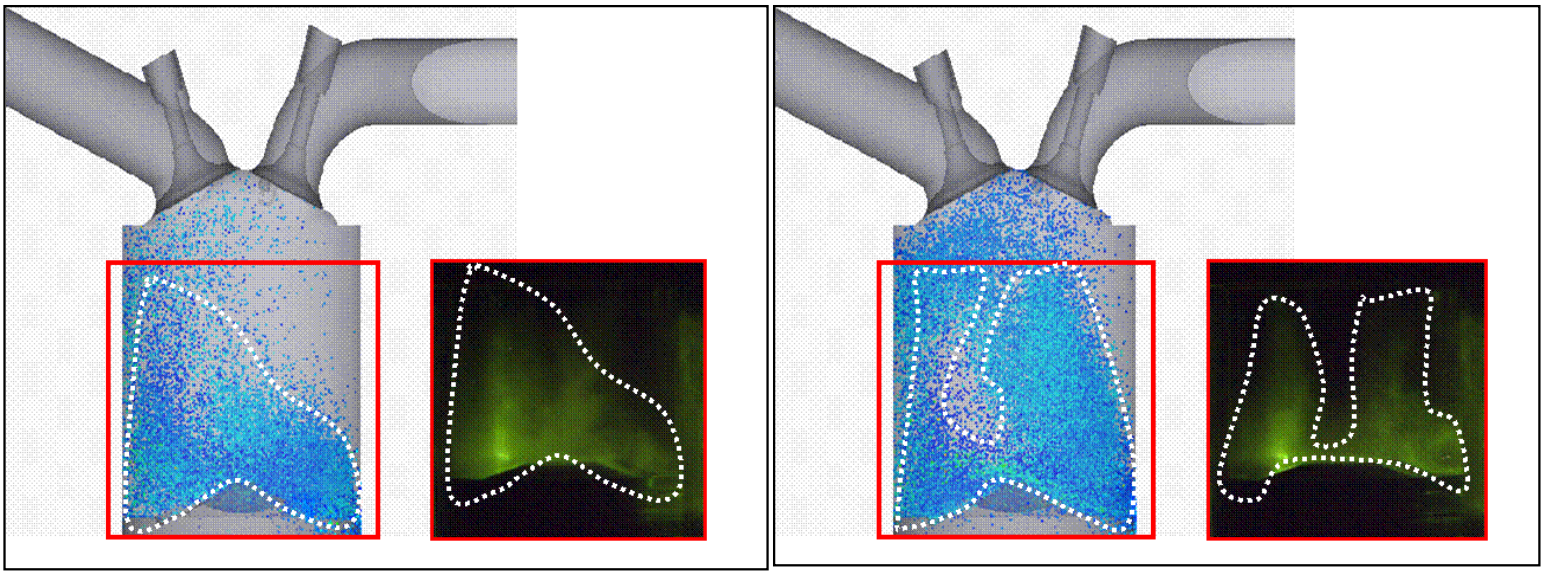

Figure 35:- Fuel Mixture Formation Comparison (Modelling and Experiments)
(Left: HPDI Multi-hole injector at 10MPa; Right: Visteon LPDI injector at 3MPa)
(Fuel: E85; Image reported at 150°BTDC)

- Results of the fuel spray tests indicate that both injectors had similar drop size distributions and spray geometry at the rated injection pressures. Impingement on piston crown is 17% higher with the LPDI injector operating at 3MPa, than the Bosch Generation 2 HPDI injector operating at 5 or 10MPa.
- A study of split injection (i.e. 2 injection pulses per cycle) had a positive effect in reducing the level of fuel impingement, while delivering adequate fuel quantity and mixture distribution.
- Fuel blend was not found to significantly affect air-fuel mixture formulation. Gasoline was observed to achieve slightly higher spray tip penetration and greater levels of impingement.
- Cold flow tests have proven that the Bosch Generation 2 HPDI injector offers less overall fuel impingement and slightly better droplet atomization than the LPDI injectors operating at 3MPa. The relative performance of these two injectors were further studied during the firing tests, to ascertain the effects on combustion.

Firing Test Experimental Setup

The test engine is a four-valve (two intake and two exhaust valves) 0.4 liter single-cylinder spark-ignition engine with a bore diameter of 83 mm, stroke length of 73.9 mm, and compression ratio of 9.75 : 1 based upon MAHLE's 3 cylinder DI3 research engine.

Figure 36**Error! Reference source not found.** shows the experimental rig for combustion visualization. An optical piston is used to provide the optical access to the cylinder. A view of the combustion chamber geometry showing intake and exhaust valves, DI injector, spark plug and the pressure transducer is shown in Figure 4.

Error! Reference source not found.

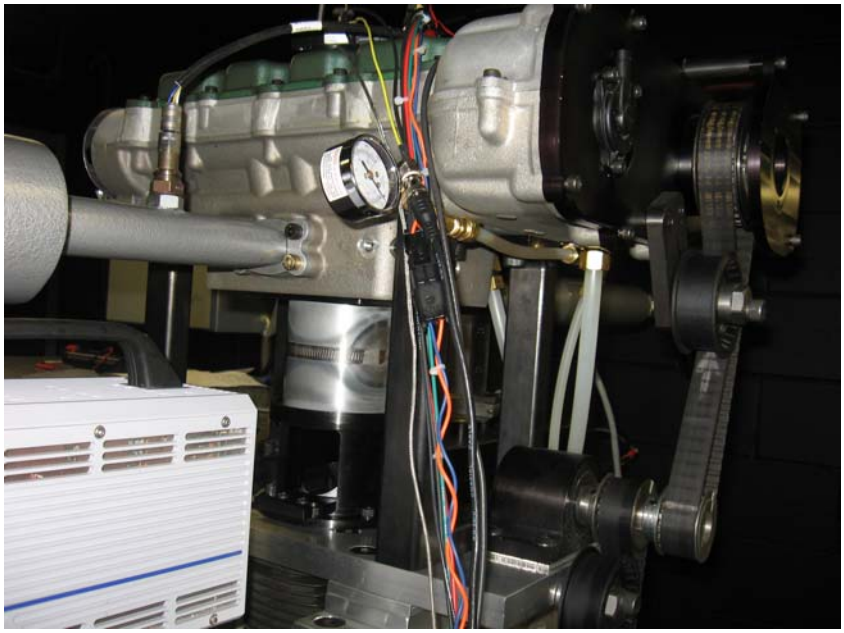

Figure 36:- Single Cylinder Optical Engine - Experimental Rig

In the setup, 0^{o} crank angle corresponds to TDC of the compression stroke, and -180^{o} CAD corresponds to BDC of the intake stroke, which is frequently referred to as 180^{o}BTDC in the rest of this report. All experiments were performed at 1500rpm engine speed with a part-load condition of 0.45bar MAP. The part load test point chosen was seen as being most representative of the DI3 engine's part load operation within the confines of the optical engine's safe operational envelope. Ignition timings were determined for each test point based on MBT timing by performing a sweep of spark timing and finding the timing that provided the maximum mean IMEP.

The effects of the following were examined:

1. Fuel injection pressure
2. Fuel injection timing
3. Air-fuel ratio, fuel type
4. Split vs. single injection.

To study injection pressure, two different injectors were used; for the 3MPa pressure case, an 8 hole LPDI injector was used, and for the 5 and 10MPa cases, a 7 hole HPDI injector was used. For testing of all other parameters (i.e. injection timing, fuel type, etc.), the HPDI injector was used with an injection pressure of 5MPa.

In all tests except those for air-fuel ratio effects, lambda (λ) was maintained at 1. In all tests except those for effects of injection timing, the single-pulse 210°BTDC injection timing was used. For the split injection cases, the first pulse was started at 210°BTDC, and the start of the second pulse was defined to be 90 CAD after the start of the first pulse at 120°BTDC; the pulse widths of each were set to be equal.

Parameter	Description
Fuel Type	gasoline, E50 and E85
Injection Pressure	3MPa (LPDI injector) 5 and 10MPa (BOSCH Generation 2 injector) 5 and 10MPa (BOSCH HDEV5 injector)
Injection Timing	240°, 210° and 180°BTDC
Number of Injections	single and split
Air Fuel Ratio	λ = 1 (stoichiometric) λ = 0.85 (rich) λ = 1.20 (lean)
Operating Condition	1500rpm, 0.45bar MAP load (same for all tests)

Table 6:- Test Parameters for Combustion Visualization Experiments

Combustion images were captured with a Photron APX-RS non-intensified high-speed CMOS camera system. The camera captures 200 frames of each of 40 consecutive cycles of firing, and during each cycle it is initially triggered in synch with the ignition spark signal so that each cycle is recorded from ignition timing through the end of combustion. The fuel injection pulse signal was adjusted for each test point in order to achieve the desired air-fuel ratio. Due to optical engine limitations, injection signal was cut off as soon as the camera finished recording the specified number of cycles.

In-cylinder pressure was recorded within one degree of crank angle resolution with a Kistler piezoelectric pressure transducer. This signal results in averaged in-cylinder pressure data which is then used to evaluate the engine performance through calculation of IMEP, peak pressures, mass fraction burned (MFB), etc. MFB and burn durations were determined using the well-known Rassweiler-Withrow method [10]. A linear model for the polytropic index during the combustion process was used to evaluate the pressure change due to the volume change [11].

Results and discussion for flat optical piston

Combustion visualization and in-cylinder pressure analysis results can provide useful insight into what happens over the combustion period by looking at the flame sizes, shapes, and textures. The images presented are a two-dimensional representation of the three-dimensional flame development inside the cylinder. Intake valves are located near the top of each image. For each variable examined (i.e. injection timing, injection pressure, air-fuel ratio, etc.), a series of images at various locations after ignition timing (AIT) are used to show the flame development and growth.

It is important to stress that due to the nature of optical engine setups, it is not useful to try to draw firm conclusions about performance based on the peak pressure and IMEP data recorded for each run. Because there is no cooling system or oil lubrication system for the cylinder, the engine is only able to be run for a short time, it never is truly able to reach a “steady state” condition. The actual operating temperature of the engine cannot be easily controlled, meaning that trying to compare pressure data between one test point and another is relatively meaningless. The pressure data is valuable for understanding what is being seen in the captured video images.

Effect of Injection Pressure

Figure 37 shows the stoichiometric combustion images of gasoline at four different CAD locations after ignition timing under the three tested injection pressures at ignition timing based on MBT and injection timing of 210°BTDC.

Flame growth is much slower with the LPDI injector at 3MPa than the HPDI injector at 5MPa which is in turn slower than the HPDI injector at 10MPa. As expected, the early flame development starts close to the in-cylinder central location (near the spark plug). The bright rich spots visible at 10MPa may be due to droplet burning, this may be due to faster spray penetration at this higher injection pressure, and hence more liquid-phase gasoline impingement on the piston top. Most multi-component fuels exhibit a tendency towards this characteristic. In the LPDI images, flame formation is much less uniform than for the HPDI 5MPa case; this could be due to better mixing being achieved with the HPDI injector.

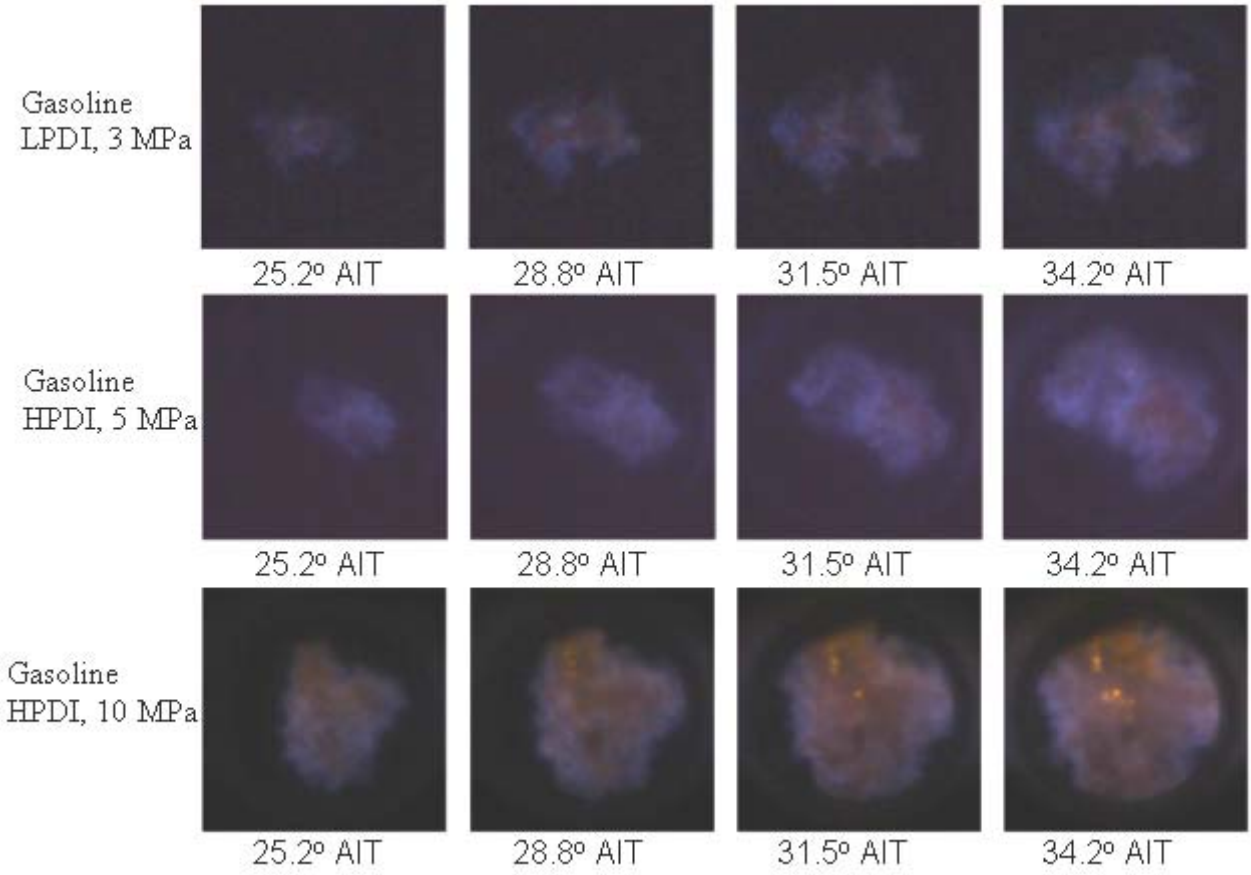

Figure 37:- Flame Images of Gasoline with Different Injection Pressures (λ=1, Ignition Timing = 35°BTDC)

Peak in-cylinder pressure was seen to increase and the crank angle at which the peak in-cylinder pressure occurred advanced with increasing injection pressure. This is consistent with the faster flame formation seen in the combustion images.

Effect of Injection Timing

Figure 38 results show that as injection timing advances, flame growth is faster, possibly due to achieving a more homogeneous mixture with early injection because of more mixing time.

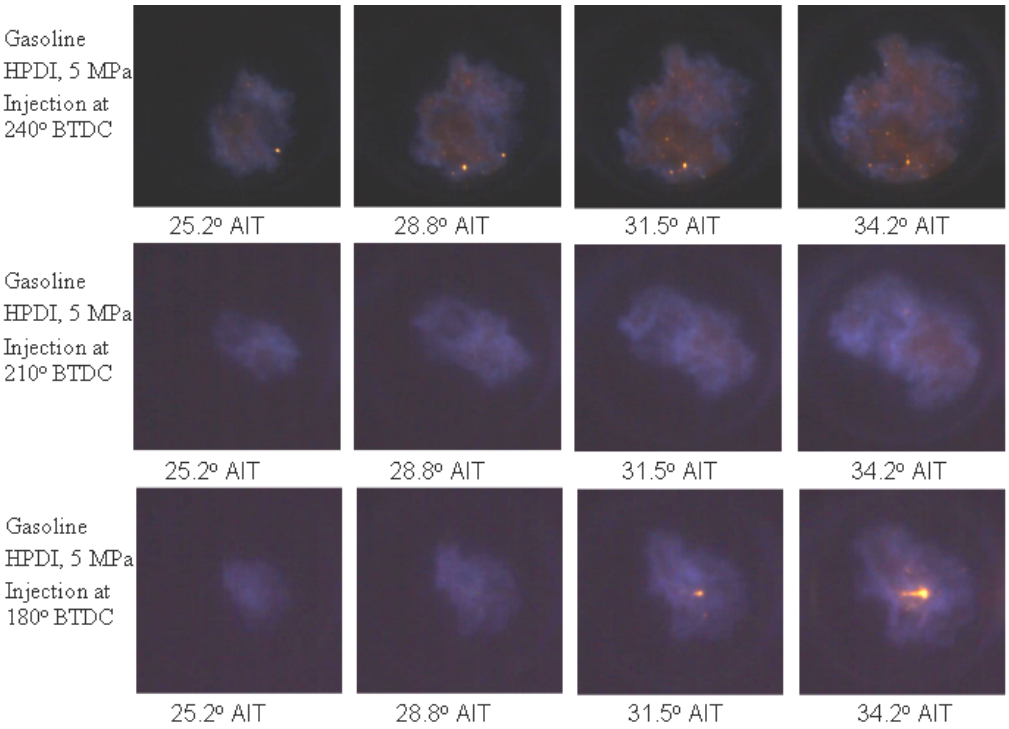

Figure 38:- Flame Images of Gasoline with Different Injection Timings (HPDI Injector at 5MPa, λ=1, Ignition Timing 35° BTDC)

Testing Using the Design Representative Pent- Roof Optical Piston

Further firing tests were performed using the target optical piston. This piston, shown in Figure 39, features a higher compression ratio than the flat piston due to the pent-roof design; motoring trace calculations put the effective compression ratio of around 12.3:1.

At this stage, the decision had been agreed with NETL to incorporate testing of the now available Bosch HDEV5 injector in lieu of cold testing.

The Bosch Generation 2 and Bosch HDEV5 HPDI injectors were tested with this piston.

Figure 39:- Target Optical Piston

Summary Results and Discussion for Target Optical Piston

Effect of Injector Type and Injection Pressure

The two Bosch injectors were tested at both 5 and 10MPa injection pressure.

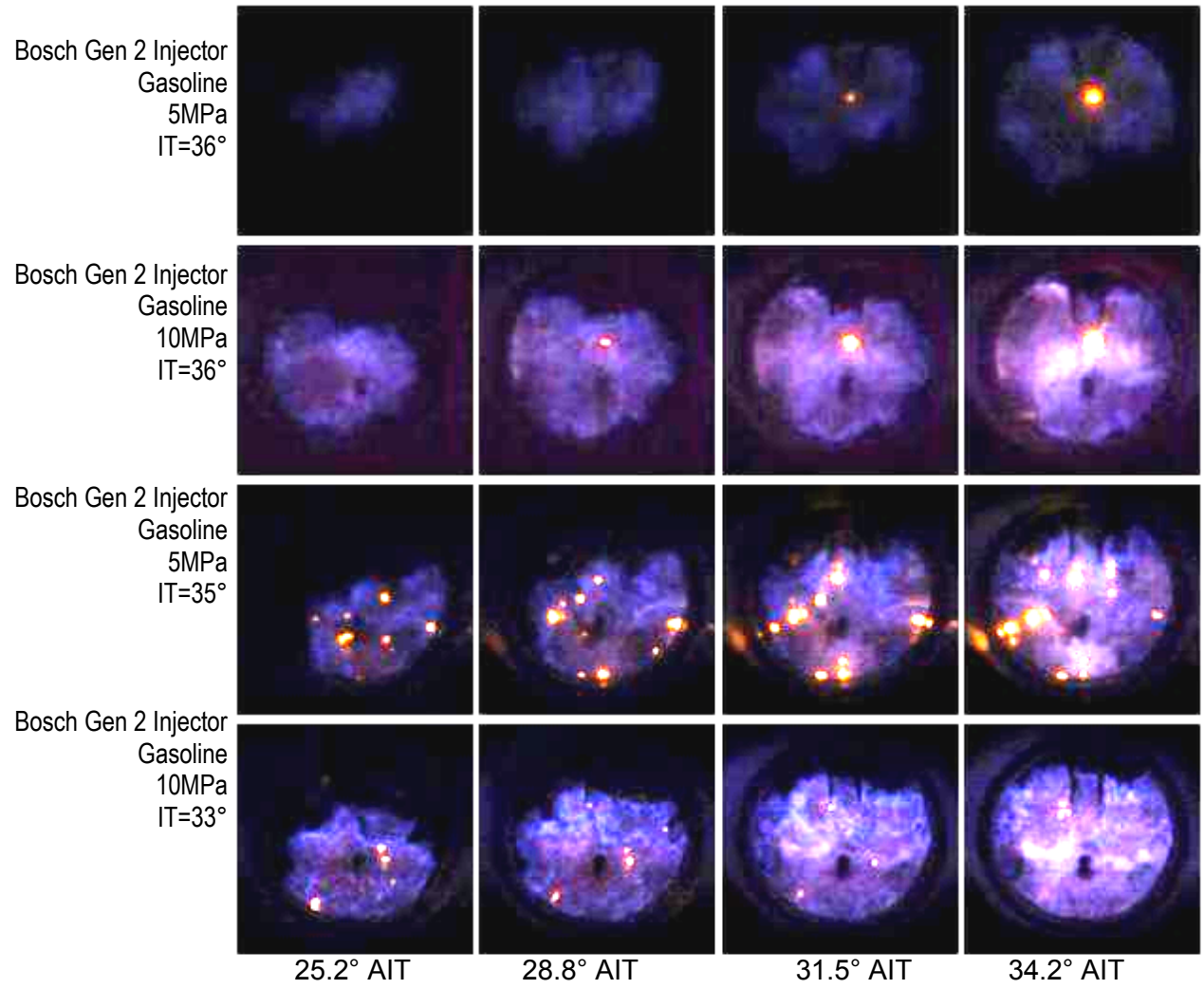

Figure 40:- Flame Images of Gasoline with Different Injectors at Different Injection Pressures (λ=1, MBT Ignition Timing)

Figure 40 shows images of stoichiometric gasoline combustion using the target optical piston. The Bosch Generation 2 and Bosch HDEV5 injectors were both used at two different injection pressures, 5 and 10MPa. For both injectors, early flame growth is faster with the higher injection pressure. The HDEV5 injector exhibits much faster flame growth at 5MPa than the Bosch Generation 2 injector; at 10MPa, the growth rate appears to be equal for both injectors.
Note the presence of many orange spots in the 5MPa HDEV5 case; these are likely droplets and have not atomized fully by the start of combustion and are contacting the piston face. These spots do not appear as vibrantly in the 10MPa case, pointing to better atomization of the fuel at this higher pressure. Also of interest is the large orange glow near the injector location in the Bosch Generation 2 injector cases; this is believed to be due to the low velocity of the last

small amount of fuel to leave the injector as it closes—it may create a rich pocket that does not mix well near the injector. This trend is seen in many of the cases with this injector.

Effect of Injection Timing

Figure 41 shows images of stoichiometric gasoline combustion using the target optical piston at three different injection timings for the Bosch Generation 2 injector; Figure 42 shows the same for the Bosch HDEV5 injector. In previous flat piston tests, a 210° injection timing was determined to be optimal; the results for an optimal timing are not as clear in these tests.

For Bosch Generation 2 injector tests, the 210° timing does exhibit a clean and even blue flame with few orange spots aside from the center rich area near the injector. The earlier 180° timing shows a less even flame with a few more small visible hot spots; this could point to a less distributed mixture due to less time in the cylinder and also injection into a fairly low-swirl / tumble environment with the piston at BDC. The cause of the orange flame color for the 240° case is not known; it may be due to fuel being sucked rapidly toward the piston face while the piston is moving downward rapidly at the time of injection, but the actual cause is unknown. This case also produced the highest peak pressures and shortest burn duration by a significant amount.

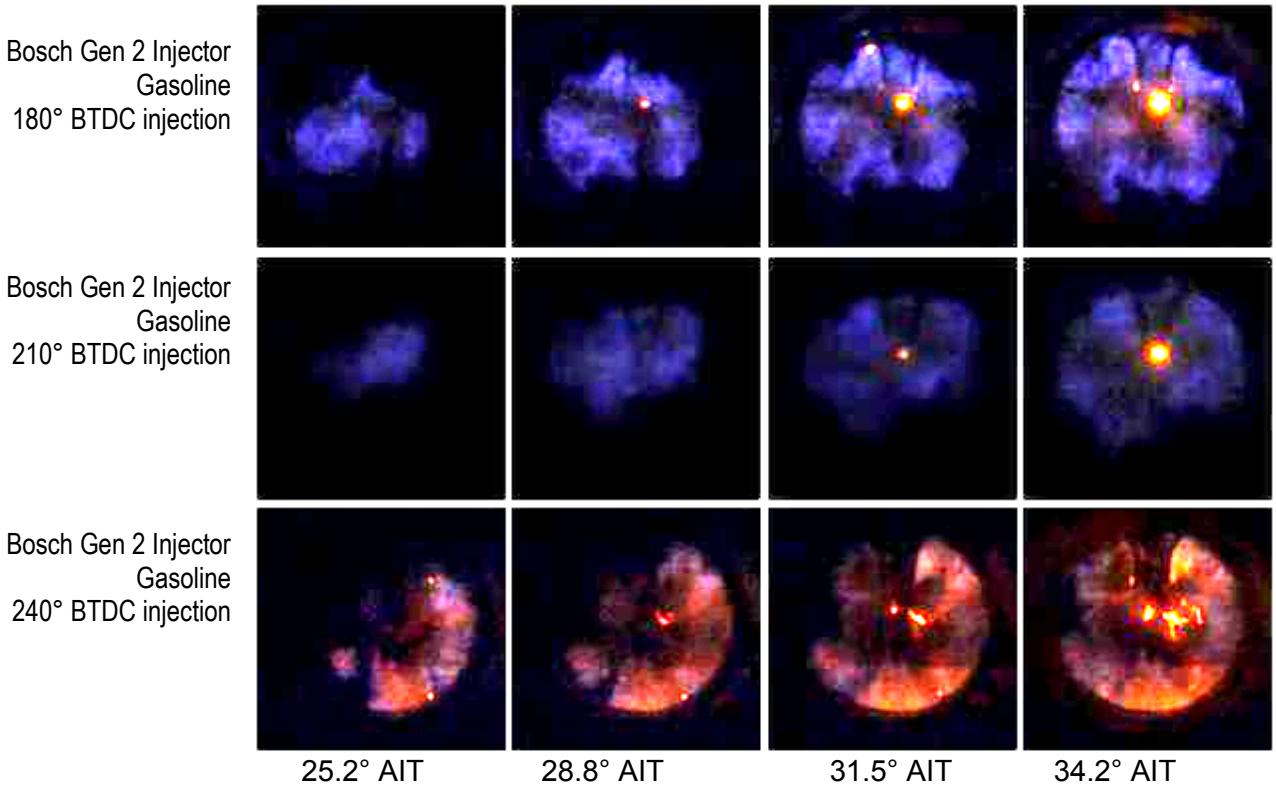

Figure 41:- Flame Images of Gasoline at Different Injection Timings with Bosch Generation 2 Injector (λ=1, MBT Ignition Timing)

The images for the Bosch HDEV5 injector show different trends. The 210° case shows many droplets burning with possible piston impingement while the 240° case shows a much more even blue flame, faster flame growth, and fewer hot spots. The 180° case shows much slower growth with no impingement but possibly poor mixing as evidenced by the more unevenly

shaped flame; it yielded much lower peak pressure and a longer burn duration than the other cases. It was difficult to obtain smooth engine operation using the 180° injection timing with this injector—every attempted run resulted in a number of misfires while all other cases with this injector ran with no such difficulties.

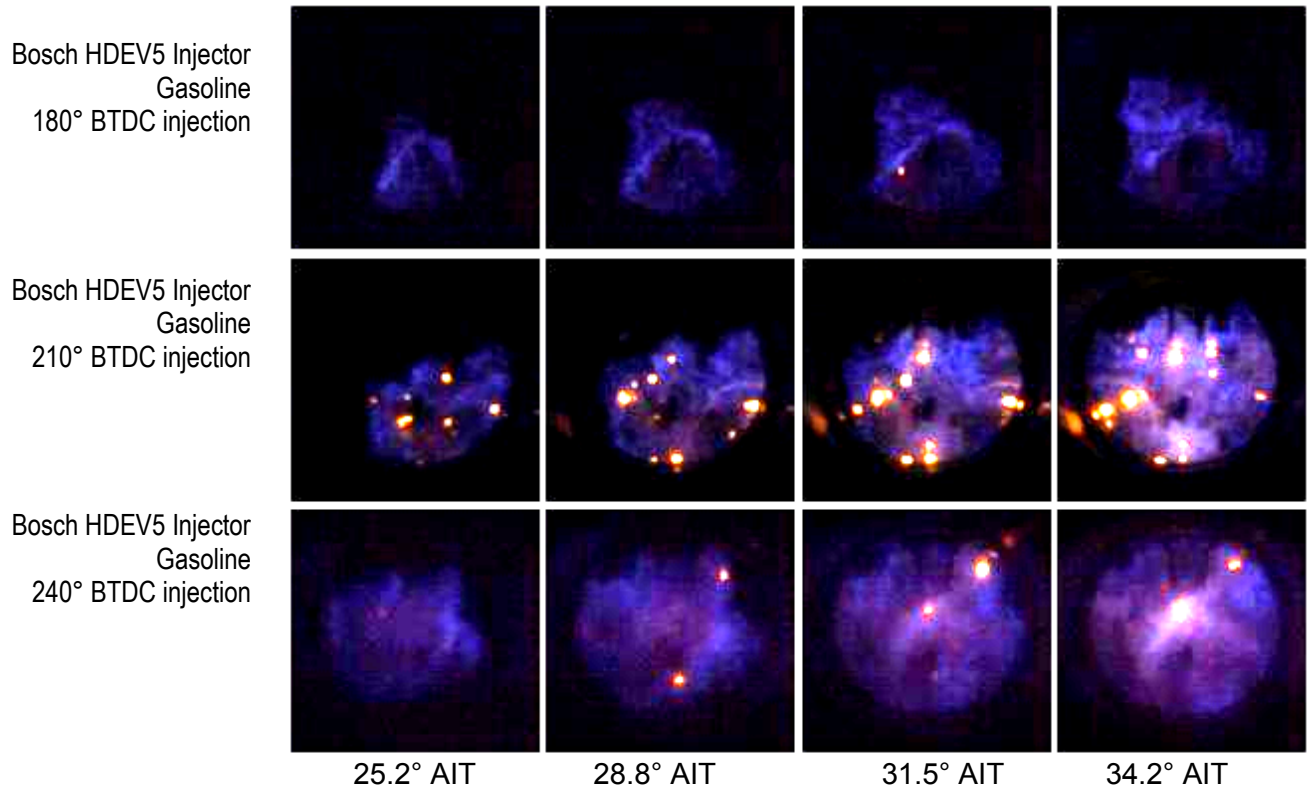

Figure 42:- Flame Images of Gasoline at Different Injection Timings with Bosch HDEV5 Injector (λ=1, MBT Ignition Timing)

Subtask 3.4.2.4 Results and discussion for Bosch HDEV5 injector, flat optical piston

Further tests with the flat piston were performed with the new Bosch HDEV5 injector that was used in some of the target piston tests. The test points used here were similar to those run with the Bosch Generation 2 injector and flat piston in the previous phase of the project. Runs with E50 and E85 were included in these tests.

Effect of Ignition Timing

Figure 43 shows flame images of stoichiometric gasoline combustion across varied ignition timings with the Bosch HDEV5 injector, flat piston, 5MPa injection pressure, and 210°BTDC injection timing. It must be noted that for each case, the images at the same angle after ignition occur at different actual crank angles. Thus, it is difficult to use these to draw conclusions about how the flame growth and engine performance are related. However, some general observations can still be made.

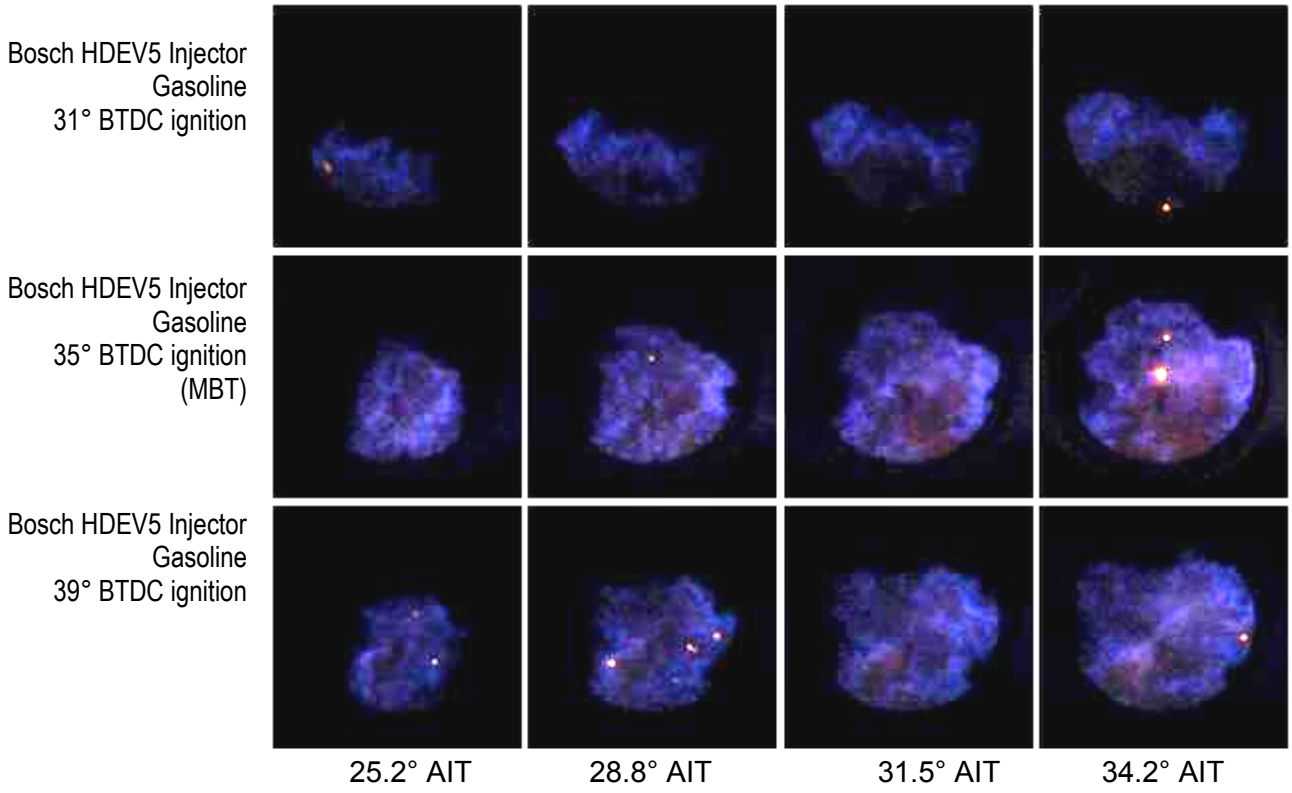

Figure 43:- Flame Images of Gasoline with Varied Spark Ignition Timing
(λ=1, Injection Timing=210°BTDC, 5MPa Injection Pressure, Flat Piston and Bosch HDEV5 Injector)

The later spark timing results in significantly later combustion and slower flame development—while the 10% burn location retards by 5 CAD compared to the 35° ignition timing case (very close to the 4 CAD difference in ignition timing), the 90% burn retards by a much larger 13.5 CAD; though combustion starts relatively similarly, it slows significantly throughout the expansion stroke compared to the earlier ignition timing cases. The images for the MBT case and the 39° ignition timing case are remarkably similar—the flame growth is very even and similarly shaped and sized at corresponding after ignition angles.

Effect of Air-Fuel Ratio

Figure 44 shows flame images of rich, stoichiometric, and lean gasoline combustion using the flat piston and Bosch HDEV5 injector at 5MPa injection pressure. The results show significantly faster, larger and more intense flame growth for the rich case, and much slower and less intense flame growth for the lean case. An interesting observation in the difference between lean and stoichiometric is that while the lean flame actually grows quicker initially, this faster growth rate, likely caused by the earlier spark timing, quickly slows down compared to the stoichiometric case and ends up with a significantly longer burn duration. Also notable is that the typical hot spot near the injector tip after the flame has developed is not visible in the lean case—it does indeed appear in images later in the cycle not seen here.

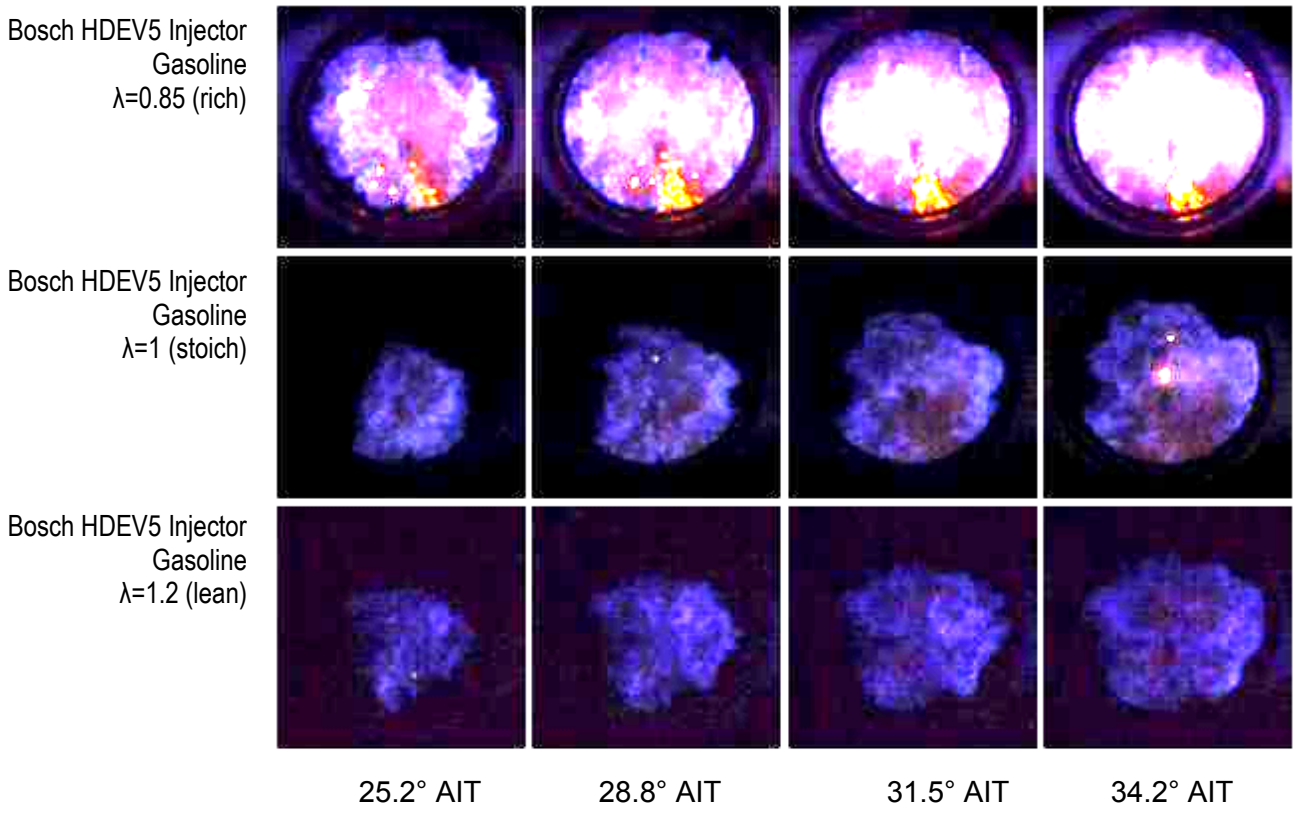

Figure 44:- Flame Images With Varied Air-Fuel Ratios - Gasoline Combustion (210° Injection Timing, MBT Ignition Timing - 5MPa Injection Pressure - Flat Piston Bosch HDEV5 Injector)

Effect of Fuel Type

Figure 45 shows flame images of the combustion of three different fuel types, gasoline, E50, and E85 with the flat piston and Bosch HDEV5 injector at 5MPa injection pressure. The images show the very different characteristic flame colors of these three fuels. One thing that becomes a difficulty with the vivid orange flame of E85 is identifying hot spots—it is not easy to tell whether bright area are impingement locations, rich locations, or simply well developed areas of a stoichiometric flame. The E50 images show a distinctive flame that looks very much like a combination of the gasoline and E85 flames, but the large bright orange areas point to possible mixing issues—these spots did not tend to simply burn in one place, but rather they began to move rapidly throughout the cylinder during the video of the full combustion cycle, leading one to think they are not impingement but rather small areas of poorly-mixed spray. Both of the ethanol blends performed smoothly—cycle-to-cycle variability was very small and no misfires were ever observed.

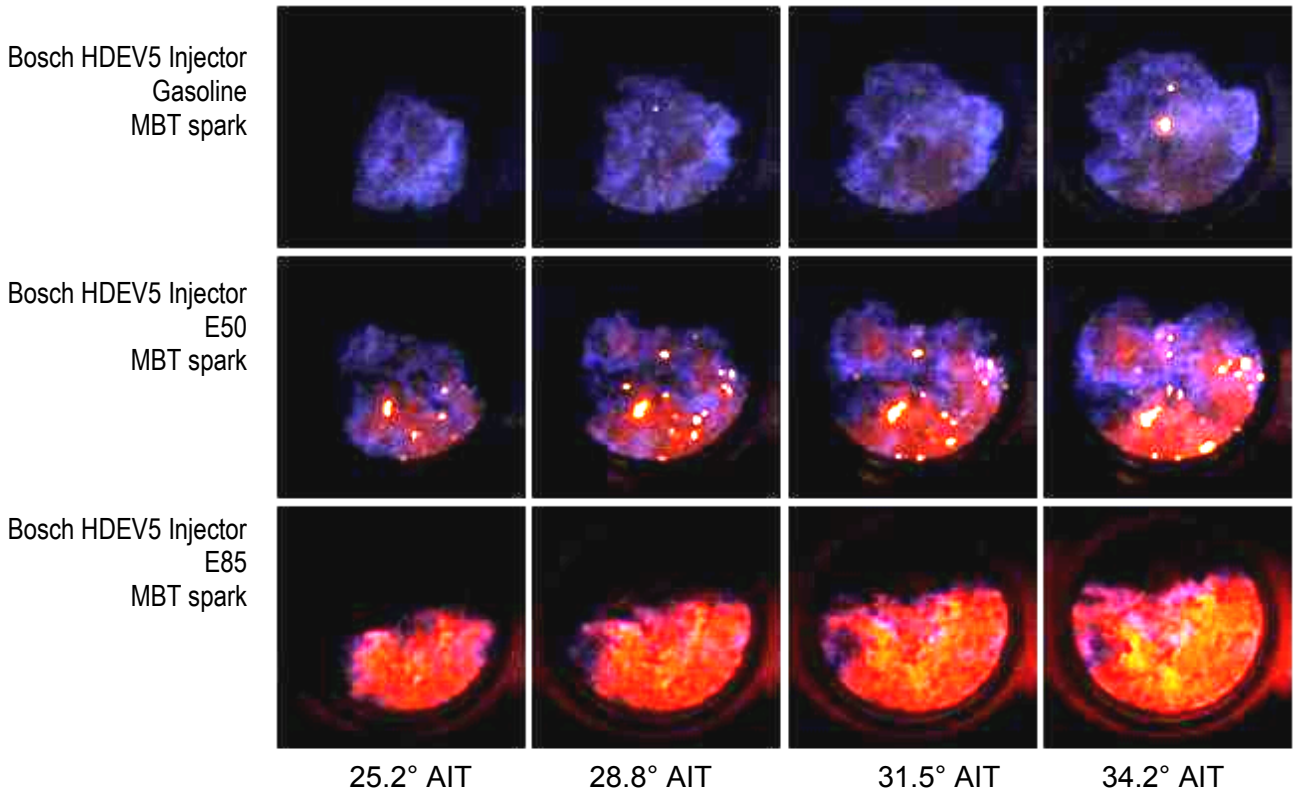

Figure 45:- Comparison of Flame Images of Gasoline, E50 and E85 (210° Injection Timing, MBT Ignition Timing - 5MPa Injection Pressure - Flat Piston Bosch HDEV5Injector)

Effect of Split Injection

Images comparing the flames of single and split injection pulse strategies for gasoline, E50, and E85 are seen in Figure 46. The single injection images are the same images found previously in Figure 45. For all three fuels, flame growth was slower, and the flames often appear to be more uneven and of lower intensity with split injection. It is possible that the second pulse of fuel simply does not have enough time to mix well in the cylinder before the start of combustion. This was also evident in the difficulty of running split injection with E85, this case exhibited much higher cycle-to-cycle variability and never ran without numerous misfires. The same hot spots visible in the single-pulse E50 case are again visible in the split case.

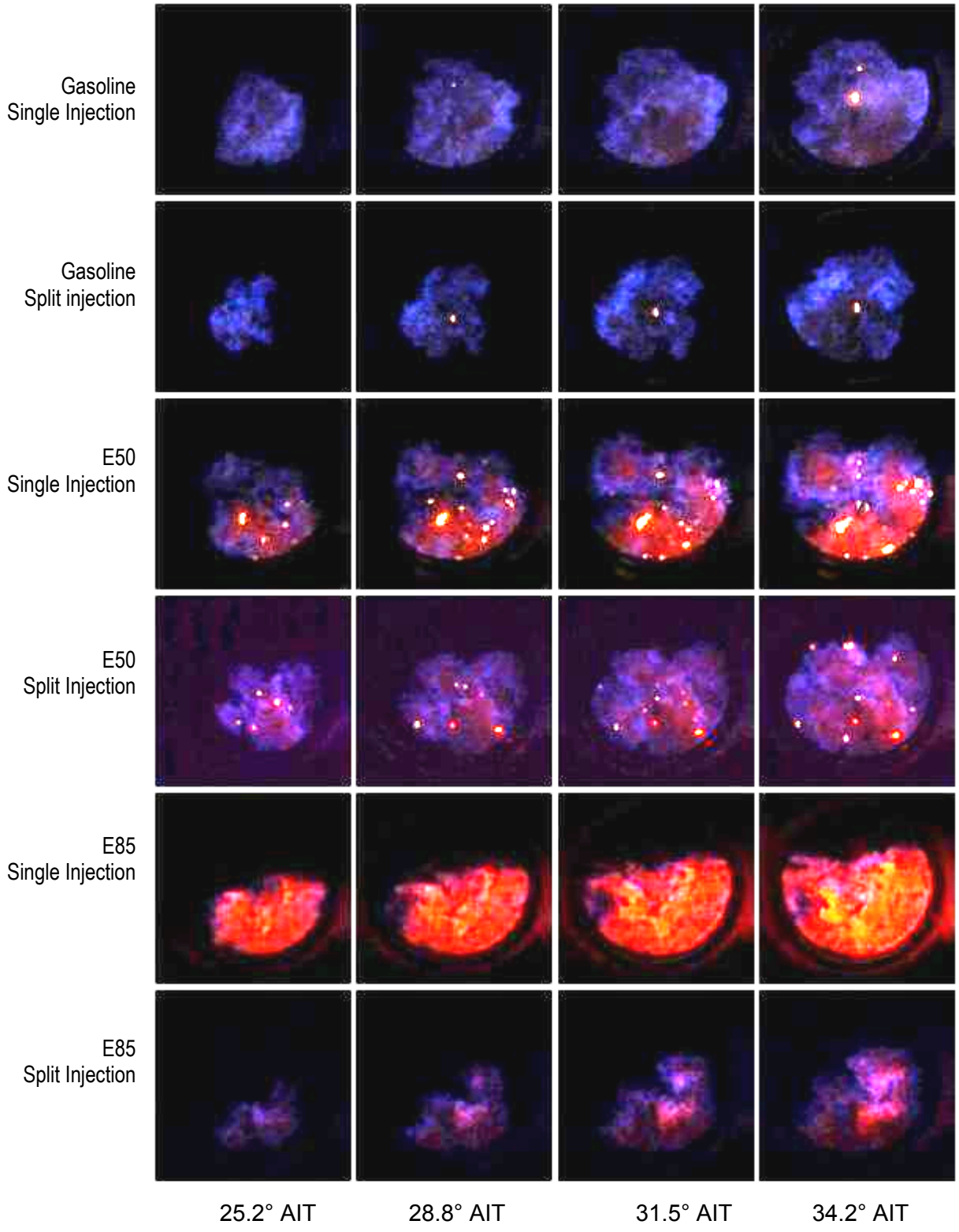

Figure 46:- Flame Images of Split vs. Single Injection Pulse For Three Different Fuel Types (MBT Ignition Timing - 5MPa Injection Pressure - Flat Piston - Bosch HDEV5 Injector)

Effect of Piston Type

Figure 47 shows comparisons of gasoline flame images of the target piston and flat piston at both 5 and 10MPa injection pressures. The target piston cases both show faster flame growth along with possible droplet impingement issues on the cylinder; impingement is much more evident in the 5MPa case.

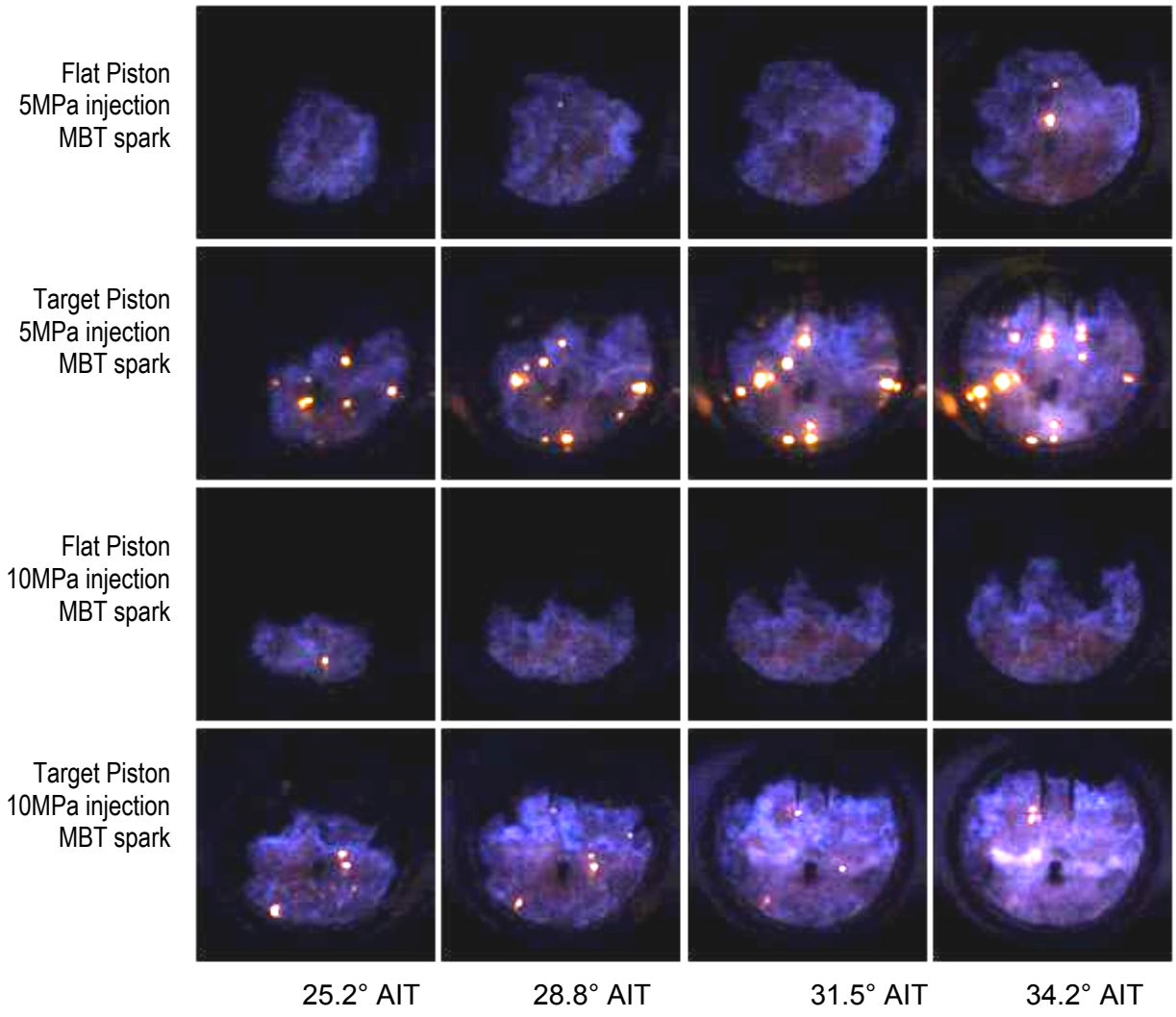

Figure 47:- Flame Images of Gasoline, Flat vs. Target Piston at Different Injection Pressures (MBT Ignition Timing, Bosch HDEV5 Injector)

Trends Observed

Injection Pressure

Combustion images generally showed that flame growth rate increased with higher fuel injection pressure, because higher pressure leads to smaller droplet size, better mixing, and less piston face impingement if the spray pattern is optimized.

Injection Timing

Generally combustion images showed that flame growth rate increased with the advancement of injection timing. Under certain conditions, late or early injection timings produced bright spots. This may have been due to impingement on the piston top at these injection timings.

Air-Fuel Ratio

Combustion images showed flame growth speed to increase with reducing AFR.

Fuel Type

Combustion images generally showed very similar flame growth rates for all three fuels. All used very similar MBT spark timings. Ethanol blends generally displayed slightly faster initial flame growth than but similar overall burn duration compared to gasoline. Ethanol blends ran extremely smoothly with the Bosch HDEV5 injector with very little cycle-to-cycle variation.

Injection Pulse

Combustion images showed that split injection generally slowed flame growth compared to the single injection case. Split injection was more likely to cause numerous visible hot spots and an uneven burn, under these conditions steady operation was difficult to achieve—cycle-to-cycle variation was large.

Compression Ratio / Piston Design

The higher compression ratio pent roof piston tended to generate a faster initial flame development, but overall longer burn and greater likelihood of piston impingement.

Conclusions

In general, the Bosch HDEV5 injector outperformed the Bosch Generation 2 injector in terms of smooth operation and even flame growth.

Task 3.4.2 Single Cylinder Metal Engine Testing

The metal components of the single cylinder engine will be configured to make use of the knowledge learned in the initial optical engine experiments in subtasks 3.4.1, the injector and combustion chamber will be reconfigured and the single cylinder metal engine experiments will be performed. Extensive testing will be conducted over the range of conditions which it is possible to operate this single cylinder engine. We expect that these iterations will continue for three to six months until reasonable performance is obtained from the single cylinder engine operating on E85.

Five test points were examined using the single cylinder metal engine in order to understand the flexibility and behavior of the two different injectors using three different gasoline-ethanol fuel blends. Figure 48 shows images of the test cell setup used for this study.

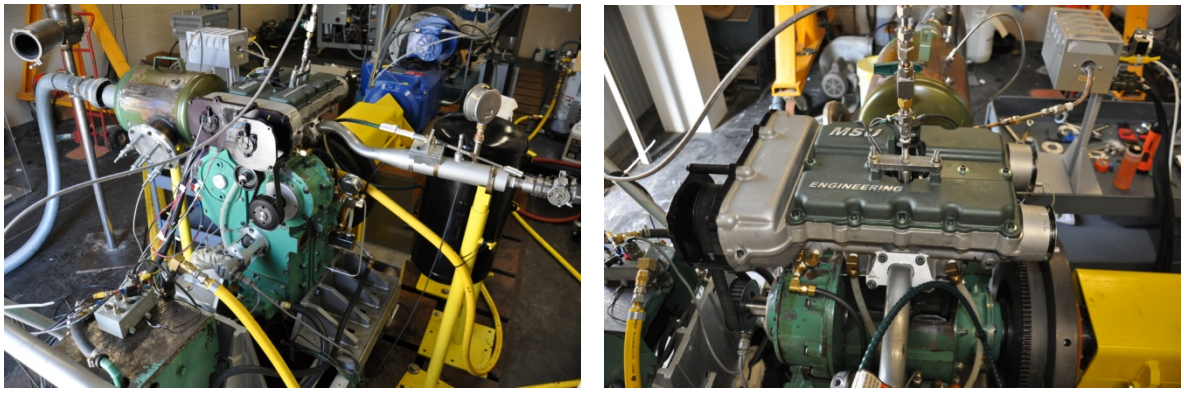

Figure 48:- Single-Cylinder Metal Engine Test Cell.

The five load / speed points tested were as follows:

- 5.6bar IMEP @ 1500rpm (medium load)
- 4.4bar IMEP @ 2000rpm (medium load)
- 3.8bar IMEP @ 1500rpm (low load)
- 3.2bar IMEP @ 2000rpm (low load)
- Wide Open Throttle @ 1500rpm (high load)

Injector Comparison

The Bosch Generation 2 and Bosch HDEV5 injector were each run at the 1500 and 2000rpm mid-load points. For each injector, all three fuels were used at the 1500 rpm mid-load point (approximately 5.6bar IMEP) at both 5 and 10MPa injection pressures with three different injection timings (180°, 210°, and 240°BTDC). At the 2000rpm mid-load point (approximately 4.4bar IMEP), only E0 and E85 were tested with both injectors; again, the same sweeps of injection pressure and injection timing were performed.

COV of IMEP

A significant difference in COV of IMEP between the two injectors was consistently evident under all conditions tested. With the Bosch Generation 2 injector, COV of IMEP values tended to run in the 2.5 to 3.5% range (generally lower at 10MPa injection pressure and higher at 5MPa), while the Bosch HDEV5 injector ran smoother with COV of IMEP values closer to the

1.5 to 2.0 range (Figure 49). This points to more consistent fuel evaporation on a cycle-to-cycle basis with the Bosch HDEV5 injector. This trend also falls in line with the previous study that the Bosch HDEV5 injector yielded smaller droplet sizes than the Bosch Generation 2 injector, particularly with E85.

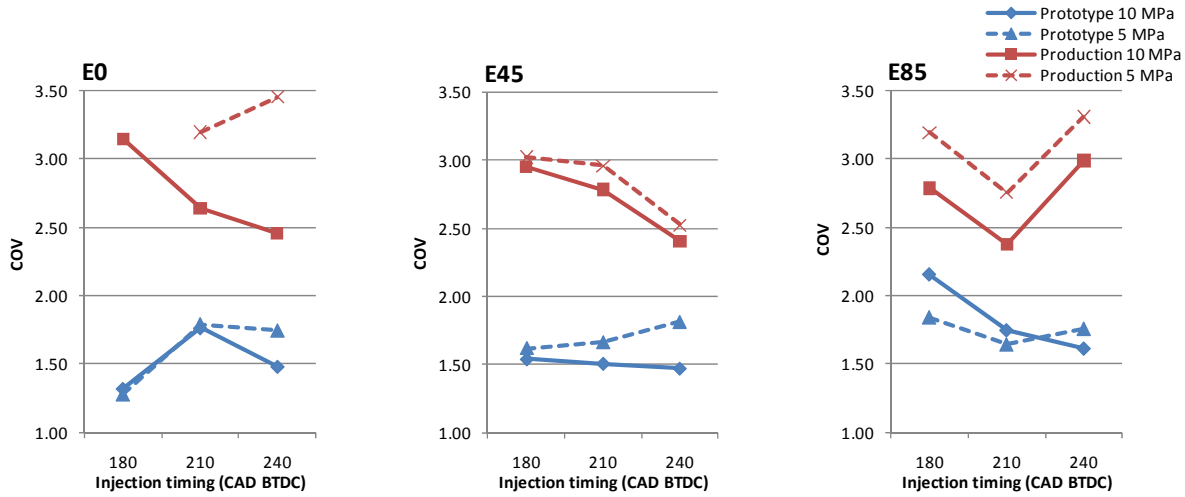

Figure 49:- COV of IMEP for E0, E45, and E85 with Bosch HDEV5 and Generation 2 Injectors 1500 rpm 5.6 bar IMEP.

At 2000 rpm, COV of IMEP generally showed the same trend.

Ion Sensor Results

Ionization sensor signals were monitored to determine the sensor's ability to detect the ethanol content of a fuel. It worked well initially, however, problems arose with extended running. It is possible that too much fuel spray impinged on the spark plug, causing a buildup of soot and possible interference with the ion signal.

Theoretically, a fuel with higher ethanol content should result in a higher signal voltage, and thus a larger area under the signal curve. This indeed was the case in initial tests done on 1500rpm mid-load cases. Figure 50**Error! Reference source not found.** shows the Ion signal averaged over 300 recorded cycles for E0, E45, and E85 at this load condition with an 18°BTDC spark timing for each fuel and both 5 and 10MPa injection pressures.

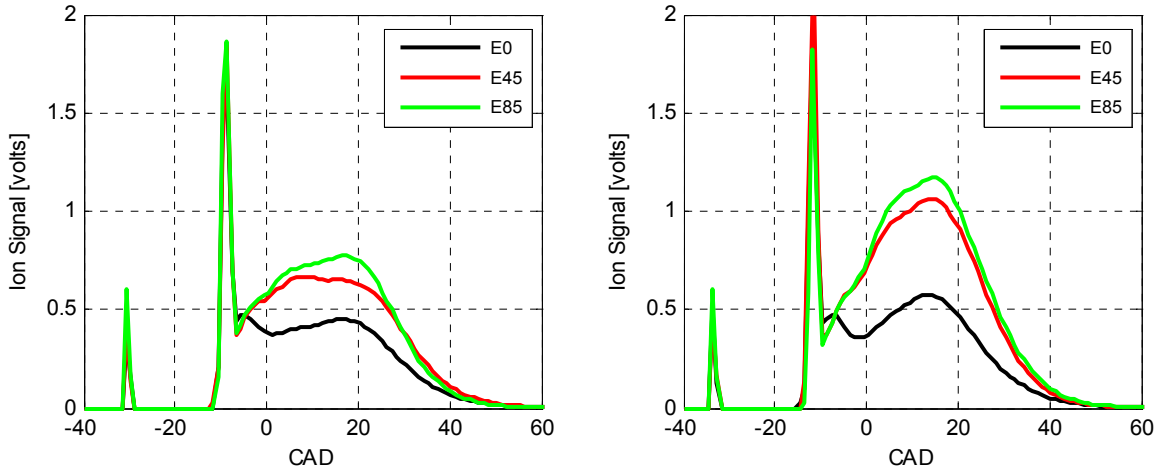

Figure 50:- Ionization Signal - 1500rpm Mid-Load
5MPa Injection Pressures (Left) - 10MPa Injection Pressures (Right)

To determine fuel type, an integration calculation can be made over a set CAD window to find the area under each curve. Integrating over a CAD window of 0° to 30°ATDC the E85 curve had the largest area and the E0 curve covers the smallest, see **Error! Reference source not found.**Table 7. However, while the area difference is easily seen between E0 and the two ethanol blends, the difference in area between E45 and E85 is less pronounced. This shows that in this application the ionization sensor is not linear with respect to the ethanol content over the entire ethanol range, and a nonlinear estimation algorithm might be required to detect the ethanol content. As a summary, the ionization signal can differentiate well between a pure-gasoline fuel and a fuel with significant ethanol content, and it may be difficult to get precise readings to differentiate between different levels of ethanol content with high ethanol concentration.

		Integrated area [volts-CAD]
5MPa injection pressure	*E0*	12.2
	E45	18.6
	E85	20.7
10MPa injection pressure	*E0*	13.5
	E45	26.2
	E85	28.9

Table 7:- Effect of Fuel Type on Integrated Ion Signal – 1500rpm Mid-Load
Integration window of 0° to 30°ATDC.

Figure 50 also shows the difference in magnitude of the raw signals with varying injection pressures. The signals with the 10MPa injection pressure all have a larger magnitude than those with the 5MPa injection pressure.

In conclusion, the ion sensor testing for ethanol fuel content determination at a single 1500rpm mid-load point indicated that fuel content determination of the processed ion signal produced robust high signal to noise results and differentiation between E0 and E45. However the system's capability to differentiate at higher blends was not proven. This could be due to the saturation of the ionization signal, which requires further study. Further investigation of capability at other speed load conditions may have provided more robust results for higher blends and would help determine the best system operating criteria for implementation in a vehicle. Unfortunately time restrictions precluded further tests.

Summary and Conclusions

The Bosch HDEV5 injector proved to be superior to the Bosch Generation 2 injector. It proved to be better with all three fuels, showing that it is well suited for flex-fuel operation with varying levels of ethanol content. This was consistent with the previous optical engine tests that showed the Bosch HDEV5 injector performing with faster and more uniform flame growth. The low-load and WOT tests helped to further enforce that it is able to effectively operate with ethanol blends over a wide range of operating conditions.

In general, the Bosch HDEV5 injector performed better with 10MPa injection pressure than with 5MPa injection pressure. This result is in agreement with the optical engine tests.

The capability of using ionization signals for identifying the ethanol content was demonstrated through dynamometer tests using the signal cylinder engine at MSU at 1500rpm with medium load. The ion based ethanol content detection was robust with low ethanol content between 0 and 45%, however at high ethanol concentration, the signal to noise ratio gets small. This could be due to the saturation of the ionization signal and further investigation is required.

Although the knock detection using ionization was not demonstrated in this project, it was demonstrated in the past research conducted at Visteon Corporation [3].

Task 3.4.3 E85 Cold Start Tests

'Upon satisfactory completion of the previous subtasks, performance measurements will commence under cold starting conditions'.

Engine cold start tests were deleted per contract modification in lieu of additional Injector testing.

Task 3.5 Receive Engine Components

'Final receipt of all multi-cylinder engine components to E85 optimized specifications, indicated by simulation and analysis'.

Engine Components were received.

Task 3.6 Assembly of Multi Cylinder Engine

'Assemble components into multi-cylinder, E85 optimized engine'

The study MAHLE DI3 engine was procured in 'stock' gasoline configuration. Optimization actions in support of Phase 4 testing were planned to be undertaken based on design direction indicated by the single cylinder engine testing. These actions were to include piston replacement to achieve increased compression ratio and up-fit of preferred fuel injection system. The necessary base engine components (piston blanks, spare cylinder head) were procured for machining to desired configuration.

Subtask 3.6.1 Assembly of Control System

'Assemble prototype control system and mate it with multi-cylinder'.

Phase 4 testing was to include utilization of the ion-sensing ignition system to enable Closed-Loop Combustion Control. The control of these systems was to be realized through utilization of an Opal RT open architecture 'rapid prototyping' control system and strategy developed by Michigan State University. Since this same control system (as described in Section 3.3) was needed by MSU to conduct the Single cylinder optical engine research, transfer of the control system to the multi cylinder engine could not take place until the completion of Phase 3.

In order to allow testing of the DI3 engine at MAHLE's test facility prior to the Opal-RT controller becoming availability, an alternative open ECU (AFT PROtroniC) was fitted to the engine, using MAHLE's proprietary control strategy. The AFT ECU was intended to be replaced by the MSU Opal RT control system as part of the optimization build, including the ionization coil ignition system however due to delays the system was still required for the single cylinder testing which carried over into Phase 4 and never became available.

Subtask 3.6.2 Dyno break in tests.

'Perform initial firing, basic functional testing and break-in of multi-cylinder, E85 optimized engine'.

The DI3 engine was broken in at MAHLE Powertrain, on gasoline fuel.

Task 3.7 Performance and Emissions Baseline of Comparator Engine

'Fuel efficiency and emissions baselines, for reference with the I3 engine work, will be generated using the comparator engine. After break-in and mapping of the production engine on gasoline, the stock engine controller will be replaced with an open architecture controller. With the open architecture controller, EGR, fueling rate and ignition timing will be adjusted to operate the engine at several different load points on various blends of fuel ranging from E10 (pump gasoline) to E85, representing the range of possibilities of fuel properties a flex fuel vehicle would face in normal usage. Engine output, fuel consumption, and emissions data will be gathered from these tests along with ionization sensor signals. This data will be used to determine a baseline for using the ionization signal to determine ignition timing, heat release, and fuel properties for a FFV. The ionization signals will also be compared to combustion light intensity signals obtained from the Visioscope for additional analysis of the combustion events'.

With the production controller fitted the GM Ecotec engine was run at a series of speed / load points to form maps of the engines fuel flow and emissions for subsequent comparison with the MAHLE DI3 engine.

Following the benchmarking with gasoline, the effects of various ethanol fuel blends on economy and emissions were investigated. E85's higher octane rating and increased heat of vaporization were seen to give improved Brake Thermal Efficiency (BTE), compared to gasoline.

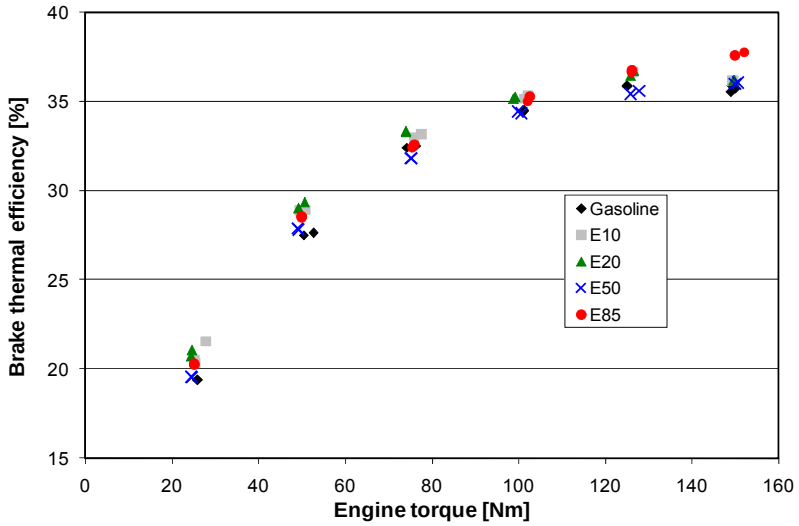

Figure 51:- Engine Torque vs. Brake Thermal Efficiency Ecotec @ 2000rpm

When running at high loads with E85 fuel it was not necessary to retard spark to avoid knock as was the case with gasoline.

Emissions testing showed that higher levels of ethanol produced lower NOx emissions.

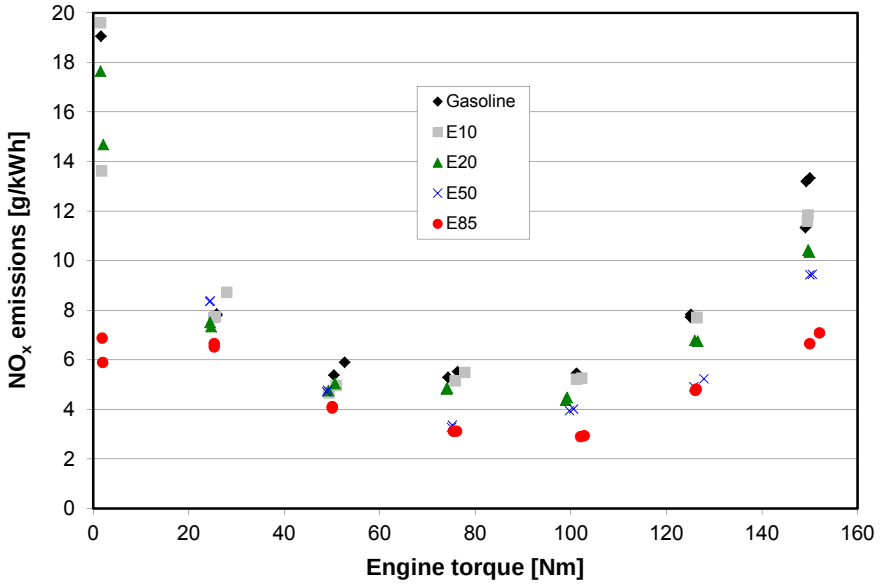

Figure 52:- Ecotec NOx Emissions

Hydrocarbon emissions were found to be relatively insensitive to the alcohol content of the fuel.

The potential for using ion sensing to determine combustion phasing, detonation and fuel composition was investigated using a range of gasoline / ethanol blends at 1500rpm 2.62bar BMEP, 1500rpm 8bar BMEP and 3000rpm 4bar BMEP.

A direct relationship was found between the phasing of cylinder pressure and the ion signal peaks, as shown in Figure 53. There is a strong linear correlation between location of 10% integrated ion sensor signal and CA10, shown in Figure 54 and between 50% integrated ion sensor signal and CA50, shown in Figure 55. There is some variation at retarded spark timings where CA50 occurs later than 20°ATDC, but the relation still trends linearly. There is a high degree of combustion variation with the retarded combustion resulting from late spark timings. However, CA50 combustion phasing of later than 20°ATDC is considered quite late, and suboptimal, for normal spark-ignition operation. Within the typical range of combustion phasing, the relation is strongly linear.

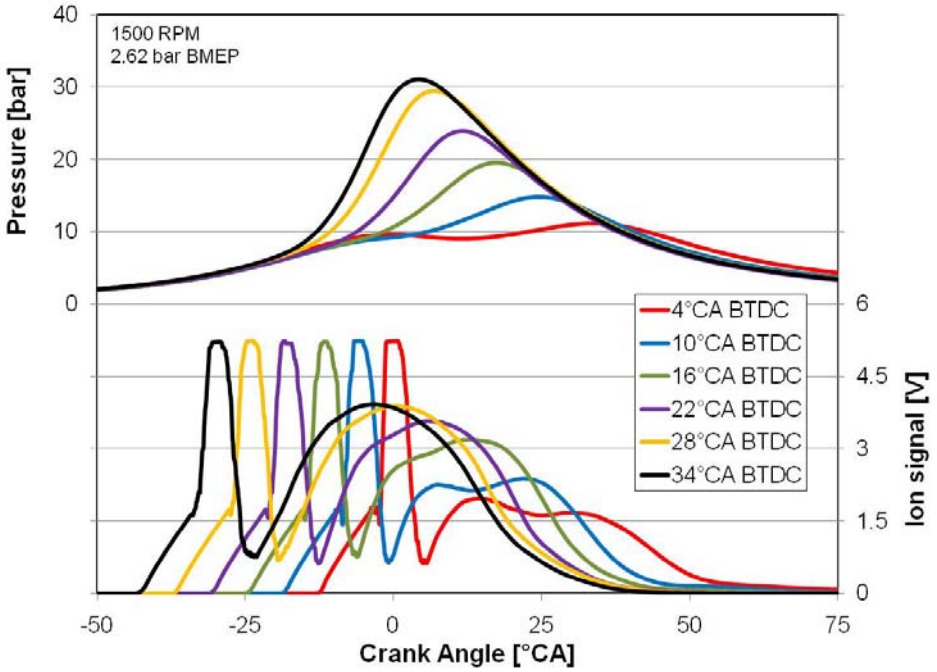

Figure 53:- Average Pressure and Ion Signal Traces for Different Spark Timing at Low Engine Load

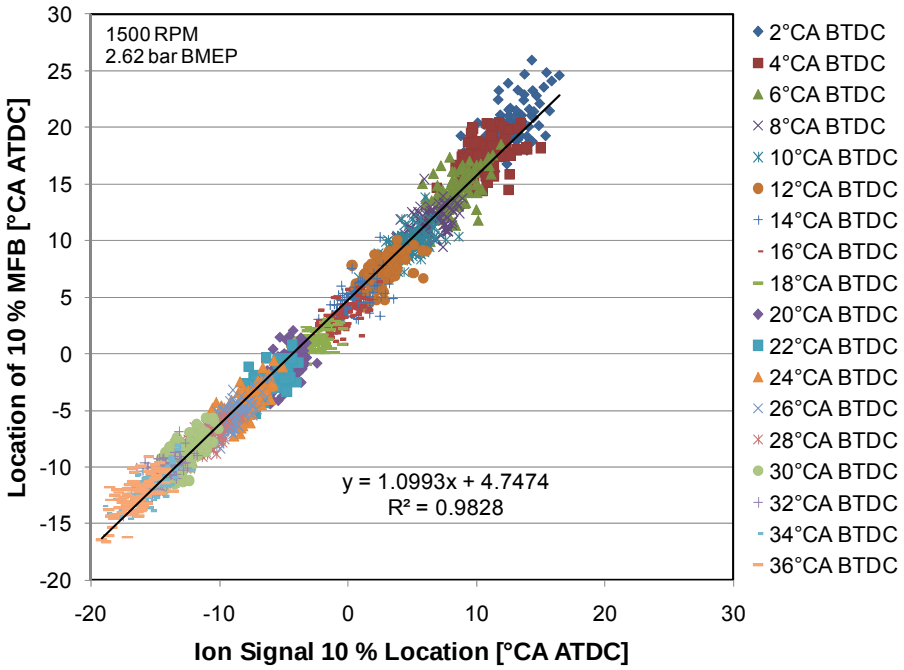

Figure 54:- 10% MFB Timing Versus 10% Ion Signal Location at Low Engine Load

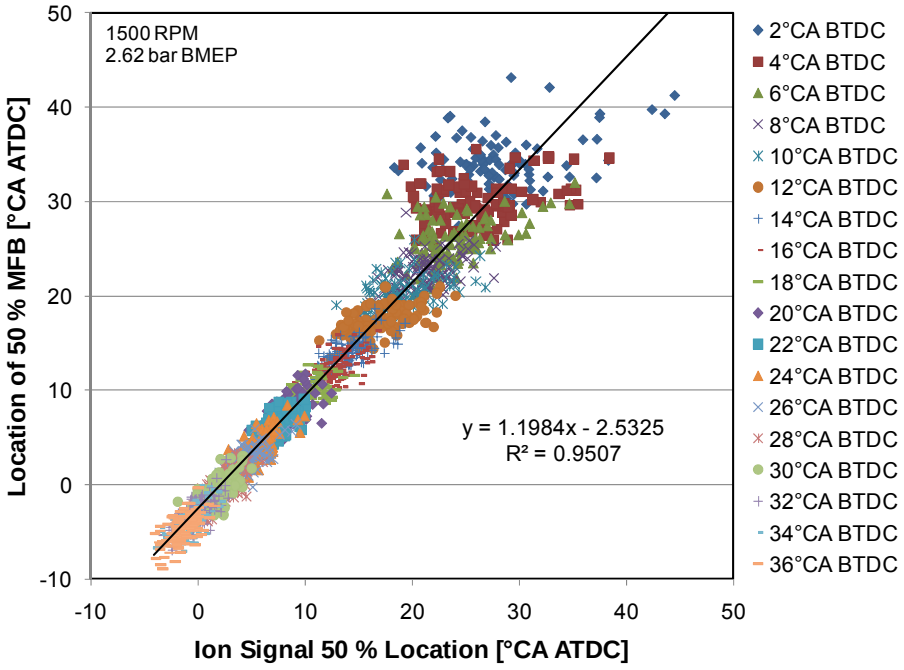

Figure 55:- 50% MFB Timing Versus 50% Ion Signal Location at Low Engine Load

Ion signal traces were studied as a means of detecting knock. Figure 56 shows individual cycle traces of cylinder pressure and ion signal at two different spark timings with varying levels of knock intensity. At the 16°BTDC spark timing, all recorded cycles featured some level of engine knock: retarding spark timing to 12°BTDC produced light knock and knock-free cycles. However, the behavior of the cycles with comparable levels of knock intensity (though different spark timings) were very close, making comparison across all points possible. Figure 56 shows that the spike and subsequent oscillations in pressure signal associated with the onset of knock are reflected in the ion signal trace. The jump in ion signal concentration is time aligned with the spike in cylinder pressure due to knock. Oscillations in ion signal come from the changes in cylinder pressure (including oscillations stemming from the rapid pressure rise due to detonation) affecting the cylinder temperature. The oscillations in cylinder pressure continue late into the expansion stroke, but the ion signal oscillations are limited by the duration of the re-ionization period. The principal component of the ion signal goes to zero at the completion of combustion and the re-ionization period, suppressing the knock-sourced oscillation.

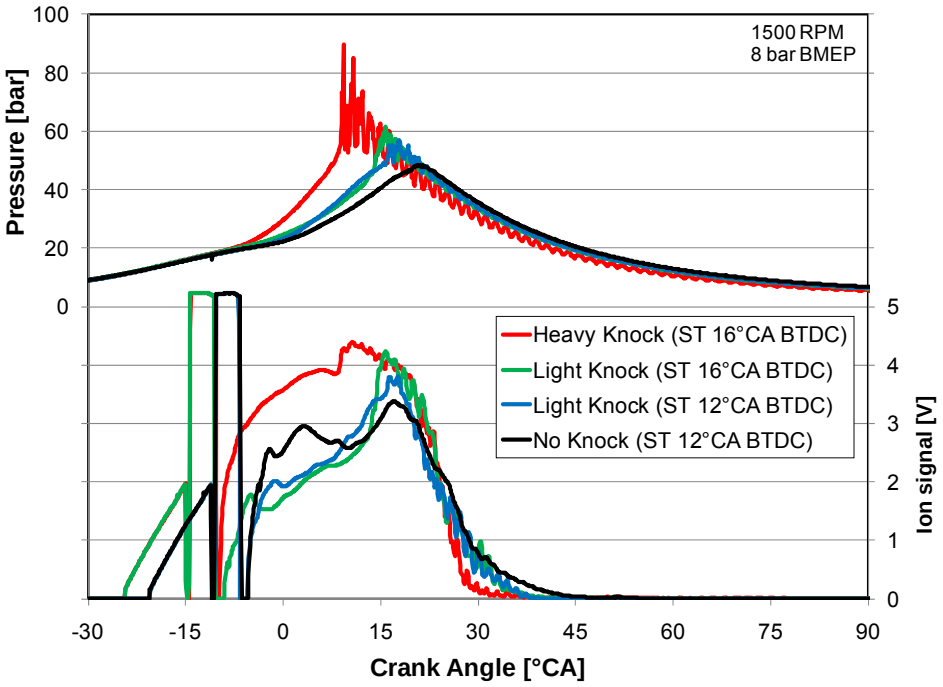

Figure 56:- Pressure Traces and Ion Signals at Knocking Conditions

A Fourier analysis of the frequency spectrum was performed on both cylinder pressure and ion signal traces for a heavy knocking engine cycles at the 16°BTDC spark timing for the condition studied, with the results shown in Figure 57 and Figure 58. The figures show the intensity (prevalence) of a given frequency versus time (in seconds) after spark timing. The graphs also include the filtered signal that was used as an input for the frequency analysis. There is a clear sustained peak in intensity in the frequency range of 5-10kHz for cylinder pressure. There is a matching, albeit shorter, peak in intensity at the same frequency within the ion signal data.

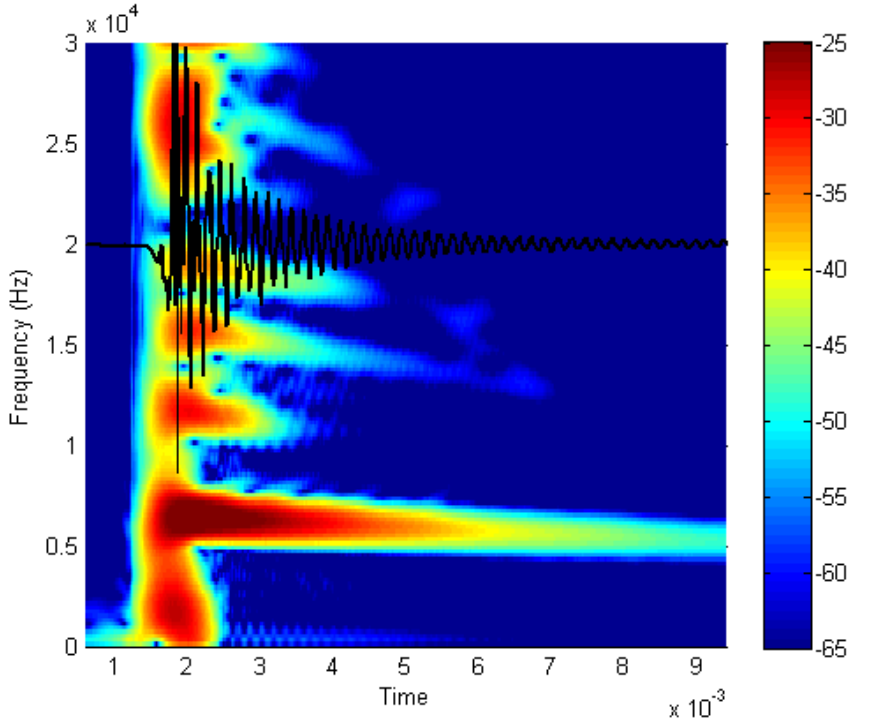

Figure 57:- Pressure Frequency Analysis for Heavy Knock Case (1500rpm, 8bar BMEP, 16 BTDC)

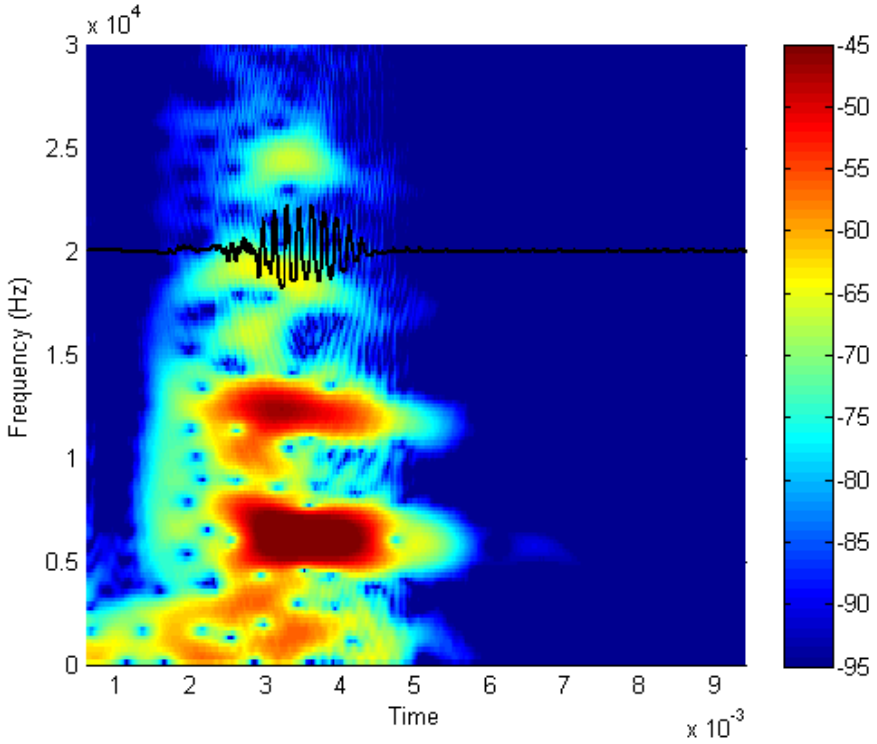

Figure 58:- Ion Signal Frequency Analysis for Heavy Knock Case (1500rpm, 8bar BMEP, 16 BTDC)

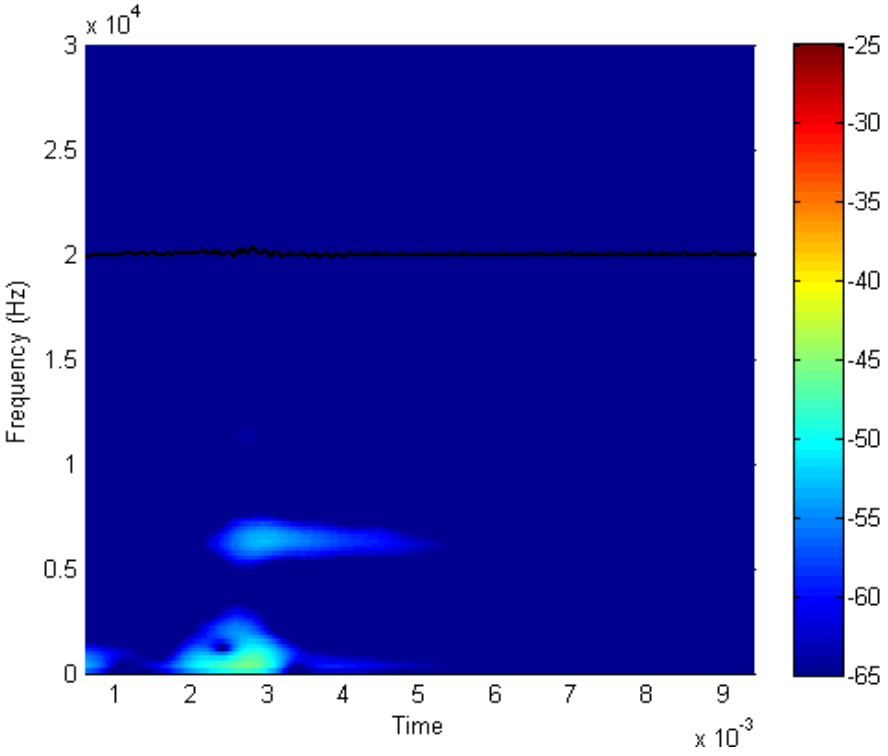

Figure 59:- Pressure Frequency Analysis for No-Knock Case (1500rpm, 8bar BMEP, 12 BTDC)

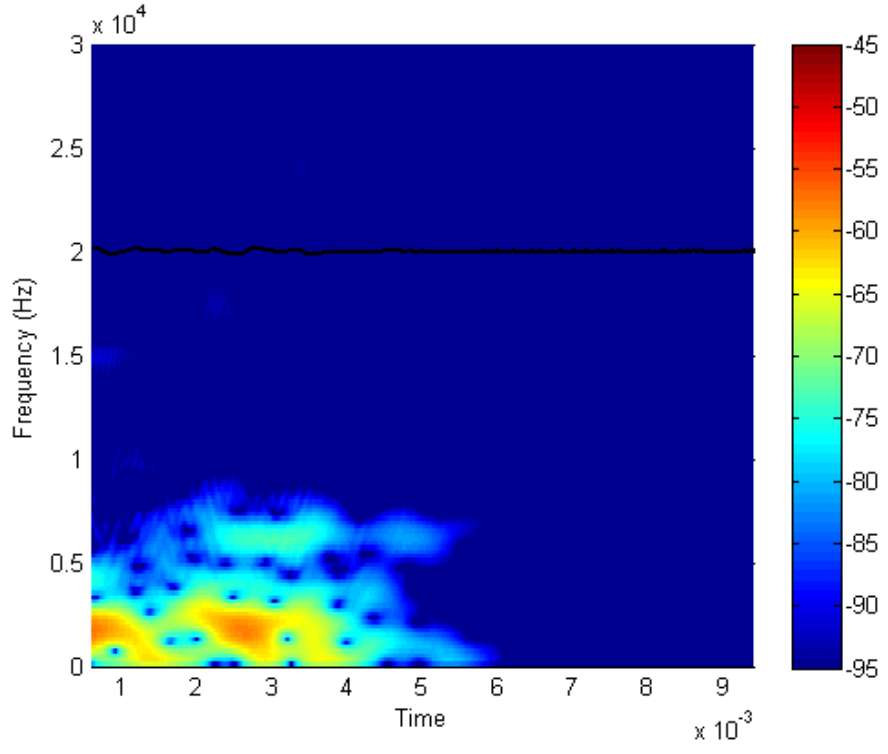

Figure 60:- Ion Signal Frequency Analysis for No-Knock Case (1500rpm, 8bar BMEP, 12 BTDC)

Figure 59 and Figure 60 show the frequency analysis results for a no knock case at 12 BTDC spark timing. For ease of comparison the scale was kept identical to the heavy knock case discussed earlier. The same frequencies in the 6kHz range are also dominant in the no knock case, however, the amplitudes are significantly lower. It is also interesting to note that the reduction in peak amplitudes of the pressure frequency analysis values is much more significant than the reduction in respective ion signal data.

Based on the frequency analysis, a highpass filter with a cutoff frequency of 6kHz was applied to both cylinder pressure and ion signal traces to isolate the high frequency oscillations typically associated with knock. The resulting filtered traces are shown in Figure 61. Like before, the traces clearly show time-alignment between the start of oscillation in the cylinder pressure signal and increased oscillation in the ion signal. The high frequency fluctuations in the filtered ion signal trace prior to TDC are primarily associated with the spark event and initial flame kernel formation. There is also an apparent trend between knock intensity and magnitude of the oscillations in ion signal, with cycles featuring more intense knock yielding fluctuations of increasing magnitude. This is especially visible between the no knock and light knock conditions, and matches the behavior exhibited by cylinder pressure. From this, Figure 62 plots the root mean squared (RMS) values of the filtered ion and cylinder pressure signals of individual cycles at a range of different spark timings. The RMS values of ion signal and cylinder pressure trend in a similar fashion: higher values of ion signal oscillation magnitude generally suggest higher levels of cylinder pressure oscillation magnitude. There is significant variation of this relationship at higher RMS levels, however, the trend may be strong enough that analyzing the magnitude of high-frequency oscillations in ion signal can classify cycles as knocking or non-knocking.

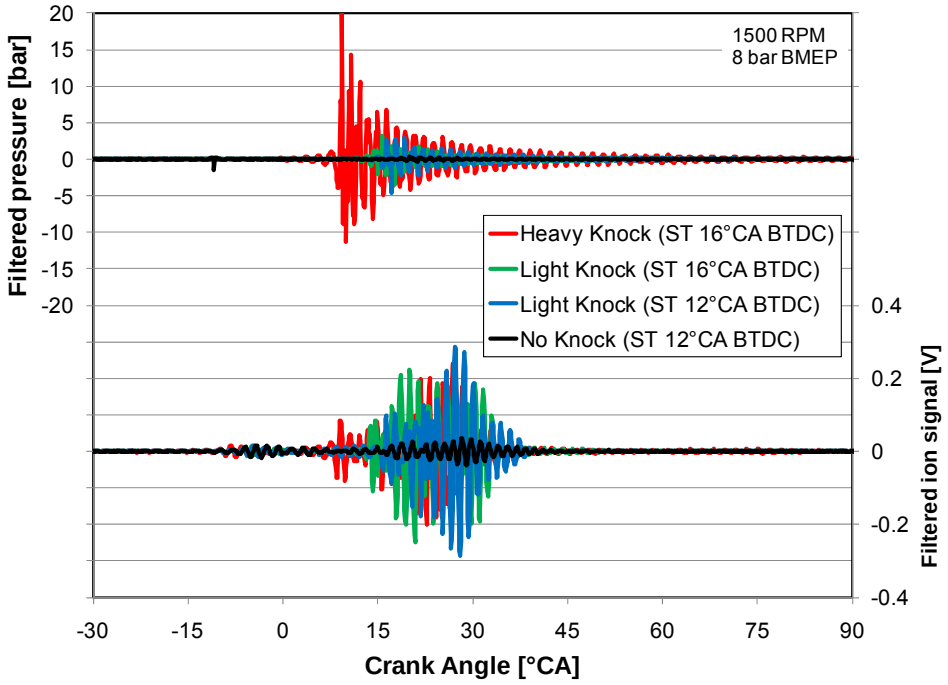

Figure 61:- Filtered Pressure Traces and Ion Signals at Knocking Conditions

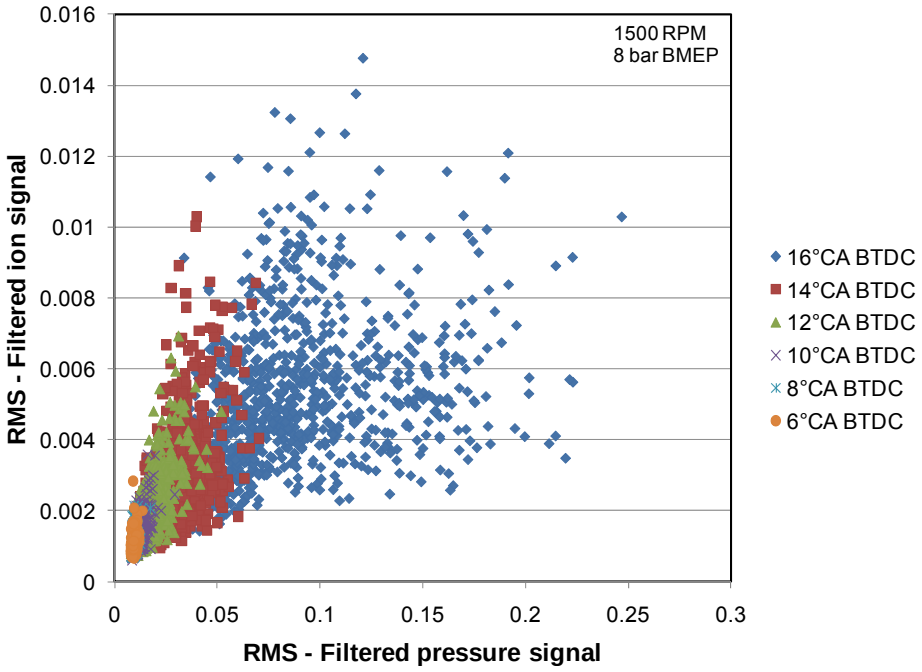

Figure 62:- Correlation Between Processed Pressure and Ion Signal for Knock Detection

With knock-induced oscillations in ion signal mimicking those found in cylinder pressure, it may be possible to use the ion sensor for knock detection, in lieu of a cylinder pressure transducer. Signals from the ion sensor show similar high frequency oscillations indicative of knock to those found in cylinder pressure. The magnitude of these fluctuations, especially as a knock versus no-knock comparison, means the ion sensor could be used to gauge the presence, and approximate intensity, of knock.

Ion signals from matching combustion conditions were examined for any behavior trending with fuel type which could serve as the basis for a fuel detection method. Cycle averaged ion sensor data is presented to give an overall representation of each fuel's behavior, since individual cycles were highly sensitive to exact conditions and cycle-to-cycle variability. Comparing individual cycles across different tests may yield erroneous results, with individual cycle differences causing changes in combustion behavior which could be attributed to fuel effects.

Fuel specific differences in ion sensor signal were apparent at the low speed / load condition. There were visible differences in the ion sensor signals between fuels at the same condition, as shown in Figure 63. These differences predominantly trend with ethanol fuel blend percentage. Gasoline fuel shows the distinct two-peak bimodal form, described as a typical ion signal in Zhu et al. [6], with a peak for flame kernel development and a second peak for re-ionization. As ethanol percentage in the fuel increases, the ion signal magnitude increases, and the two separate peaks merge to form one continuous peak across the whole combustion event. With an apparent constant production rate, the increased ion production due to the flame kernel extends the initial peak, merging it with the second (re-ionization) peak and obscuring the inflection points between the two peaks. This data indicates there could be differences in the ion production behaviour between ethanol and gasoline combustion.

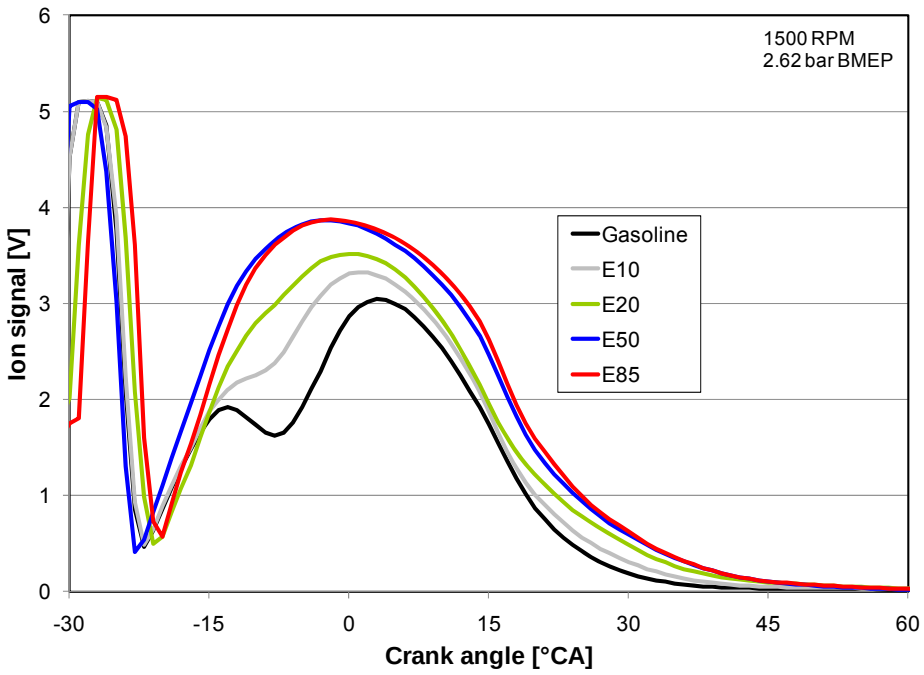

Figure 63:- Average Ion Signal Traces with Ethanol Addition at Low Engine Load

The high load condition did not yield the same distinct fuel-dependent differences in ion-signal that were shown at the low load case. At this operating condition, ECU knock control was active. This results in both cycle-to-cycle phasing variation and phasing variation between different fuels. Increasing ethanol blend percentage increases the knock resistance of a fuel, allowing earlier combustion phasing. This results in significant changes in cylinder pressure and rate of heat release curves, which will have some effect on the ion signal curves. However, though phasing varies between the fuels, the overall shape of the ion signals can be compared. All fuels show very similar ion signal traces, displayed in Figure 64, featuring a single ion peak from combustion following the initial spike from the ignition event. Accounting for the differences in combustion phasing no significant differences were apparent between the ion signals for each different fuel.

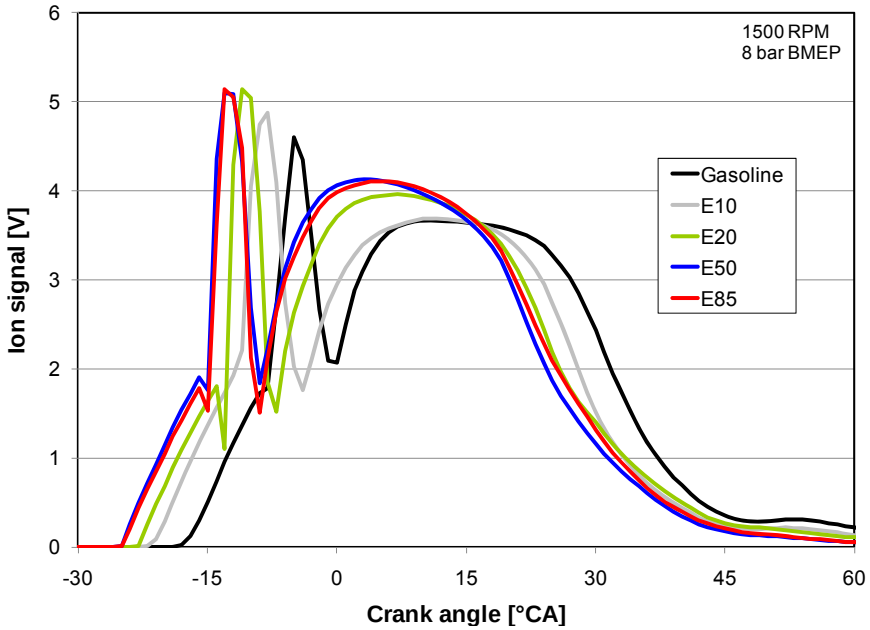

Figure 64:- Average Ion Signal Traces with Ethanol Addition at High Engine Load

Like the high load condition, the 3000rpm 4bar BMEP condition did not yield the same distinct fuel-dependent differences in ion-signal that were shown at the low load case.

From these results, it is clear that the ion signal only exhibits distinct differences from fuel type in select operating conditions. Clear fuel dependent trends were apparent at the light load condition, but not at the high load or high speed conditions. The ion signals are highly sensitive to combustion conditions, cycle-to-cycle variation, and the operating point. No distinct universal changes in ion signal from fuel composition were found in these tests, suggesting that using an ion sensor for fuel composition detection over the entire speed and load range may not be a robust solution. Although the types of differences in ion signal noted at the low load case are not optimal for basing a control scheme around, it might be possible to infer fuel blends in certain operating windows of the engine.

Experimental results yielded the following conclusions:

- Increasing ethanol content increases the efficiency of the DISI engine.
- The part-load combustion characteristics of all tested fuel blends (gasoline, E10, E20, E50 & E85) were found to be similar in terms of heat release and pressure.
- NOx emission decreased slightly as ethanol content was increased, HC remained similar.
- It was possible to use ionization signals to determine combustion phasing by linking the integral of the ion signal to the 10% and 50% mass fraction burned.
- Analysis of the ignition ionization signals show that the system is effective in knock detection.
- Use of the ionization signal for inference of fuel blend was found to be suitable only in certain operational conditions. It is suggested that a fuel blend determination algorithm may need to be 'windowed' to certain conditions. It is recognized that a conventional ethanol fuel sensor or alternative method of fuel blend determination may be required.

3.8 Highly Diluted Combustion Analyses

'A key factor in attaining the improved efficiency from the HECCE is to maximize its efficiency in low-load conditions typical of much of normal engine operation in light-duty vehicles. The HECCE concept addresses this important objective from the start by using a high static compression ratio, engine downsizing, using LPDI and CLCC, and two-stage boosting. Another critical element of the HECCE concept is the use of high levels of cooled EGR. Using dilute combustion reduces pumping losses while increasing the knock tolerance of the engine. HDC will be investigated using the aforementioned concepts as appropriate, pushing the limits of dilute combustion to the maximum to improve operating efficiency at this critical operating point. Using new technology to visualize combustion under these cool conditions through endoscopic spectroscopy, the engine's operating range will be extended to the limits of combustion control using the CLCC. As EGR levels increase, emission spectroscopy will be used to understand the limits of dilution using different fuel blends and interpret the ionization signals that are obtained to control the combustion events over the range of ethanol / gasoline blends to extract the most work from the least amount of fuel. This knowledge of HDC will be used to improve the overall efficiency of the HECCE under loads most often associated with everyday driving'.

Early on in the Task 3.8, a review by the project team members, agreed that further continuation by ANL with the remaining scope would not be productive or the best use of available funding. This action was subsequently approved by the DOE.

Justification: It was determined that endoscopic access to the combustion chamber, required for the "endoscopic spectroscopy" portion of task 3.8, was not feasible due to space limitations in the cylinder head. In addition, although the GM L850 engine is equipped with an external EGR system, the stock EGR system is not equipped with an EGR cooler. Therefore, while high dilution EGR operation as outlined in the SOPO text - Task 3.8 can be accomplished, preliminary results do not reflect the full potential expected of cooled EGR operation.

Based on the initial data, it is clear that results with uncooled EGR from the comparator engine at Argonne cannot be directly linked to progress made on the engine developed as part of the overall project. A joint effort was made with the other project partners to redefine the scope of work to be performed at Argonne to be of greater utility to the project partners and more closely aligned with the overall goals of the project. However, it was determined that a redefined project is not feasible due to budget and time constraints, and that the most responsible solution is to not continue past the preliminary tests already completed.

5 PHASE 4 – ENGINEERING DEVELOPMENT

Task 4.1 Agree Detailed Test Plan

'Create detailed test plan for multi-cylinder, E85 optimized engine testing, including development of 'mini-map' test point matrix, to facilitate estimation of drive-cycle (i.e. FTP – Federal Test Procedure) fuel economy from steady-state dynamometer data.'

The agreed test plan was developed to satisfy the two distinct parts of the planned engine testing. The first goal was to quantify part load efficiency improvements. The second goal was to quantify engine performance with the selected test fuels.

Part Load Test Point Selection.

Drive cycle fuel economy was established using GT Drive. GT Drive requires a fuel flow surface, or map, as one of its primary inputs. The selection of the part load test points was driven by the need for good coverage of the speed / load conditions encountered during the drive cycles under consideration. Fuel use during the FTP75 and HWFET Drive Cycles was analyzed. **Error! Reference source not found.**Figure 65 and Figure 66 show the percentage of total fuel used at each speed / load condition (blue bubbles) and the test points subsequently selected (green bubbles) for the FTP75 and HWFET Drive Cycles.

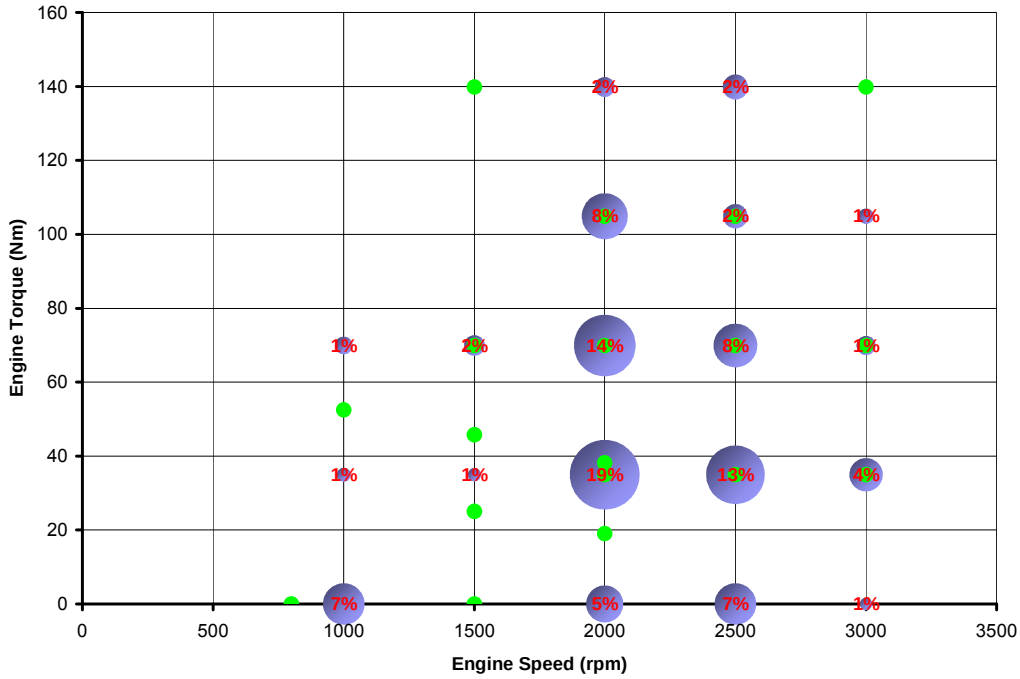

Figure 65:- Fuel Usage Distribution for FTP75 Drive Cycle

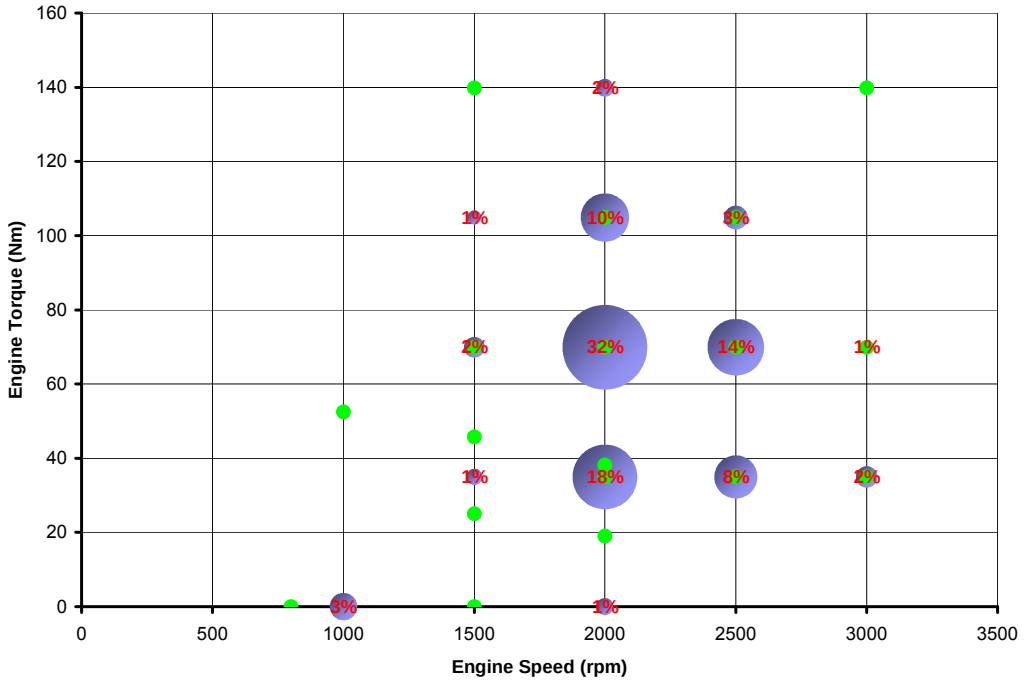

Figure 66:- Fuel Usage Distribution for HWFET Drive Cycle

The test points selected cover the most important conditions for both the FTP75 and HWFET drive cycles. Test points were established as 'engine speed' / 'engine torque' sites, rather than 'engine speed' / 'engine BMEP' sites as the MAHLE DI3 engine and the Opel 2.2L Ecotec Direct engine have different displacements. The part load test points selected are shown in Table 8.

Engine Speed (rpm)	Engine Torque (Nm)	DI3 BMEP (bar)	Ecotec BMEP (bar)
800	0.0	0.00	0.00
1000	52.5	5.50	3.00
1500	0.0	0.00	0.00
1500	25.0	2.62	1.43
1500	45.8	4.80	2.62
1500	69.9	7.33	4.00
1500	139.9	14.66	8.00
2000	19.1	2.00	1.09
2000	35.0	3.66	2.00
2000	38.2	4.00	2.18
2000	69.9	7.33	4.00
2000	104.9	10.99	6.00
2500	35.0	3.66	2.00
2500	69.9	7.33	4.00
2500	104.9	10.99	6.00
3000	35.0	3.66	2.00
3000	69.9	7.33	4.00
3000	139.9	14.66	8.00

Table 8:- *Part Load Test Points*

Due to changes in project structure and personnel, GT Drive was used in place of Advisor (used in Phase 1 of the project) for drive cycle fuel economy predictions. GT Drive effectively works in the same way as Advisor. Vehicle, engine and cycle data are analyzed and cycle fuel economy or vehicle performance are output.

Full Load Test Point Selection.

To quantify engine performance, power tests were conducted at two different performance levels. Firstly at the same performance as the comparator engine, and secondly at a performance level of 25bar BMEP (238Nm). The testing at 25bar BMEP was included to keep open the option of "downspeeding" the MAHLE engine.

Optimization.

The following parameters were varied using the engine controller.

- Intake Valve Timing
- Exhaust Valve Timing
- External EGR Rate
- Fuel Injection Pressure
- Fuel Injection Timing
- Spark Timing
- Air Fuel Ratio (Full Load Only – For Part Load Running AFR was kept at $\lambda = 1$ to enable use of a three way catalyst)

At each test point the sensitivity of the engine's fuel consumption to these parameters was assessed. At the combination found to deliver best fuel economy data was recorded. Certain constraints were put on the optimization.

- Maximum turbine entry temperature of 950^{o}C.
- Maximum peak cylinder pressure of 140bar.
- The engine was not allowed to detonate or pre-ignite.
- Maximum COV of IMEP of 5% at part load or 2.5% at full load.
- Maximum cylinder pressure rise rate of 7bar/^{o}ca.

In addition to optimization of the above variables, tests were planned with compression ratios of 9.25, 11.5 and 13.7 :1. Downsizing was also seen as a key contributor to fuel economy gains.

Additionally further part load testing was conducted on the 2.2L Ecotec Direct at Argonne National Laboratory to provide data that could be used to generate a fuel flow surface for use in subsequent GT Drive analysis.

Task 4.2 Final Performance and Emissions Test

Subtask 4.2.1 Gasoline Fuel Baseline Test

'Perform testing and calibration of multi-cylinder, E85 optimized engine running on 100% gasoline to provide baseline fuel economy and performance data.'

Testing and calibration were conducted on the MAHLE DI3 engine as outlined in the response for Task 4.1 in MAHLE Powertrain's Novi facility.

Figure 67:- MAHLE DI3 Engine in Test Cell

Testing was only conducted at two compression ratios, 9.25 and 11.25 : 1. The findings at the 11.25 : 1 compression ratio made testing at the 13.7 : 1 compression ratio unnecessary. Again due to issues found during testing, additional tests were conducted on a second turbocharger. The original turbocharger, a Borg Warner 5303 988 0005 was found to offer poor low speed torque on the DI3 engine. Tests were conducted on a second turbocharger, a Borg Warner 5303 988 0069 to address this issue. The results found are presented and analyzed in the response for Task 4.3 in this report.

Subtask 4.2.2 E85 Fuel & Fuel Blends Test

'Perform testing and calibration of multi-cylinder, E85 optimized engine running on E85 and other fuel blends, such as E22 and E50 (depending upon availability) for comparison with data recorded in task 4.2.1.'

Testing and calibration were conducted on the DI3 engine as outlined in the response for Task 4.1 using E85 fuel only. Testing on other blends, E22 and E50 was not conducted. The rational for this decision was twofold. Firstly, with the performance of E85 and gasoline well defined, both worst case fuel economy (E85) and the worst case full load performance (gasoline) would be identified. The performance of other blends would fall between what was found on E85 and gasoline. Secondly due to delays with the single cylinder testing, confirmation tests examining the suitability of ion sensing to detect the ethanol content of fuels were not conducted on the multi-cylinder DI3 engine. The results found are presented and analyzed in the response for Task 4.3 in this report.

Subtask 4.2.3 Cold Start Test

'Assess cold starting capability of multi-cylinder, E85 optimized engine running on E85.'

This scope was deleted in preference to additional injector characterization and testing in the single cylinder engine.

Task 4.3 Analysis and Summary of Engine Efficiency and Fuel Economy Data.

'Conduct a full analysis of the test results and compare to targets.'

Part Load Fuel Economy Test Data

Figure 68 shows the optimized fuel consumption at a selection of the part load test points. It can be seen that:

1. The relative efficiencies of the DI3 engine and the 2.2L Ecotec Direct engine were not constant, but varied greatly with engine load set point.
2. The DI3 engine was generally more efficient when the compression ratio was 11.25 : 1 than when the compression ratio was 9.25 : 1.
3. The DI3 engine used less fuel (mass based) when fueled by gasoline than when fueled by E85.

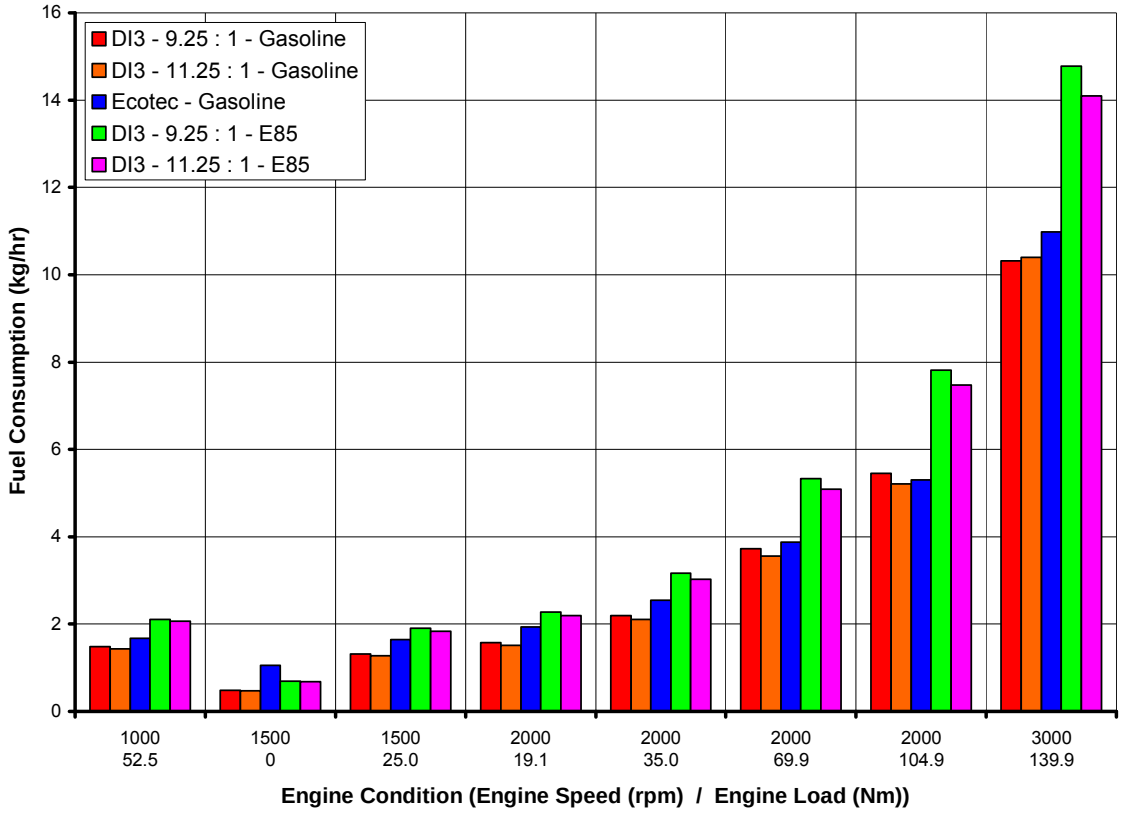

Figure 68:- Fuel Consumption Test Results

Effect Of Engine Load On Relative Fuel Economy

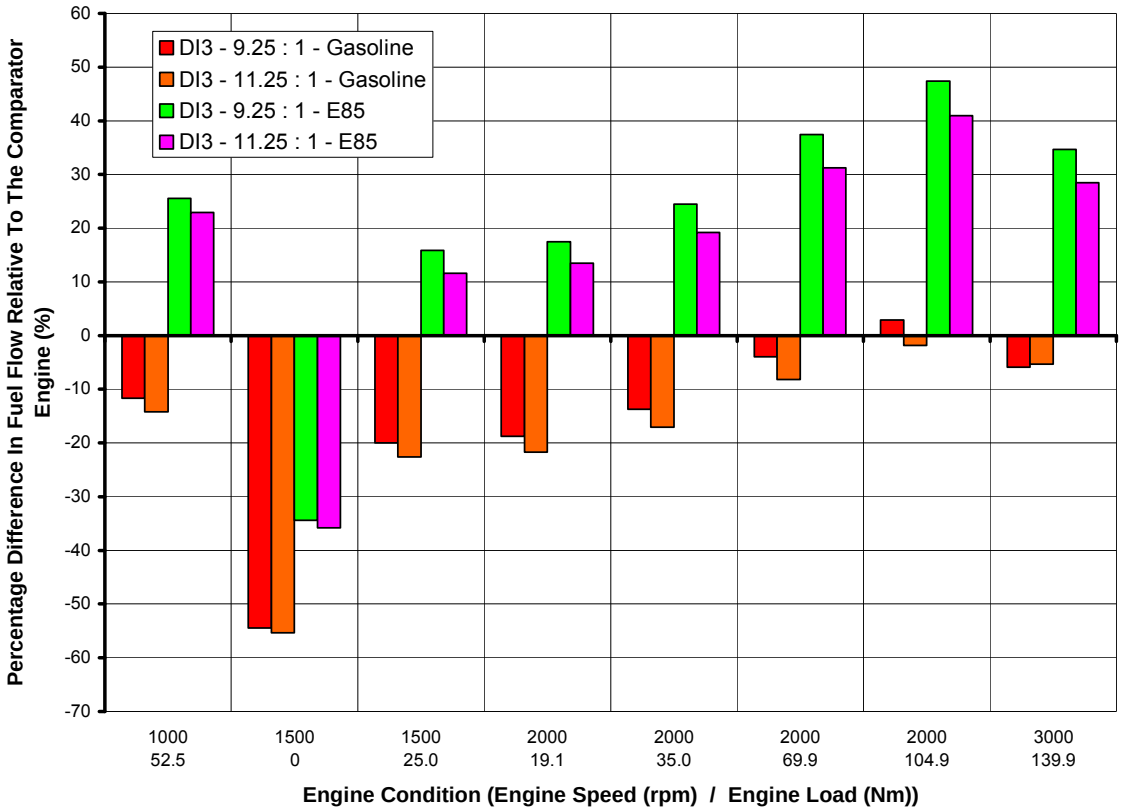

Figure 69:- Relative Fuel Consumption of the DI3 Engine Compared to the Ecotec

Figure 69 shows that the DI3 engine (irrespective of fuel type or compression ratio) relative to the Ecotec engine was comparatively more efficient at light loads than at high loads. The primary reason for the difference in relative fuel efficiency at different loads is downsizing. Downsizing is a technique increasingly being used to improve vehicle fuel economy. The fuel economy of a smaller (downsized) engine will be better than a larger incumbent engine as it will run in a more efficient area of its operational envelope at light loads.

Figure 70 shows the fuel consumption of the gasoline fueled 9.25 : 1 MAHLE DI3 relative to the Ecotec at 2000rpm.

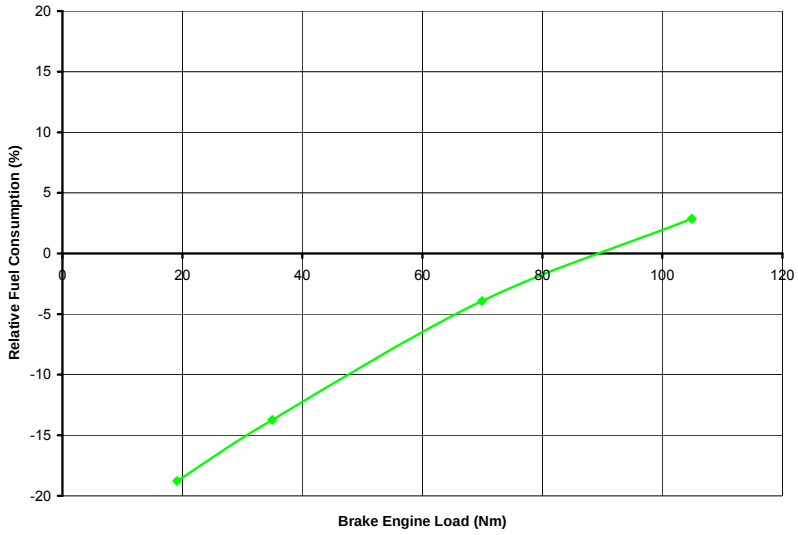

Figure 70:- Relative Fuel Consumption of the DI3 Engine Compared to the Ecotec at 2000rpm

Relative fuel consumption was calculated as shown in the equation below.

$$\text{Relative Fuel Consumption} = \frac{(\text{Fuel Flow Rate DI3} - \text{Fuel Flow Rate Ecotec})}{\text{Fuel Flow Rate Ecotec}} \times 100\%$$

At light loads (20Nm) the MAHLE DI3 engine used 19% less fuel than the 2.2L Ecotec Direct, at high loads (105Nm) the MAHLE DI3 engine used 3% more fuel.

To understand the trend the following measures must be considered:

1. The indicated load. This is a measure of the gross output of the engine (i.e. it includes load required to overcome pumping and frictional losses, not just the load taken from the flywheel).
2. The indicated specific fuel consumption. This is a measure of how efficiently fuel is converted into indicated load.

Pumping losses

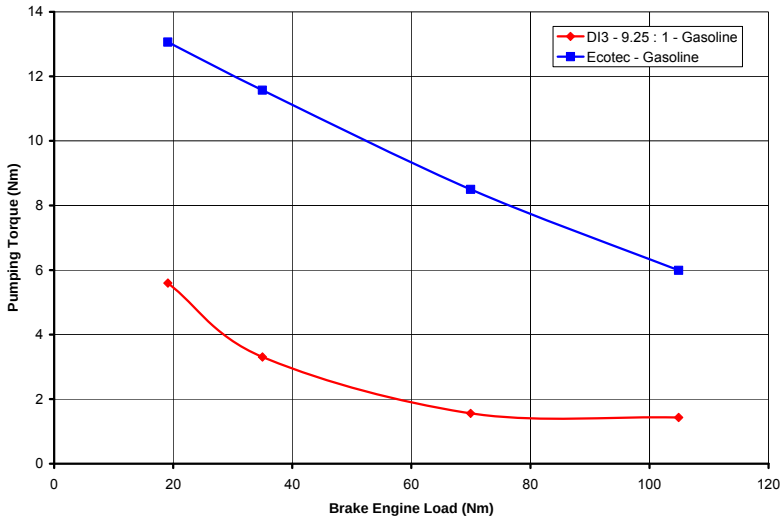

Figure 71:- Pumping Torque Variation with Brake Load of the MAHLE DI3 and 2.2L Ecotec Direct Engines

Figure 71 shows the following:

1. For a given output torque the pumping torque of the DI3 engine is lower than that of the 2.2L Ecotec Direct. The difference is 7Nm at 19Nm (39% of brake load) and 4Nm at 105Nm (4% of brake load), this is consistent with the principals of downsizing. At light loads the reduction in pumping work represents a significant reduction in indicated load for the DI3. As the brake load is increased the significance of the pumping reductions decreases.
2. The slope of the curve for the DI3 is far less linear than the curve for the 2.2L Ecotec Direct. The DI3 utilizes variable valve timing which will modify the pumping torque curve shape.

Friction losses

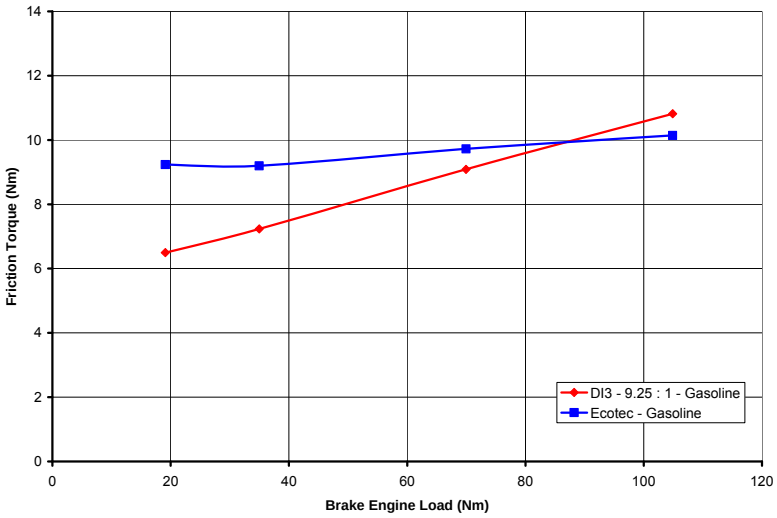

Figure 72:- Friction Torque Variation with Brake Load of the MAHLE DI3 and 2.2L Ecotec Direct Engines

Figure 72 shows the following:

1. The friction torque of the DI3 engine is lower than that of the 2.2L Ecotec Direct at light break loads and the same as the Ecotec at higher loads.
2. The slope of the curve for the DI3 is steeper than the curve for the 2.2L Ecotec Direct, indicating that the friction of the DI3 is more sensitive to changes in engine load.

Indicated Load

The total savings from pumping and friction improvements may be established by comparing Indicated Load.

Indicated Load = Brake Load + Pumping Load + Friction Load

Brake Load (Nm)	Indicated Load (Nm)		Difference	
	DI3	Ecotec	Absolute (Nm)	(%)
19.1	31.2	41.4	-10.2	-24.7
35.0	45.5	55.7	-10.2	-18.4
69.9	80.6	88.2	-7.6	-8.6
104.9	117.2	121.0	-3.9	-3.2

Table 9:- Comparison Of Indicated Load Differences Between MAHLE DI3 and Ecotec Engines

Indicated Fuel Consumption

The savings in fuel consumption are smaller than the reductions in indicated load. The reason for this are differences in how efficiently the two engines convert the fuel supplied into indicated work.

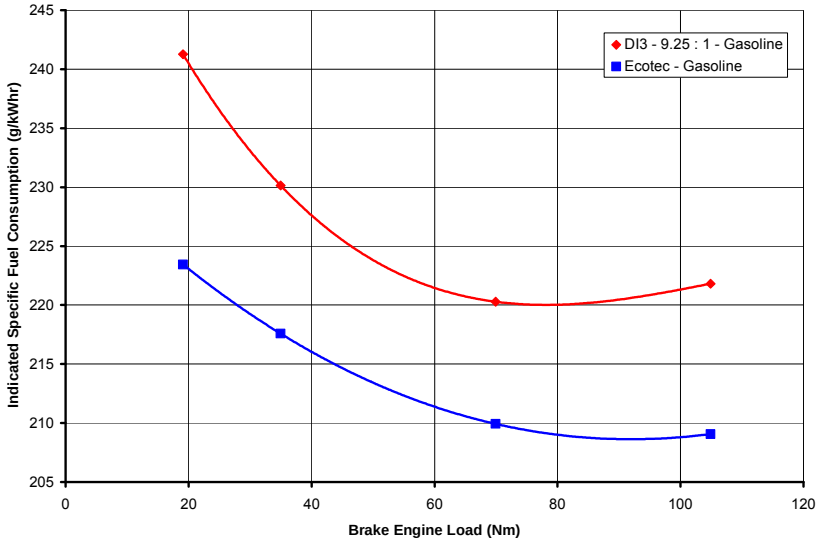

Figure 73:- Indicated Specific Fuel Consumption Variation with Brake Load of the MAHLE DI3 and 2.2L Ecotec Direct Engines

Figure 73 shows that from a fuel conversion standpoint the Ecotec engine is more efficient than the DI3 engine.

The primary reasons for the difference in ISFC between the DI3 and Ecotec are differences in heat transfer, compression ratio and specific heats of the charge. These are considered below:-

1. Heat Transfer.

   The more heat lost from the combustion process to the coolant, lubricant etc, the less that is available for useful work, resulting in higher ISFC. Higher combustion temperatures lead to greater heat loss. The combustion temperature at each load condition was greater for the DI3 than for the Ecotec; it was not measured directly but can be inferred from the in-cylinder pressure measurements.

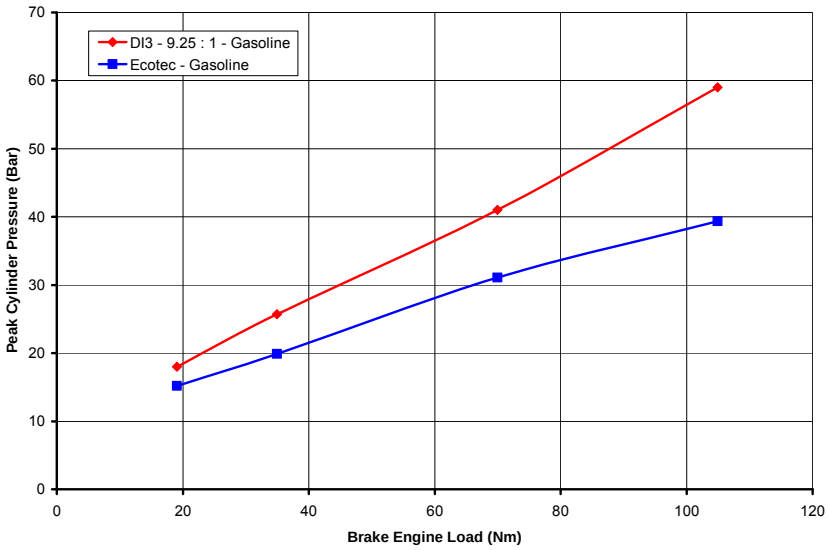

Figure 74:- Peak Cylinder Pressure Variation with Brake Load of the MAHLE DI3 and 2.2L Ecotec Direct Engines

2. Compression Ratio.

   Thermo dynamically, higher compression ratios lead to lower indicated specific fuel consumption.
   If the engine cycle is assumed to have constant volume combustion and the working fluids are assumed to be ideal gases, the gross fuel conversion efficiency is given by the equation

$$\eta_{f,ig} = 1 - \frac{1}{CR^{\gamma-1}}$$

Where $\eta_{f,ig}$ = Gross Fuel Conversion Efficiency
CR = Compression Ratio
γ = Specific Heat Ratio

Equation 2 [12].

Research has shown the thermal efficiency will increase with increasing compression ratio up to a maximum value of 14 to 15 : 1 [12]. The DI3 was run with a geometric

compression ratio of 9.25 : 1 and the Ecotec with a compression ratio of 12.0 : 1. An increase in compression ratio of this magnitude, if nothing else was changed would tend to improve ISFC by about 5%.

When comparing the DI3 with the 2.2L Ecotec Direct, the effective compression and expansion ratios are dictated not only by the geometric compression ratio but by the intake valve closing (IVC) timing and the exhaust valve opening (EVO) timing. The Ecotec ran with fixed cam timings, IVC = 120°BTDC and EVO = 135.5°ATDC. The DI3 has variable valve timing; the tests at 2000rpm were run with IVC timings between 152° and 162°BTDC and EVO timings between 121 and 126°ATDC.

3. Specific Heat Ratio, γ, c_p/c_v.

   If the engine cycle is again assumed to have constant volume combustion and the working fluids are assumed to be ideal gases (Equation 2), the gross fuel conversion efficiency decreases with γ. The value of γ is sensitive to in-cylinder gas temperatures; as temperature increases the value of γ decreases, decreasing the gross fuel conversion efficiency and increasing the indicated fuel consumption [12]. As previously discussed, it may be inferred from cylinder pressure data that at any given engine load the peak cycle temperature for the MAHLE DI3 engine was higher than for the Ecotec engine.

   Thus the trend in fuel consumption is due to three distinct mechanisms, pumping losses, friction losses and fuel conversion efficiency differences. The table below approximates the makeup of the fuel economy improvements of the DI3 compared to the Ecotec for each brake load condition.

	Contribution To DI3 Fuel Economy Improvement Over Ecotec (%)			
Brake Load (Nm)	Pumping	Friction	Fuel Conversion	Total
19.1	19.6	7.2	-8.0	18.8
35.0	15.7	3.7	-5.8	13.7
69.9	8.1	0.7	-4.9	3.9
104.9	3.7	-0.5	-6.1	-2.9

Table 10:- Contribution Of Different Mechanisms To Fuel Economy Differences Between The MAHLE DI3 and 2.2L Ecotec Direct Engines.

Effect Of Compression Ratio On Fuel Economy

Figure 68 showed that the fuel consumption of the DI3 engine improved with increasing compression ratio. This improvement can be seen more clearly in the chart below.

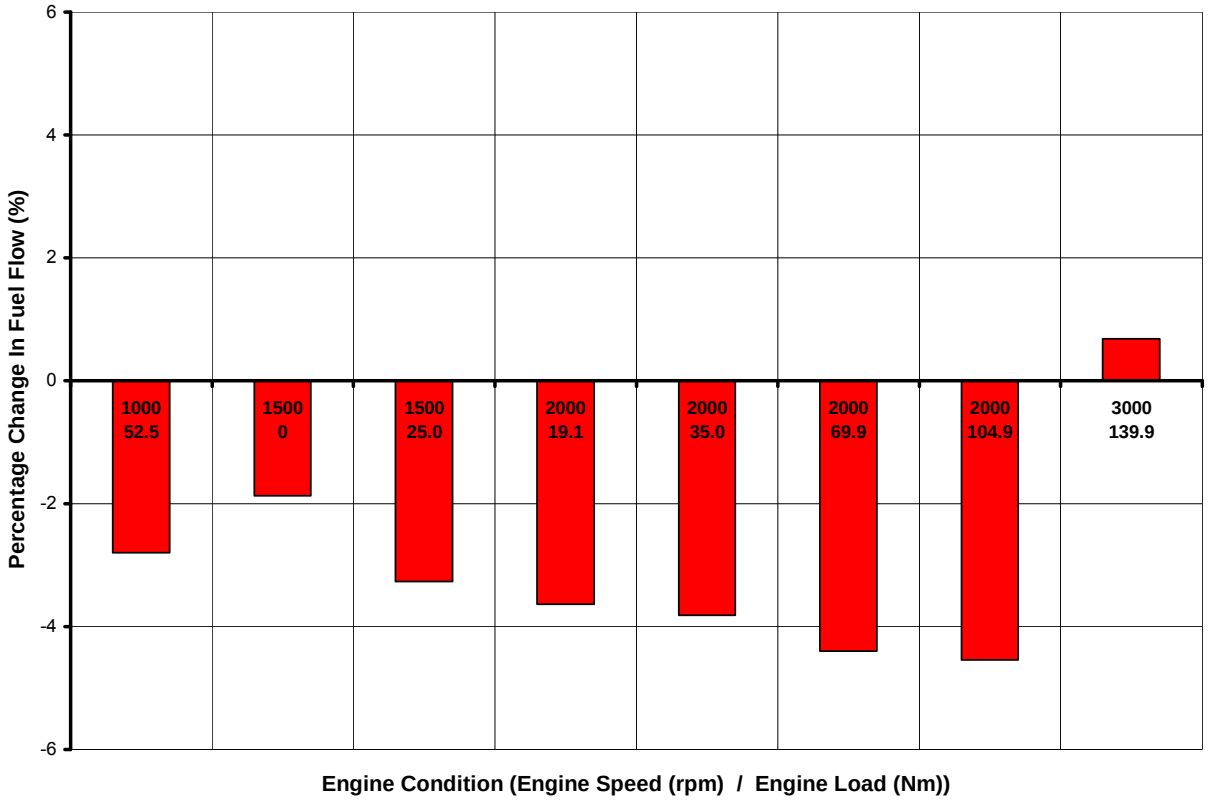

Figure 75:- Fuel Consumption Reduction Associated with Increasing DI3 Compression Ratio From 9.25 : 1 To 11.25 : 1 (Gasoline Fuel).

Fuel consumption was reduced (improved) by an average of around 4% when the compression ratio was increased from 9.25 : 1 to 11.25 : 1. A decrease in fuel consumption would be expected with a higher compression ratio, again with reference to Equation 2, if γ is assumed to be 1.3, the gross fuel conversion efficiencies would be 49% and 52% for compression ratios of 9.25 and 11.25 respectively, representing a 6% improvement in gross fuel conversion efficiency for the 11.25 : 1 engine.

Equation 2 is a representation of an ideal cycle and does not account for many of the losses in a real engine. The losses present in the DI3 engine meant that the recorded values of gross fuel conversion efficiency were lower than those predicted by the ideal cycle. The 6% improvement in gross fuel conversion efficiency predicted for an ideal cycle with increasing compression ratio was not realized during testing because of increased losses associated with the 11.25 : 1 compression ratio. At the higher compression ratio, cylinder pressures and thus temperatures were higher, consequently heat losses were higher and the ratio of specific heats less favorable.

Figure 75 shows the average fuel consumption improvement was about 4%, however at the 3000rpm 139.9Nm test point the fuel consumption deteriorated as the compression ratio was increased. With a compression ratio of 9.25 : 1 the spark timing could be optimized (50%mfb = 8.7^{o}ATDC). At a compression ratio of 11.25 : 1 it was necessary to retard the spark timing from

its optimum value to avoid detonation (50%mfb = 17.5°ATDC), consequently the combustion was less efficient at 11.25 : 1.

With E85 fuel, increasing the compression ratio from 9.25 : 1 to 11.25 : 1 improved fuel consumption by approximately 4%.

Effect Of Fuel Type On Fuel Economy

The DI3 engine used less fuel (mass based) when fueled by gasoline than when fueled by E85 due to the relative net heating values of the two fuels. The net heating values for the gasoline and E85 fuels used were 42.8MJ/kg and 29.2MJ/kg respectively. So purely on an energy basis it might be expected that the DI3 would use 32% less fuel when fueled with gasoline. The difference in net heating values of the two fuels does not account for all of the differences seen. Figure 76 shows a comparison of the brake thermal efficiency of the MAHLE DI3 engine with the two different fuels at 9.25 : 1 compression ratio.

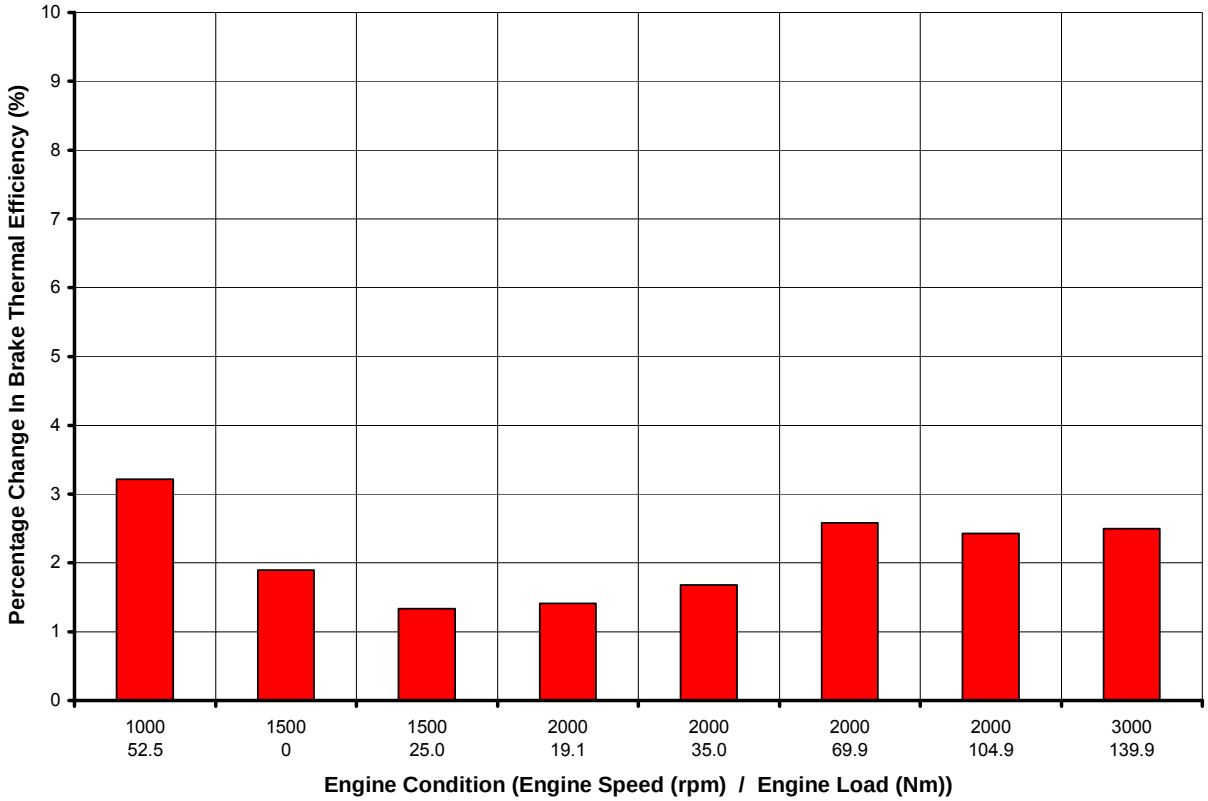

Figure 76:- Brake Thermal Efficiency Improvement of E85 Over Gasoline DI3 Engine 9.25 : 1 Compression Ratio

The DI3 engine shows an average 2% improvement in BTE when fueled by E85 compared to gasoline. The reason for this is the lower combustion temperatures of E85 [13 and 14]. Due to E85's increased heat of vaporization (the heat of vaporization for E85 is 760kJ/kg compared with 305kJ/kg for gasoline) it has much greater charge cooling effect than gasoline, this results in lower temperatures during the compression stroke, and subsequently lower combustion

temperatures. The temperatures can be inferred from the cylinder pressure traces recorded during testing.

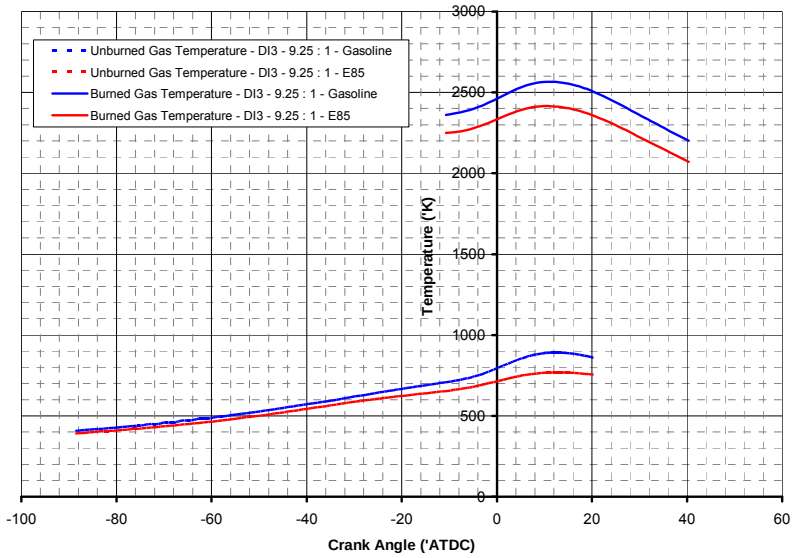

Figure 77:- The Sensitivity of Burned and Unburned Temperatures to Fuel Type 9.25 : 1 Compression Ratio – 2500rpm - 104.9Nm

The lower combustion temperatures of E85 yields two efficiency benefits, firstly decreased heat transfer to the combustion chamber and secondly a more favorable ratio of specific heats, γ.

Figure 78 shows a comparison of the brake thermal efficiency of the MAHLE DI3 engine when fueled with E85 and gasoline at 11.25 : 1 compression ratio.

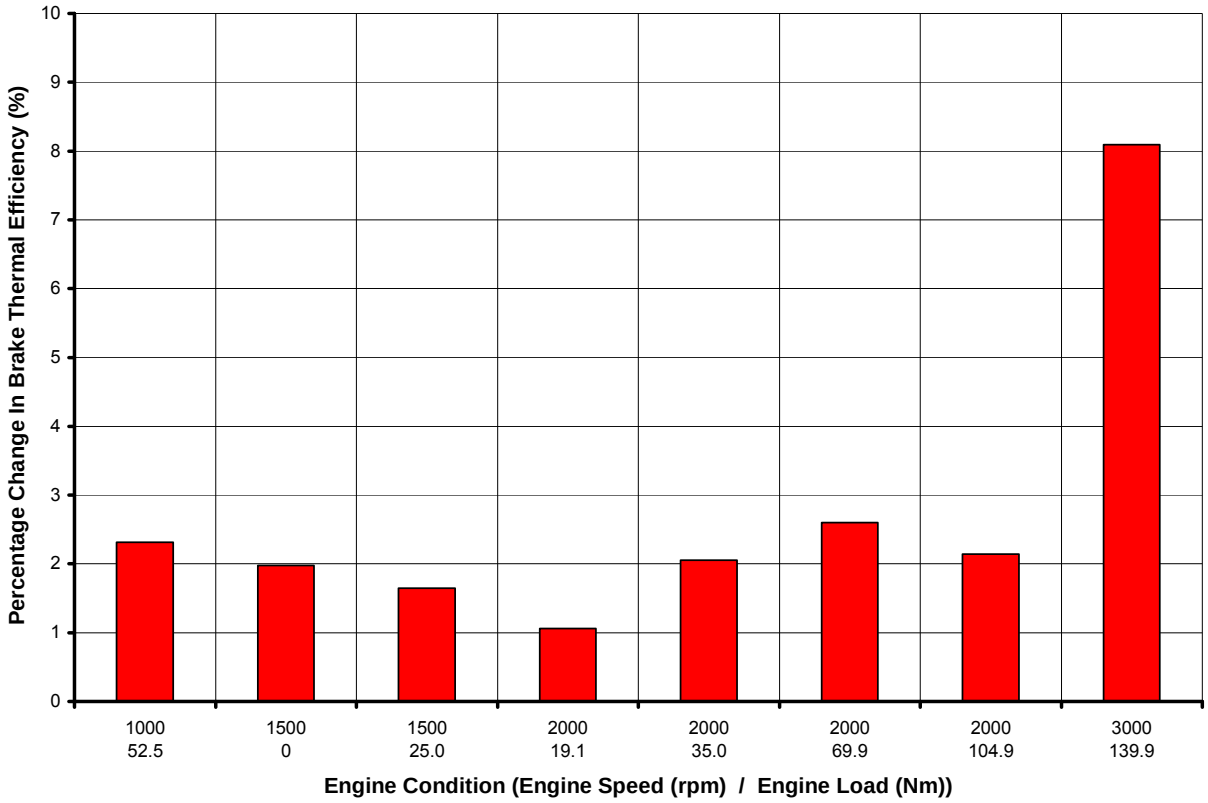

Figure 78:- Brake Thermal Efficiency Improvement of E85 Over Gasoline DI3 Engine 11.25 : 1 Compression Ratio

At the 3000rpm 139.9Nm test point the BTE was seen to improve by more than the average 2% when using E85 fuel. With E85 fuel the spark timing could be optimized at this condition, however, with gasoline fuel it was necessary to retard the spark timing from its optimum value to avoid detonation, resulting in less efficient combustion. E85 is less prone to detonation than gasoline, since typically the RON for E85 is around 104 compared to 97 for the test gasoline.-.

GT Drive Analysis

The optimized part load fuel economy data obtained in Task 4.2 was used in a GT Drive fuel economy prediction model. The predictions are for a Chevrolet HHR. The Chevrolet HHR was used for the predictions rather than the Chevrolet Cobalt used with Advisor because GM ceased production of the Cobalt in 2010. A summary of the predictions are shown in the Table 11

Engine Configuration	Fuel	City Fuel Consumption (MPG)	Highway Fuel Consumption (MPG)	Combined Fuel Consumption (MPG)
2.2L Ecotec Direct	Gasoline (E0)	26.2	34.4	29.3
MAHLE DI3 9.25 : 1	Gasoline (E0)	29.8	35.0	31.9
MAHLE DI3 9.25 : 1	E85	21.8	25.5	23.3
MAHLE DI3 11.25 : 1	Gasoline (E0)	31.1	36.7	33.4
MAHLE DI3 11.25 : 1	E85	22.8	26.8	24.4

Table 11:- Drive Cycle Fuel Economy – Corrected For True E85 Fuel.

The formula used to calculate City fuel consumption was as follows:

City Fuel Consumption = 0.9 * FTP75 Fuel Consumption

The formula used to calculate Highway fuel consumption was as follows:

Highway Fuel Consumption = 0.78 * HWFET Fuel Consumption

The formula used to calculate Combined fuel consumption was as follows:

$$\frac{1}{\text{Combined}} = \frac{0.55}{\text{City}} + \frac{0.45}{\text{Highway}}$$

The fuel consumption of the different DI3 configurations is compared to 2.2L Ecotec Direct engine in the table below.

Engine Configuration	Fuel	City Fuel Economy Improvement Over 2.2L Ecotec Direct (%)	Highway Fuel Economy Improvement Over 2.2L Ecotec Direct (%)	Combined Fuel Economy Improvement Over 2.2L Ecotec Direct (%)
MAHLE DI3 9.25 : 1	Gasoline (E0)	13.7	1.8	8.8
MAHLE DI3 9.25 : 1	E85	-16.9	-25.8	-20.6
MAHLE DI3 11.25 : 1	Gasoline (E0)	18.9	6.6	13.8
MAHLE DI3 11.25 : 1	E85	-13.0	-22.2	-16.8

Table 12:- Drive Cycle Fuel Economy – DI3 Configurations Relative To 2.2L Ecotec Engine.

Table 12 shows a 16.8% the fuel economy penalty of using the optimized DI3 engine running on E85 compared to the 2.2L Ecotec Direct Engine in the Chevrolet HHR, typically the penalty for running with E85 over gasoline is quoted as 30%.

Commercially available gasoline fuel generally contains 10% ethanol. Commercially available E85 fuel does not always contain 85% ethanol. The American Society of Testing and Materials in its standard, ASTM D 5798 “Standard Specification for Fuel Ethanol for Automotive Spark-Ignition Engines” [15], specifies three “Volatility Classes” of E85.

- Volatility Class 1 - For use in warm ambient temperatures, 79% to 83% ethanol.
- Volatility Class 2 - For use in intermediate ambient temperatures, 74% to 83% ethanol.
- Volatility Class 3 - For use in cold ambient temperatures, 70% to 83% ethanol.

Two studies were financed by the Coordinating Research Council to determine the actual ethanol content of E85 fuel sold in the US. The first study [16] analyzed 47 samples taken from 10 states during the spring and summer of 2006. The average ethanol content of the fuels analyzed was 76.2%. The second study [17] analyzed 55 samples taken from 15 states during the winter of 2007. The average ethanol content of the fuels analyzed was 71.5%. The average ethanol content of all the fuels analyzed was 73.7%.

Consequently, the actual fuel economy realized with gasoline fuel would be worse, and the fuel economies with E85 would be better than previously predicted if consideration is given to commercially available fuels.

Correcting the predictions in Table 11 for the ethanol contents of commercially available fuels yields the following results:

Engine Configuration	Fuel	City Fuel Consumption (MPG)	Highway Fuel Consumption (MPG)	Combined Fuel Consumption (MPG)
2.2L Ecotec Direct	E10	25.3	33.3	28.4
MAHLE DI3 9.25 : 1	E10	28.8	33.9	30.9
MAHLE DI3 9.25 : 1	E73.7	22.9	26.9	24.5
MAHLE DI3 11.25 : 1	E10	30.1	35.5	32.3
MAHLE DI3 11.25 : 1	E73.7	24.0	28.2	25.7

Table 13:- Drive Cycle Fuel Economy – Corrected For Commercially Available Fuels.

This will in turn modify the fuel consumption penalty when comparisons are made between the DI3 and the 2.2L Ecotec Direct engine:

Engine Configuration	Fuel	City Fuel Economy Improvement Over 2.2L Ecotec Direct (%)	Highway Fuel Economy Improvement Over 2.2L Ecotec Direct (%)	Combined Fuel Economy Improvement Over 2.2L Ecotec Direct (%)
MAHLE DI3 9.25 : 1	E10	13.7	1.8	8.8
MAHLE DI3 9.25 : 1	E73.7	-9.5	-19.3	-13.5
MAHLE DI3 11.25 : 1	E10	18.9	6.6	13.8
MAHLE DI3 11.25 : 1	E73.7	-5.3	-15.2	-9.4

Table 14:- Drive Cycle Fuel Economy Comparison – Commercially Available Fuels DI3 Configurations Relative To 2.2L Ecotec Direct Engine

Table 14 shows that if a “consumers” approach to fuel economy is sought, and comparisons are made between the Ecotec engine fueled with commercially available “gasoline” and the optimized DI3 engine running on commercially available “E85”, the fuel economy penalty would be only 9.4%, a marked improvement over the typically quoted 30%.

Note that the fuel consumption of the MAHLE DI3 engine with both compression ratios and both fuels relative to the 2.2L Ecotec Direct engine are significantly better when calculated over the City than the Highway Cycle. The section discussing the Effect Of Engine Load On Relative Fuel Economy considered the effect of engine load on the relative fuel economies of the DI3 and Ecotec engines. Compared to the Ecotec the DI3 is relatively much more efficient at lighter loads. Figure 65 and Figure 66 show how the HWFET is more highly loaded than the FTP75, consequently greater gains were seen in City fuel economy with the DI3 engine.

HC Emissions

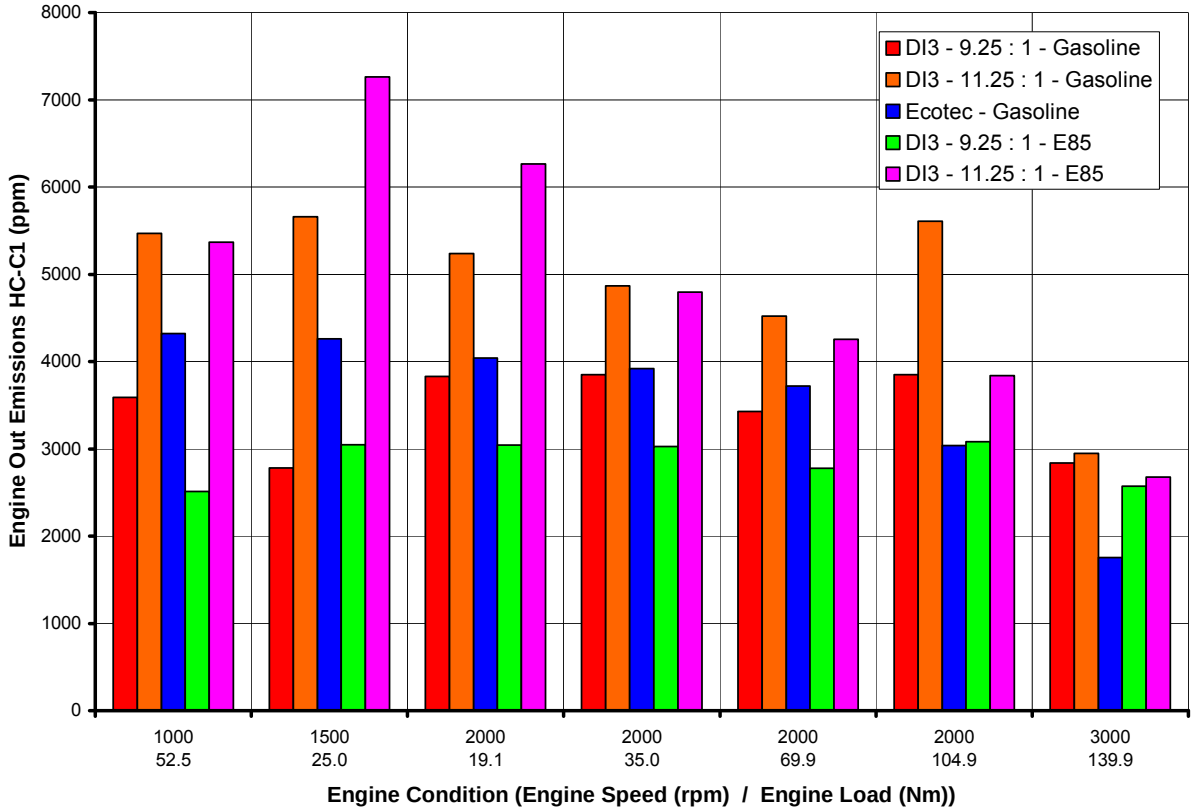

Figure 79:- Engine Out HC Emissions Comparison

Figure 79 shows the engine out HC emissions of each of the major engine configurations tested. The emissions concentrations are all in a range that could be easily converted to meet current emissions legislation with similar after treatment technologies (three way catalyst).

Therefore in consideration that meeting legislated emissions levels was not an issue and the focus of this investigation was fuel economy not hydrocarbon emissions, the hydrocarbon emissions were not optimized at any of the speed load conditions.

NOx Emissions

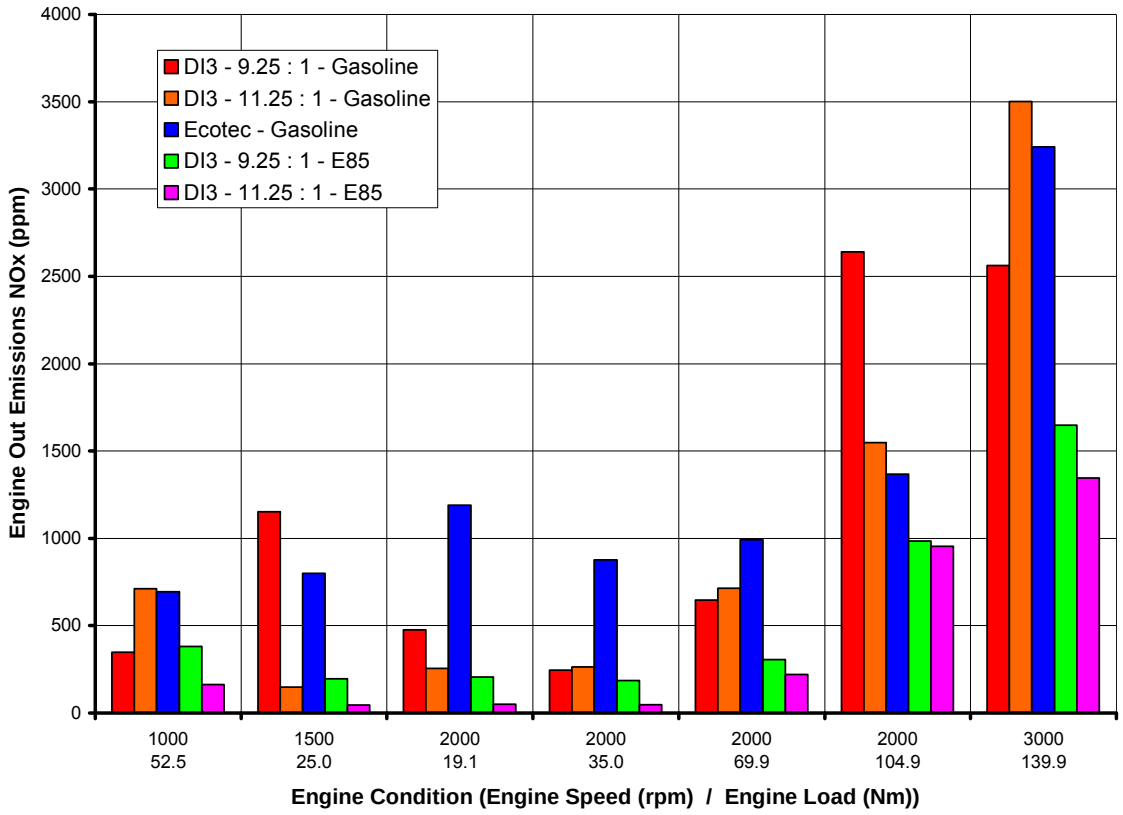

Figure 80:- Engine Out NOx Emissions Comparison

Figure 80 shows the engine out NOx emissions of each of the major engine configurations tested. The emissions concentrations are all in a range that could be easily converted to meet current emissions legislation with similar after treatment technologies (three way catalyst).

Therefore in consideration that meeting legislated emissions levels was not an issue and the focus of this investigation was fuel economy not NOx emissions, the NOx emissions were not optimized at any of the speed load conditions. The dominant factor driving NOx emissions is the amount of EGR used to optimize fuel economy.

CO Emissions

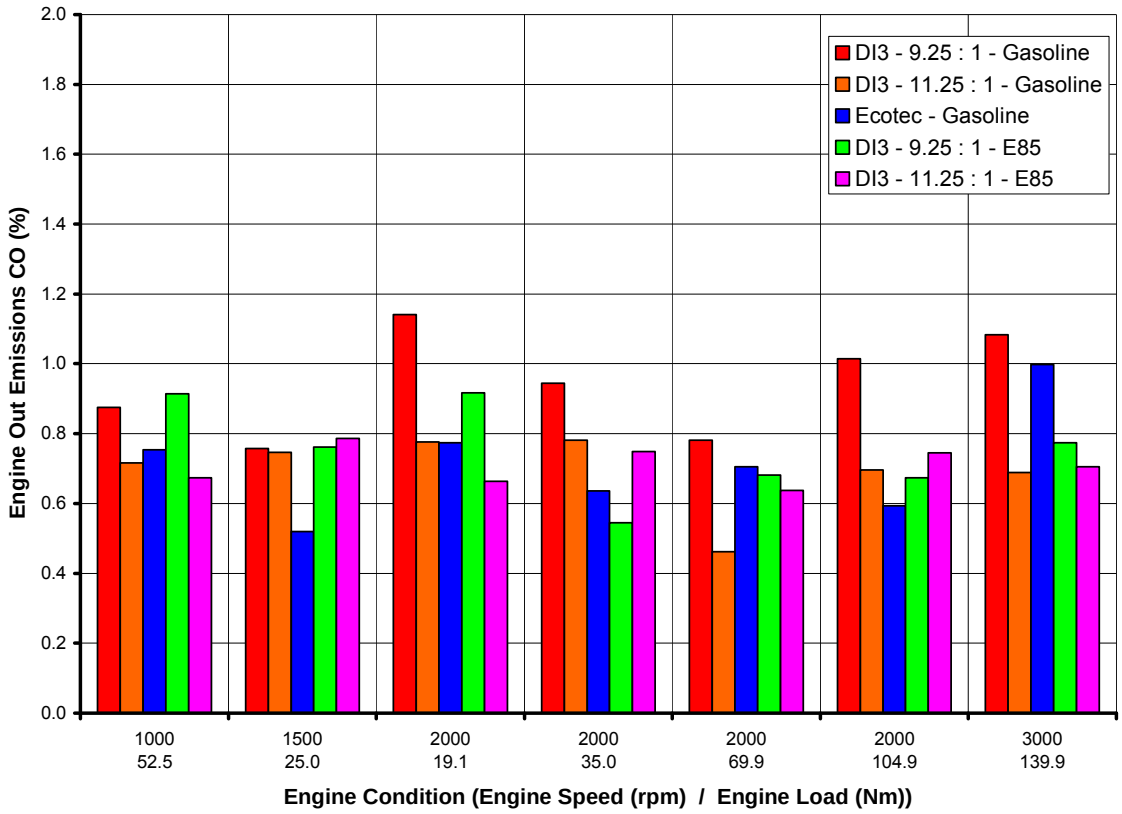

Figure 81:- Engine Out CO Emissions Comparison

Figure 81 shows the engine out CO emissions of each of the major engine configurations tested. The emissions concentrations are all in a range that could be easily converted to meet current emissions legislation with similar after treatment technologies (three way catalyst).

The CO emissions were all similar in a fairly tight band around 0.7%. CO emissions are very sensitive to air fuel ratio, as both the Ecotec and the DI3 engine were run with closed loop fuel control, the dominant factor affecting the CO emissions presented was the quality of the closed loop fuel control.

Full Load Test Data

Power curves were conducted with the following configurations (Hardware – Fuel – Turbocharger – Performance Level):

1. DI3 Engine – 9.25 : 1 Compression Ratio – Gasoline Fuel – Borg Warner 5303 988 0005 Turbocharger – Ecotec Performance Level.
2. DI3 Engine – 9.25 : 1 Compression Ratio – Gasoline Fuel – Borg Warner 5303 988 0005 Turbocharger – 25bar BMEP Performance Level.
3. DI3 Engine – 9.25 : 1 Compression Ratio – E85 Fuel – Borg Warner 5303 988 0005 Turbocharger – Ecotec Performance Level.
4. DI3 Engine – 9.25 : 1 Compression Ratio – E85 Fuel – Borg Warner 5303 988 0005 Turbocharger – 25bar BMEP Performance Level.
5. DI3 Engine – 11.25 : 1 Compression Ratio – Gasoline Fuel – Borg Warner 5303 988 0005 Turbocharger – Ecotec Performance Level.
6. DI3 Engine – 11.25 : 1 Compression Ratio – Gasoline Fuel – Borg Warner 5303 988 0005 Turbocharger – 25bar BMEP Performance Level.
7. DI3 Engine – 11.25 : 1 Compression Ratio – E85 Fuel – Borg Warner 5303 988 0005 Turbocharger – Ecotec Performance Level.
8. DI3 Engine – 11.25 : 1 Compression Ratio – E85 Fuel – Borg Warner 5303 988 0005 Turbocharger – 25bar BMEP Performance Level.
9. DI3 Engine – 11.25 : 1 Compression Ratio – Gasoline Fuel – Borg Warner 5303 988 0069 Turbocharger – Ecotec Performance Level.
10. DI3 Engine – 11.25 : 1 Compression Ratio – Gasoline Fuel – Borg Warner 5303 988 0069 Turbocharger – 25bar BMEP Performance Level.
11. DI3 Engine – 11.25 : 1 Compression Ratio – E85 Fuel – Borg Warner 5303 988 0069 Turbocharger – Ecotec Performance Level.
12. DI3 Engine – 11.25 : 1 Compression Ratio – E85 Fuel – Borg Warner 5303 988 0069 Turbocharger – 25bar BMEP Performance Level.

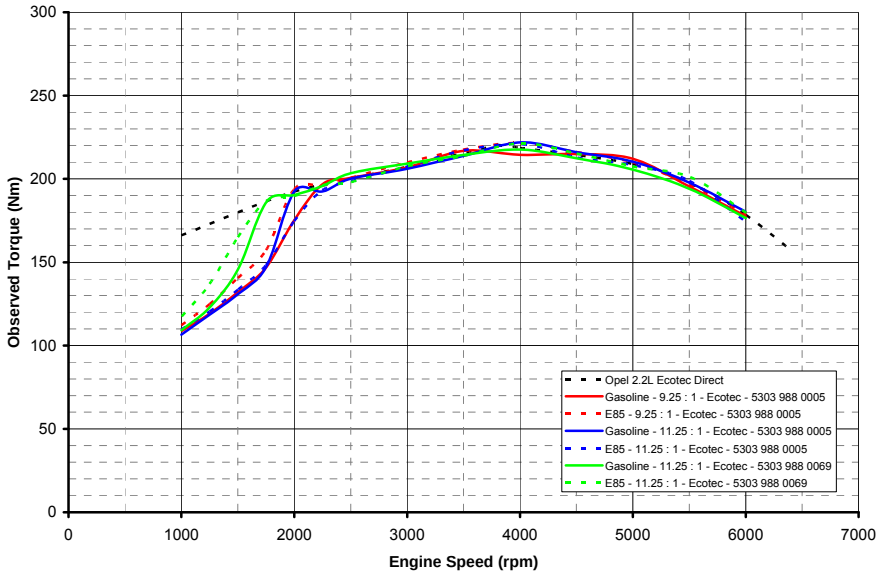

Figure 82:- Comparison of Engine Torque Output for Tests Run at Ecotec Performance Levels

Figure 82 shows the torque outputs from each configuration of the DI3 engine run at Ecotec performance levels compared with the Ecotec. Unfortunately, because of dynamometer limitations it was not possible to run a complete full load test on the Opel 2.2L Ecotec Direct Engine at Argonne National Laboratory. Full load performance was obtained from an MTZ article titled "2,2 l ECOTEC DIRECT – The New All-Aluminum Engine with Gasoline Direct Injection for the Opel Signum" [18].

At engine speeds above 2000rpm all configurations of the DI3 engine met the performance levels of the 2.2L Ecotec Direct engine. Additional improvements were realized with a Borg Warner 5303 988 0069 turbocharger, the DI3 engine with an 11.5 : 1 compression ratio met the performance of the 2.2L Ecotec Direct engine at all speeds above 1750rpm.

Low engine speed torque is typically an issue with turbocharged gasoline engines. This is apparent when comparing the DI3 engine with Opel 2.2L Ecotec Direct, at low engine speeds there is not enough energy in the exhaust for the turbo to make much boost (see Figure 86), hence the engine performance is close to what it would be in naturally aspirated form.

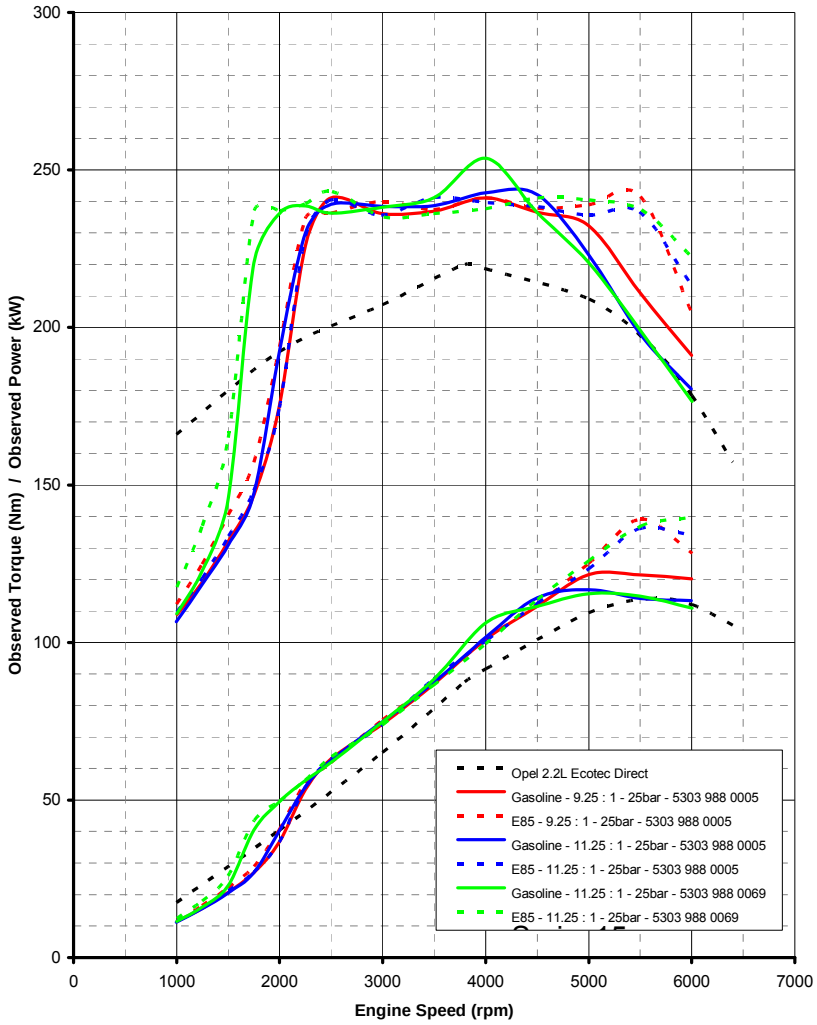

Figure 83:- Engine Torque and Power Output for Tests Run at 25bar Performance Levels

Figure 83 shows the torque outputs from each configuration of the DI3 engine run at the 25bar BMEP performance level. At engine speeds between 2250rpm and 4500rpm all configurations of the DI3 engine could achieve the 25bar BMEP (238Nm) performance level. With a Borg Warner 5303 988 0069 turbocharger fitted the 25bar BMEP performance could be achieved at engine speeds as low as 1750rpm, with both gasoline and E85 fuels. With E85 fuel 25bar BMEP could be maintained to an engine speed of 5500rpm at both compression ratios with either turbo fitted.

The DI3 engine was tested at the 25bar performance level so downspeeding could be considered. For down speeding to be an option the DI3 engine would need to make the same (or similar) power as the 2.2L Ecotec Direct Engine but at lower speeds, so as to maintain vehicle performance with higher gearing.

The peak power output of the 2.2L Ecotec Direct Engine is 114kW at 5600rpm, at the 25bar performance level the DI3 engine makes this power at around 4500rpm. Thus downspeeding should be possible without compromising maximum engine speed.

Effect Of Fuel Type On DI3 Full Load Performance.

To illustrate the different characteristics of gasoline and E85 and the effects they had on the full load performance of the DI3 engine, comparisons will be made between the tests run at 9.25 : 1 at the 25bar performance level.

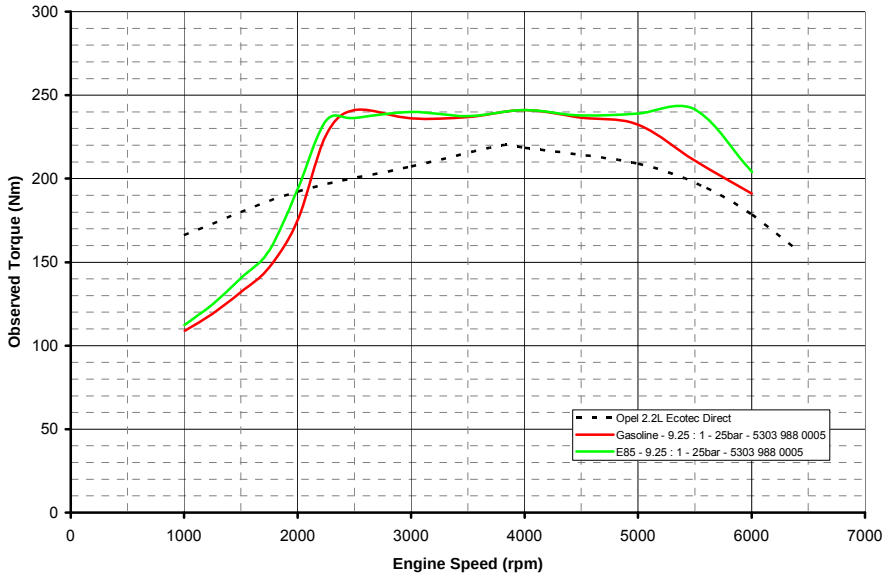

Figure 84:- Comparison of Engine Torque Output with Gasoline and E85 Fuels
DI3 Engine – 9.25 : 1 Compression Ratio – Borg Warner 5303 988 0005 Turbocharger
25bar Performance Level

Figure 84 shows a slight increase in low speed torque when the engine is run on E85, and a more significant increase in high speed torque. Although the brake performance of the engine is similar between 2250rpm and 5000rpm (modulated by the turbocharger wastegate) the efficiency with which 25bar BMEP is achieved is significantly different for the two fuels.

E85 is less prone to detonation than gasoline, due to its higher octane number. Due to its relative resistance to detonation the combustion phasing for E85 was more favorable than for gasoline.

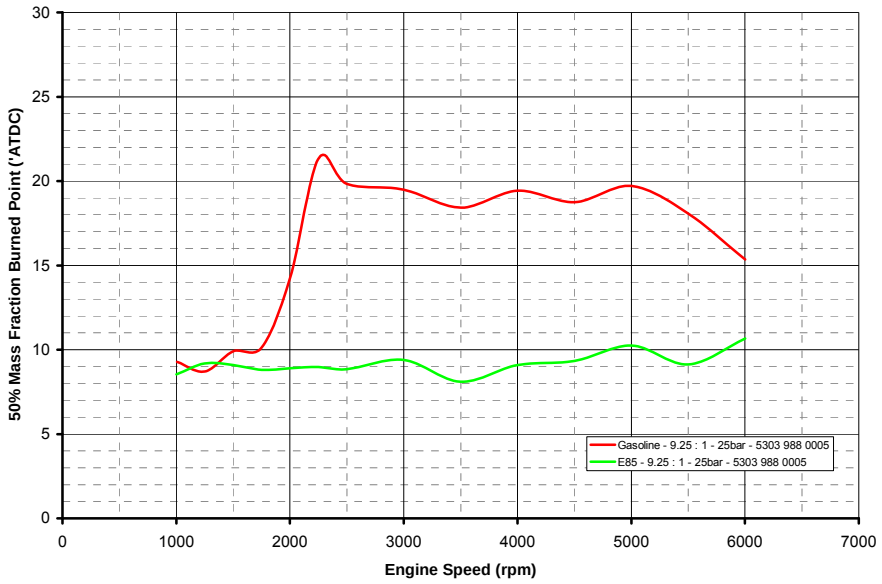

Figure 85:- Comparison of 50% Mass Fraction Burned Point with Gasoline and E85 Fuels DI3 Engine – 9.25 : 1 Compression Ratio – Borg Warner 5303 988 0005 Turbocharger 25bar Performance Level

An engine is typically most efficient when the 50% mass fraction burned point is between 8° and 10°ATDC. Figure 85 shows that with E85 fuel the DI3 engine could be run with optimum spark timing at all speeds, however, with gasoline as soon as the turbo was able to make significant boost it was necessary to retard the spark timing significantly.

Due to inefficiencies brought about by retarded combustion it was necessary to run with increased boost for the gasoline fueled DI3, see Figure 86.

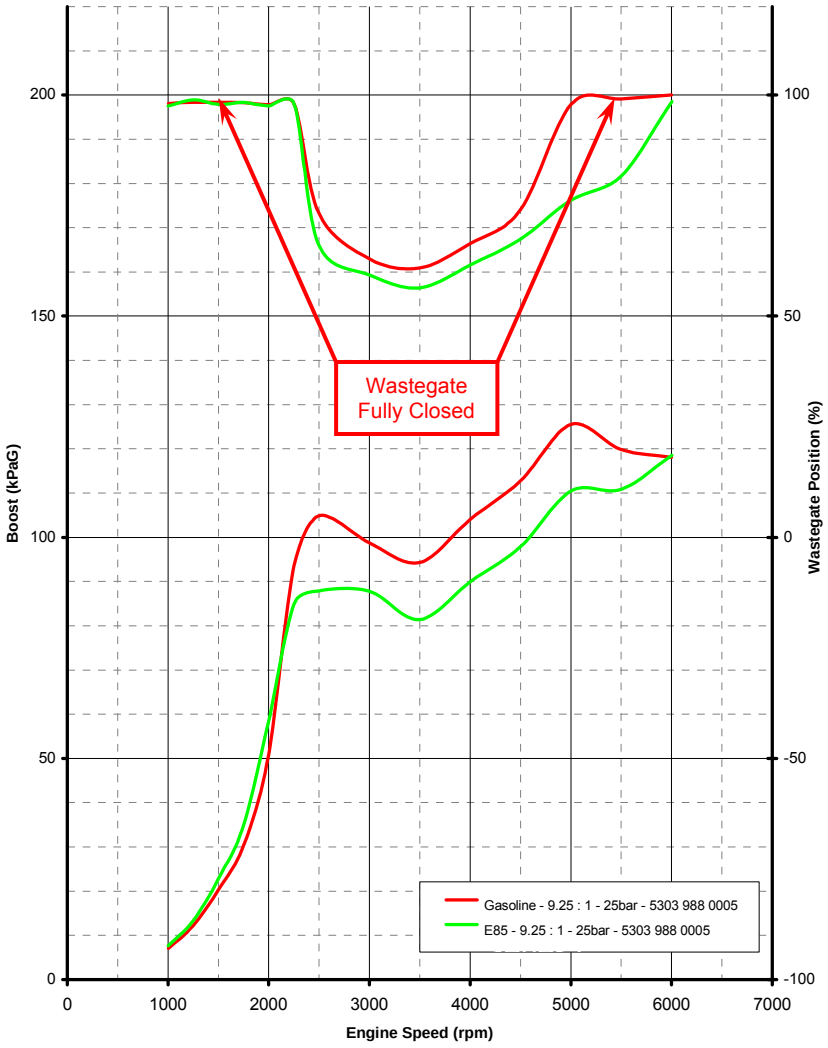

Figure 86:- Comparison of Boost and Wastegate Positions with Gasoline and E85 Fuels DI3 Engine – 9.25 : 1 Compression Ratio – Borg Warner 5303 988 0005 Turbocharger 25bar Performance Level

Figure 84 shows that 25bar BMEP can be achieved at speeds up to 5500rpm for E85 fuel but only 4500rpm with gasoline fuel. The turbocharger as fitted can only generate a certain amount of airflow, the amount is modulated by the wastegate up to a certain maximum amount, when the wastegate is fully closed the maximum possible airflow is achieved. With E85 fuel the available air is used more efficiently, as indicated by the lower boost levels.

The torque output for the engine with gasoline fuel drops above 4500rpm because the wastegate is fully closed. The wastegate is not fully closed until 6000rpm with E85 fuel, consequently it is at 6000rpm that the BMEP drops below 25bar.

A consequence of retarded combustion phasing is deteriorating combustion stability. One of the constraints for full load testing was that the COV of IMEP could not exceed 2.5%.

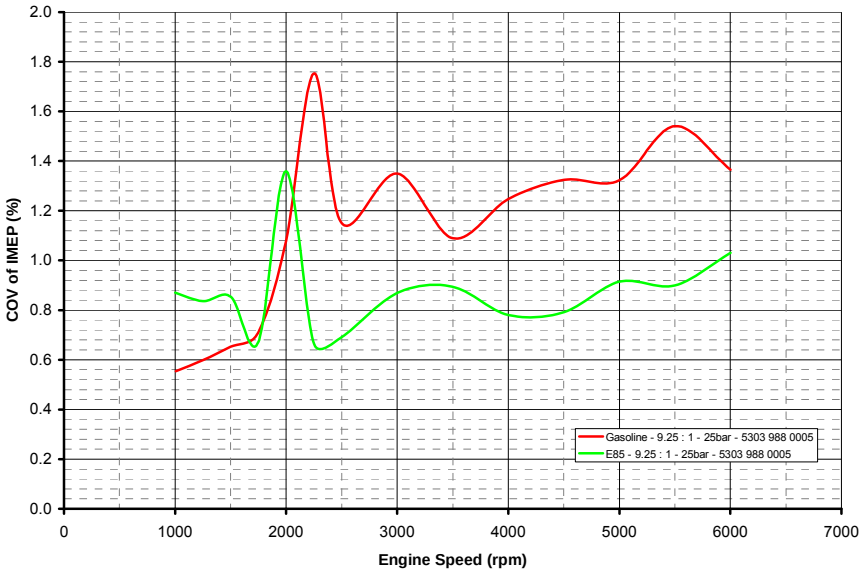

Figure 87:- Comparison of COV Of IMEP with Gasoline and E85 Fuels
DI3 Engine – 9.25 : 1 Compression Ratio – Borg Warner 5303 988 0005 Turbocharger
25bar Performance Level

Although the stability is not near the COV of IMEP limit of 2.5%, the stability of the DI3 engine when fueled with gasoline is worse than when fueled with E85.

Due to the higher heat of vaporization of E85 and the retarded spark timing of gasoline, exhaust gas temperatures tend to be higher with gasoline.

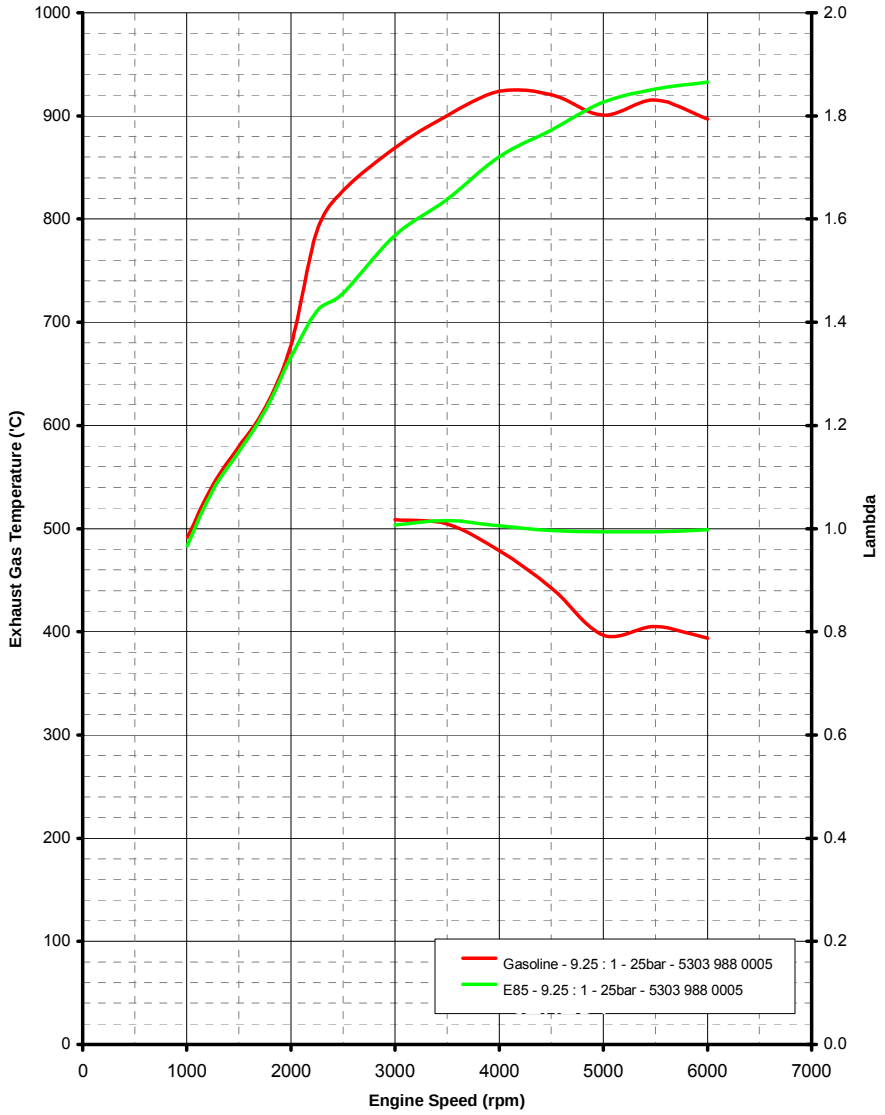

Figure 88:- Comparison of Exhaust Gas Temperatures and Lambda with Gasoline and E85 Fuels DI3 Engine – 9.25 : 1 Compression Ratio – Borg Warner 5303 988 0005 Turbocharger 25bar Performance Level

In order to keep the exhaust gas temperatures below the maximum permissible temperature of 950°C, it was necessary to add extra fuel for gasoline operation. The excess fuel acts as a diluent, increasing the heat capacity of the charge. This reduces the compression temperatures, reducing the tendency of the engine to knock and reduces combustion, expansion and hence exhaust gas temperatures. **Error! Reference source not found.** It was possible to run lambda = 1 at all speeds with E85.

The results of the retarded combustion and over fuelling are that torque output at high speeds are reduced with gasoline fuel compared to E85 and that the fuel consumption is compromised with gasoline.

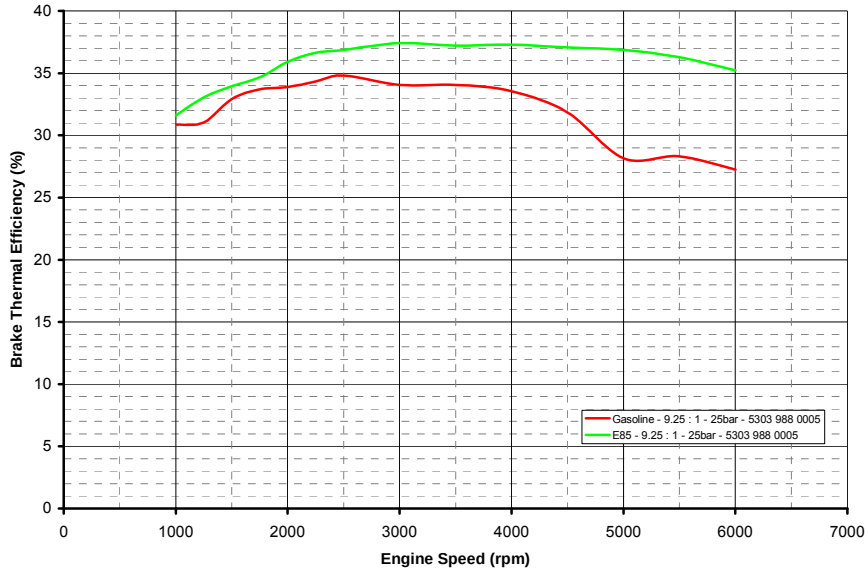

Figure 89:- Comparison of Brake Thermal Efficiency with Gasoline and E85 Fuels DI3 Engine – 9.25 : 1 Compression Ratio – Borg Warner 5303 988 0005 Turbocharger 25bar Performance Level

Figure 89 shows the brake thermal efficiency of gasoline deteriorating with engine speed when compared to E85.

Effect Of Compression Ratio On DI3 Full Load Performance.

To illustrate the effect compression ratio had on the full load performance of the DI3 engine, comparisons will be made between the tests run on gasoline at the 25bar performance level with the Borg Warner 5303 988 0005 turbocharger.

Figure 90 shows the torque output of the DI3 engine at compression ratios of 9.25 : 1 and 11.25 : 1 together with the torque output of the comparator engine.

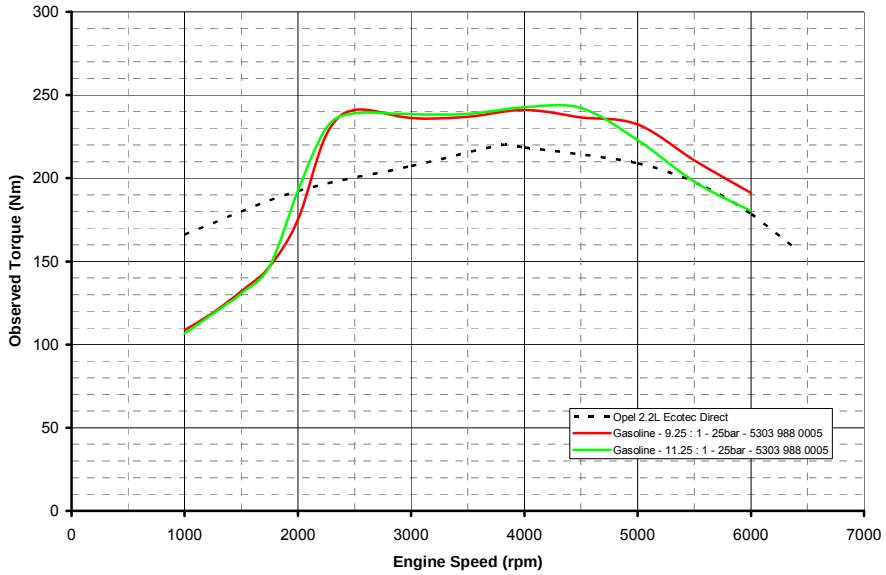

Figure 90:- Comparison of Engine Torque Output with 9.25 and 11.25 :1 Compression Ratios DI3 Engine – Gasoline Fuel – Borg Warner 5303 988 0005 Turbocharger – 25bar Performance Level.

Figure 90 shows a degradation in high speed engine performance with the higher compression ratio. The degradation in performance is due to increasingly retarded combustion phasing, the result of an increased tendency for detonation due to increased compression ratio.

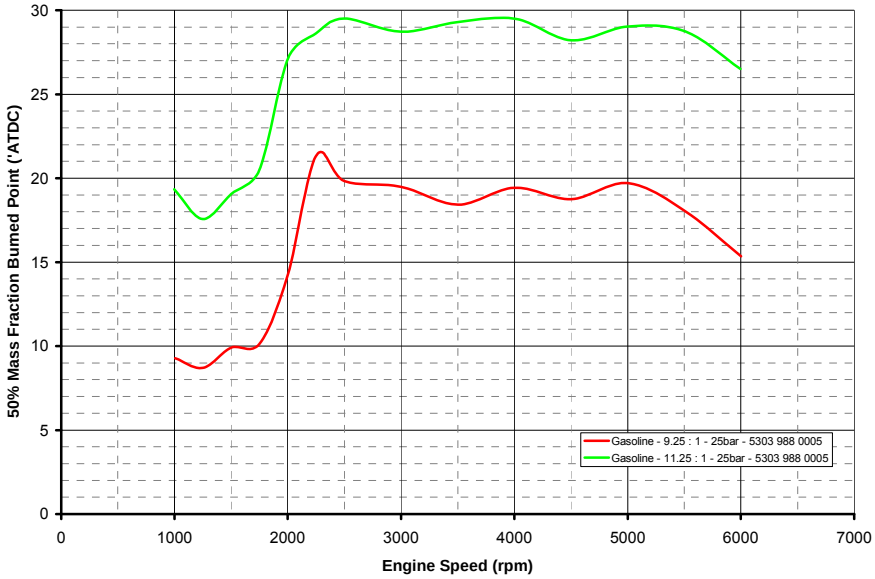

Figure 91:- Comparison of 50% MFB with 9.25 and 11.25 :1 Compression Ratios
DI3 Engine – Gasoline Fuel – Borg Warner 5303 988 0005 Turbocharger – 25bar Performance Level.

Figure 91 shows that the combustion phasing is significantly more retarded for the 11.25 : 1 compression ratio than for the 9.25 : 1 compression ratio. Between engine speeds of 2500rpm and 5500rpm the 50% mass fraction burned point for the 11.25 : 1 compression ratio is around 29°ATDC, when combustion is so retarded the engine is very inefficient.

Due to the inefficient combustion it was necessary to provide the 11.25 : 1 engine with more boost, and consequently more airflow than the 9.25 : 1 engine to achieve the same torque.

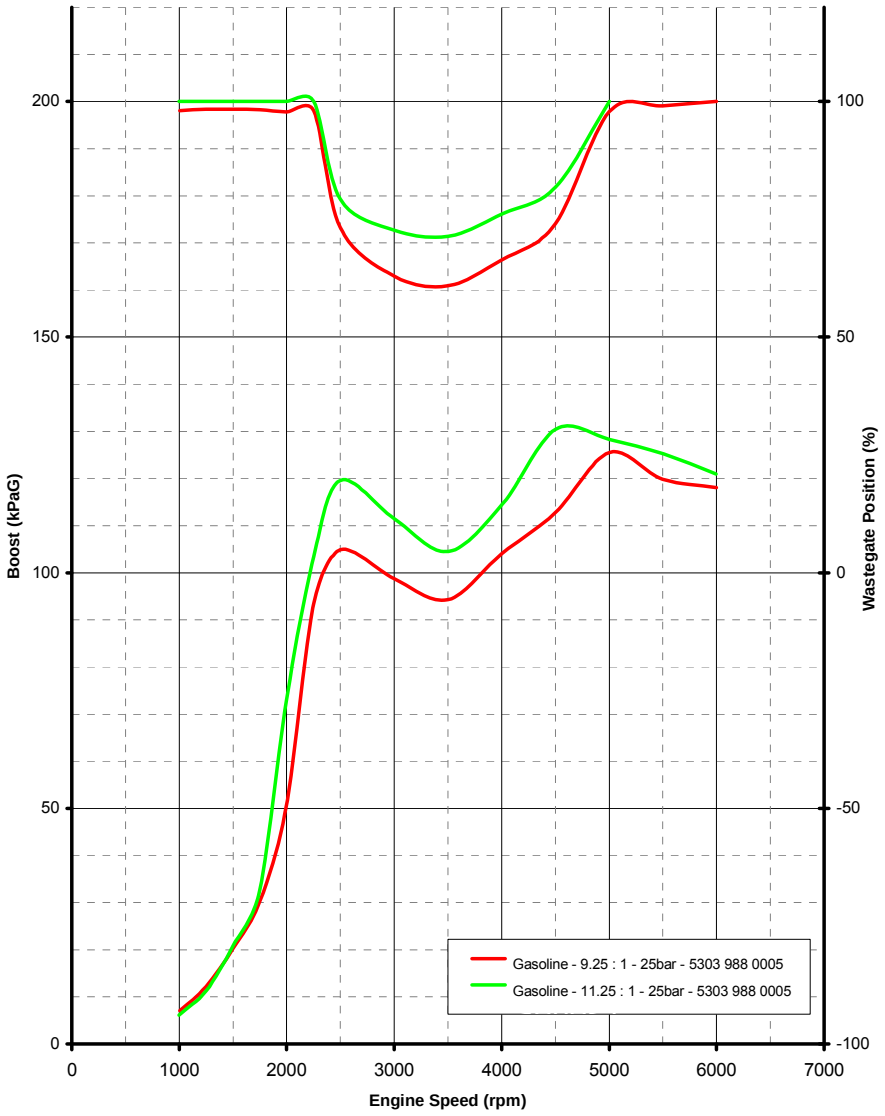

Figure 92:- Comparison of Boost and Wastegate Position with 9.25 and 11.25 :1 Comp Ratios DI3 Engine – Gasoline Fuel – Borg Warner 5303 988 0005 Turbocharger – 25bar Performance Level.

At a mass fraction burned point of 29°ATDC combustion stability will tend to be poor.

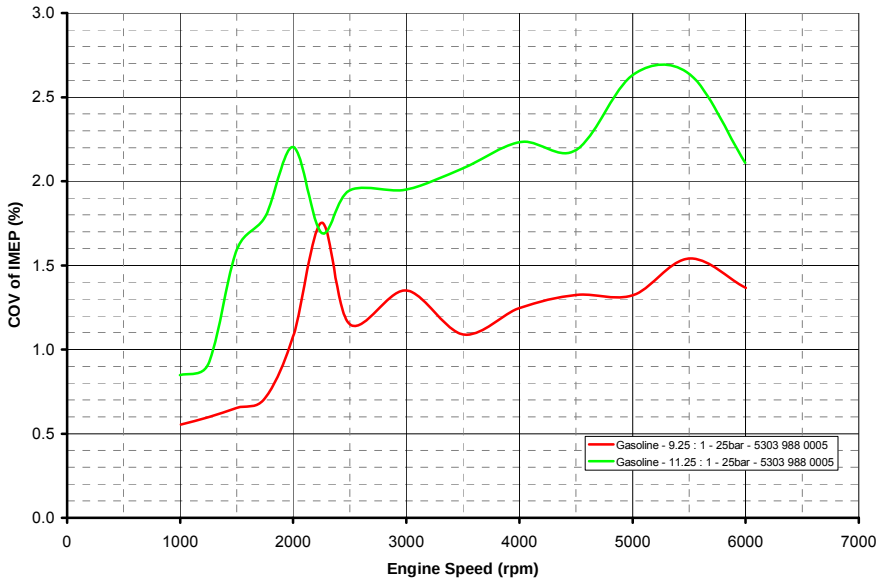

Figure 93:- Comparison of COV Of IMEP with 9.25 and 11.25 :1 Compression Ratios DI3 Engine – Gasoline Fuel – Borg Warner 5303 988 0005 Turbocharger – 25bar Performance Level.

There is a significant degradation in combustion stability seen with the increased compression ratio. At 5000 and 5500rpm with an 11.25 : 1 compression ratio the stability was in excess of the limit value of 2.5% due to the retarded combustion phasing. As previously stated the combustion phasing is limited by detonation. Typically combustion phasing may be advanced with the addition of a diluent, either excess fuel or cooled EGR.

The amount of additional excess fuel that can be added is limited. Fuel is already rich at $\lambda \geq 0.76$ to cool the turbine. The addition of more fuel may degrade combustion stability and torque output and will reduce efficiency. Any degradation of combustion stability or torque output will be offset (maybe mitigated) by combustion phasing improvements made possible. Any torque loss greater than can be cancelled by combustion phasing improvements cannot be easily made up, as increasing the boost pressure would result in a greater tendency for the engine to detonate, necessitating the combustion phasing be retarded.

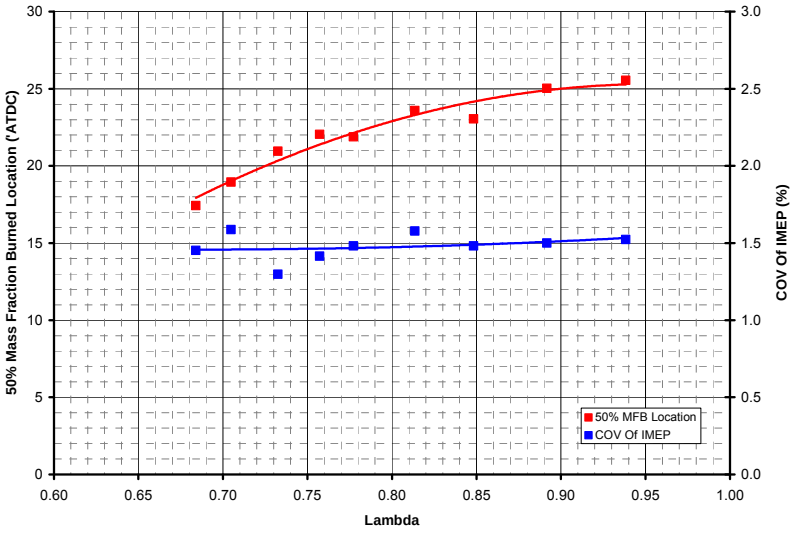

Figure 94:- The Sensitivity of Combustion Phasing and Combustion Stability to Excess Fuel DI3 Engine – Gasoline Fuel - 11.5 : 1 Compression Ratio – IMOP 80°ATDC – EMOP 100°BTDC Zero EGR - 2500rpm - 2.2L Ecotec Direct Performance Level.

Figure 94 shows the sensitivity of combustion phasing and combustion stability to excess fuel. Although combustion phasing is improved with excess fuel, the combustion stability remains effectively constant.

Another method that has been used to improve combustion phasing is the addition of cooled EGR, however, the amount of EGR that can be added is limited. Any EGR addition will necessitate boost pressure be increased (the addition of EGR causes there to be a lower percentage of oxygen in the cylinder, consequently there needs to be more charge inducted / pushed into the cylinder) and as shown in Figure 92 at higher speeds the wastegate is closed. Typically large quantities of EGR are needed to have a significant effect on combustion phasing.

Figure 95 and Figure 96 show the effect of adding cooled EGR to the torque, boost pressure, wastegate position, combustion phasing and combustion stability of the gasoline fueled DI3 engine.

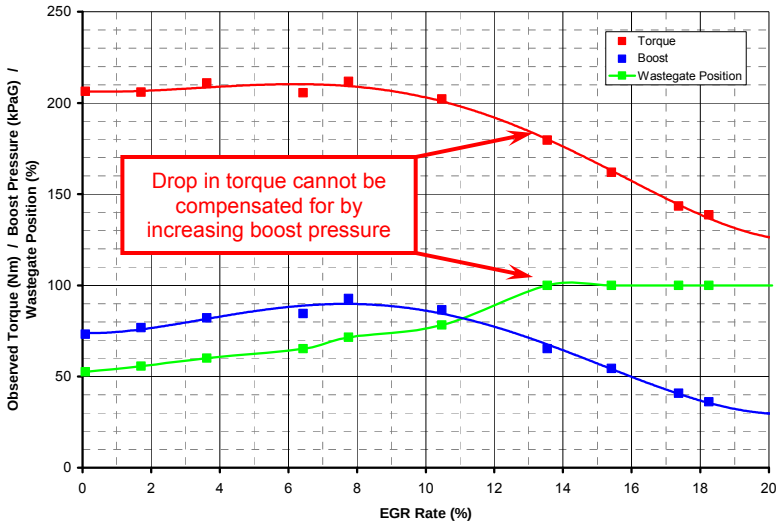

Figure 95:- The Sensitivity of Torque, Boost Pressure and Wastegate Position to Cooled EGR DI3 Engine – Gasoline Fuel - 11.5 : 1 Compression Ratio – IMOP 80°ATDC – EMOP 100°BTDC 3000rpm - 2.2L Ecotec Direct Performance Level

Adding EGR causes the torque to drop but up to an EGR rate of 10% the torque drop can be made up by increasing boost pressure. With more than 10% EGR the wastegate is fully closed, consequently there is no way to make up for lost performance. This test was conducted at 3000rpm at the 2.2L Ecotec Direct performance level. With no EGR it was necessary to have wastegate 50% open to make the desired torque. At the 25bar performance level with zero EGR to make the desired performance the wastegate needs to be much closer to its closed position, see Figure 92, consequently there is less room to regain the performance loss associated with increasing amounts of EGR. At engine speeds of 5000rpm and above the wastegate is fully closed in order to try and make the 25bar BMEP performance, consequently the addition of any EGR will cause torque to drop. Further optimization of the boosting system would be required to enable higher EGR rates.

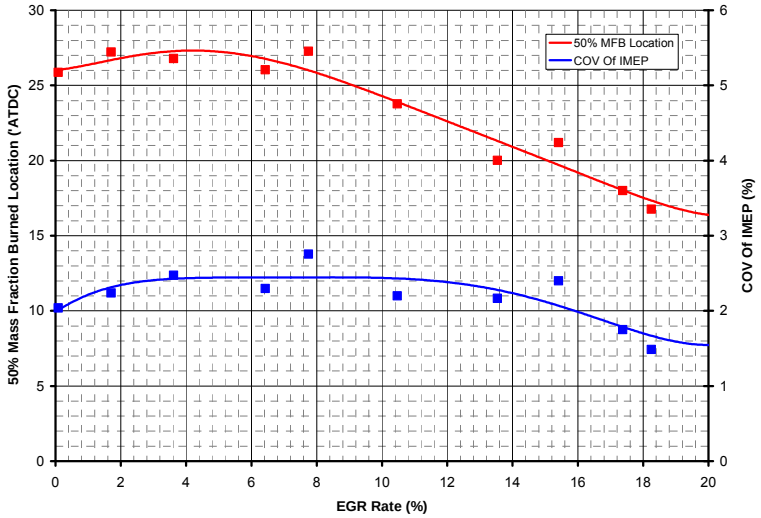

Figure 96:- The Sensitivity of Combustion Phasing and Combustion Stability to Cooled EGR DI3 Engine – Gasoline Fuel - 11.5 : 1 Compression Ratio – IMOP 80°ATDC – EMOP 100°BTDC 3000rpm - 2.2L Ecotec Direct Performance Level.

Figure 96 shows that combustion phasing and combustion stability are insensitive to the addition of cooled EGR at levels up to 10%. At levels in excess of 10% both the combustion phasing and combustion stability are seen to improve, however, as discussed previously at these levels of EGR the torque also falls.

Neither adding excess fuel nor EGR look promising as methods for improving combustion stability on the DI3 engine tested. Any further increase in compression ratio would necessitate the combustion phasing be retarded further. Consequently the combustion stability of the gasoline fueled DI3 engine would be further degraded. Thus if performance with gasoline fuel is to be maintained 11.25 : 1 would seem to be the maximum compression ratio for this engine. Figure 90, shows that with a compression ratio of 11.25 : 1 at engine speeds in excess of 5500rpm the peak torque does not exceed that of the 2.2L Ecotec Direct, any increase in compression ratio would cause the performance of the gasoline DI3 to drop below the levels of the comparator engine.

The exhaust gas temperature tends to be higher with retarded combustion phasing, it causes the peak cylinder pressure and temperature to occur later in the expansion stroke, consequently, expansion takes place over a smaller volume change before the exhaust valve opens, thus the temperature (and pressure) of the exhaust gasses are higher. At high engine speeds (greater than 4000rpm) exhaust gas temperature (turbine entry temperature) is a concern. There are two diluents commonly used to control exhaust gas temperature, either excess fuel or cooled EGR. The sensitivity of exhaust gas temperature and brake thermal efficiency to excess fuel is shown in Figure 97.

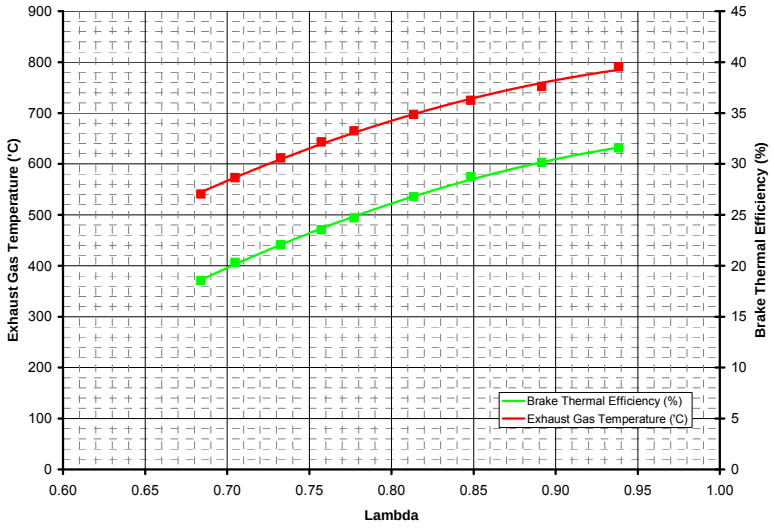

Figure 97:- The Sensitivity of Exhaust Gas Temperature and BTE to Excess Fuel - DI3 Engine Gasoline Fuel - 11.5 : 1 Compression Ratio – IMOP 80°ATDC – EMOP 100°BTDC - Zero EGR 2500rpm - 2.2L Ecotec Direct Performance Level.

The addition of excess fuel increases the heat capacity of the charge, reducing combustion temperatures improving combustion phasing, see Figure 94. Figure 97 also shows that adding excess fuel has a detrimental effect on fuel consumption. At 2500rpm 200Nm, when the DI3's fuelling was richened from $\lambda = 0.95$ to $\lambda = 0.7$ the brake thermal efficiency was reduced from 31% to 20%.

The sensitivity of exhaust gas temperature to cooled EGR is shown in Figure 98.

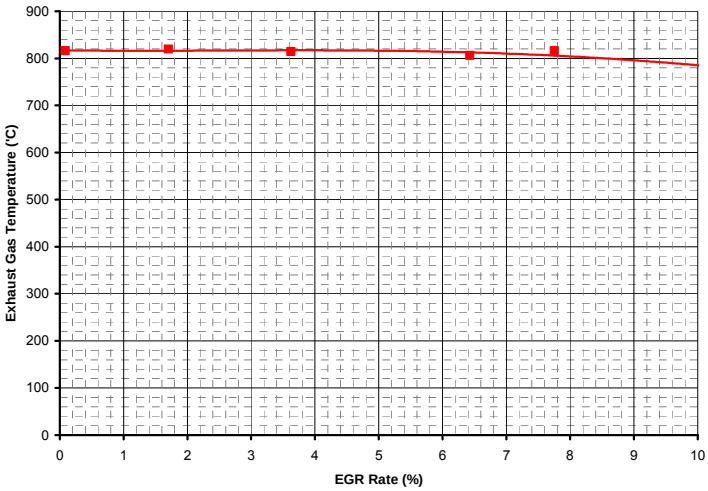

Figure 98:- The Sensitivity of Exhaust Gas Temperature to Cooled EGR
DI3 Engine – Gasoline Fuel - 11.5 : 1 Compression Ratio – IMOP 80°ATDC – EMOP 100°BTDC
3000rpm - 2.2L Ecotec Direct Performance Level.

The exhaust gas temperature of the DI3 at full load was surprisingly insensitive to the addition of cooled EGR under full load conditions, this may have been because it was not possible to add sufficient amounts of EGR due to performance degradation.

To keep exhaust gas temperatures below the 950°C limit the fuel was enriched.

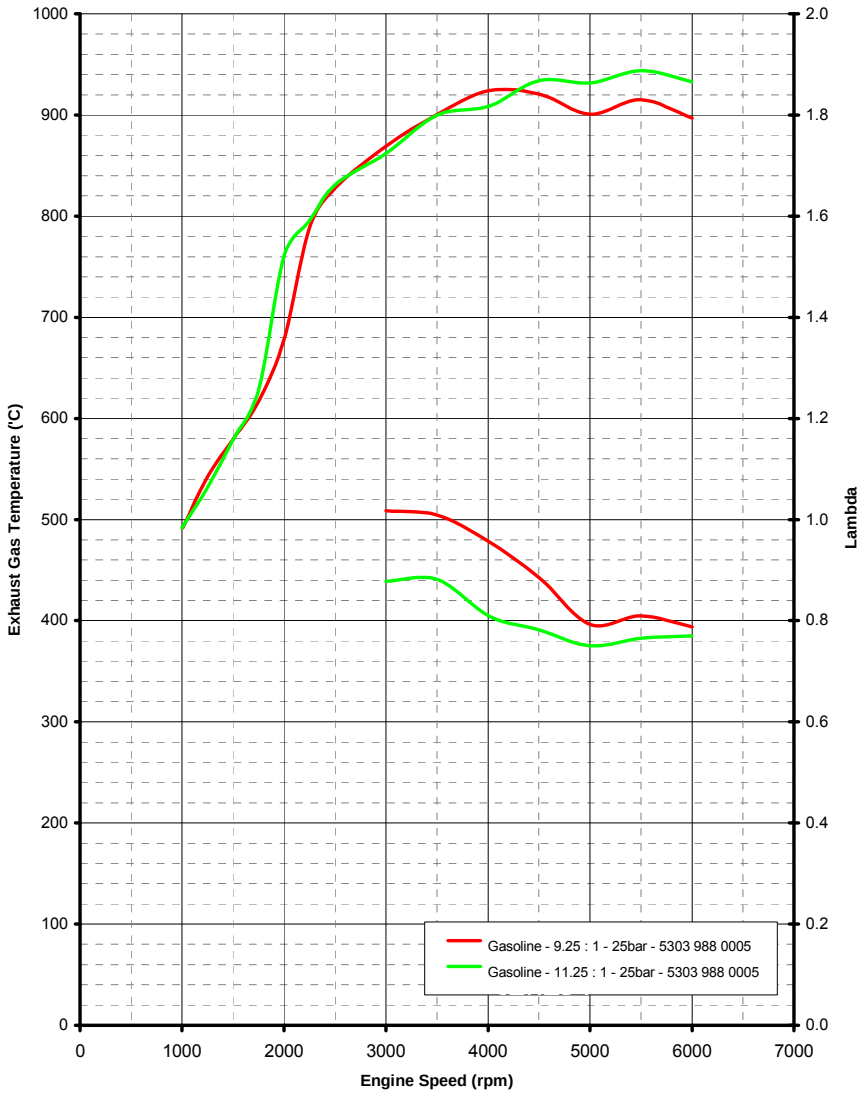

Figure 99:- Comparison of Lambda with 9.25 and 11.25 :1 Compression Ratios
DI3 Engine – Gasoline Fuel – Borg Warner 5303 988 0005 Turbocharger – 25bar Performance Level.

Figure 99 shows that because of the increasingly retarded combustion of the 11.25 : 1 engine it was necessary to add more fuel to keep the exhaust gas temperatures cool.

The result of the retarded combustion and over fuelling is a reduction in torque at high engine speeds (see Figure 90), and reduced thermal efficiency with the higher compression ratio.

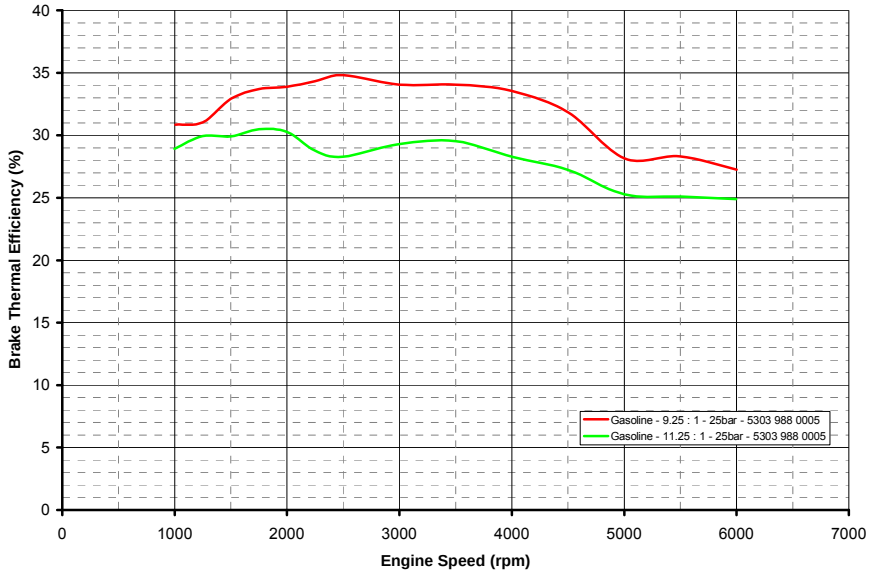

Figure 100:- Comparison of Brake Thermal Efficiency with 9.25 and 11.25 :1 Compression Ratios DI3 Engine – Gasoline Fuel – Borg Warner 5303 988 0005 Turbocharger – 25bar Performance Level.

To eliminate Pre-ignition experienced at 11.25 : 1 compression ratio the fuelling was enriched.

Effect Of Turbocharger Type On DI3 Full Load Performance.

To illustrate the effect the two different turbochargers had on the full load performance of the DI3 engine, comparisons will be made between the tests run at the 25bar performance with E85 fuel. Because of the higher octane number and higher heat of vaporization, previously discussed, it was not necessary to retard the combustion phasing due to detonation or add excess fuel to keep the exhaust cool.

The chart below shows the engine torque output of the DI3 engine with both the Borg Warner 5303 988 0005 and the Borg Warner 5303 988 0069 together with the torque output of the comparator engine.

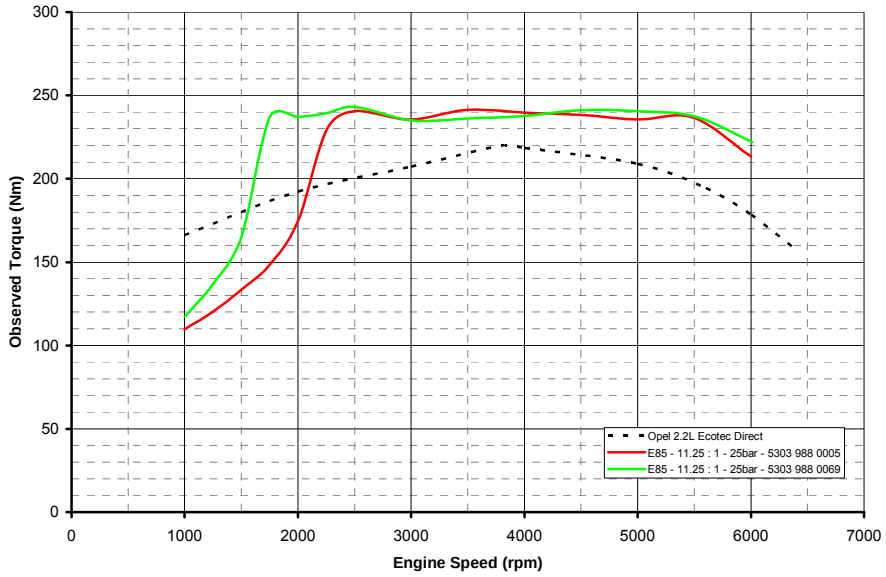

Figure 101:- Comparison of Engine Torque Output with 0005 and 0069 Turbochargers DI3 Engine – Gasoline Fuel – 11.25 :1 Compression Ratio – 25bar Performance Level.

Figure 101 shows significantly improved low speed torque with the 5303 988 0069 turbocharger. With the 5303 988 0069 turbocharger 25bar BMEP can be achieved at engine speeds as low as 1750rpm, with the 5303 988 0005 turbocharger 25bar BMEP cannot be achieved until 2250rpm. This improvement in low speed torque will improve the response of any vehicle in which the engine is fitted. As discussed previously low speed torque is typically an issue with turbocharged gasoline engines. The 5303 988 0069 addresses many of these issues. The torque of the 2.2L Ecotec Direct can be achieved at speeds as low as 1500rpm.

The increase in low speed torque is due to the improved low speed boost afforded by the Borg Warner 5303 988 0069 turbocharger.

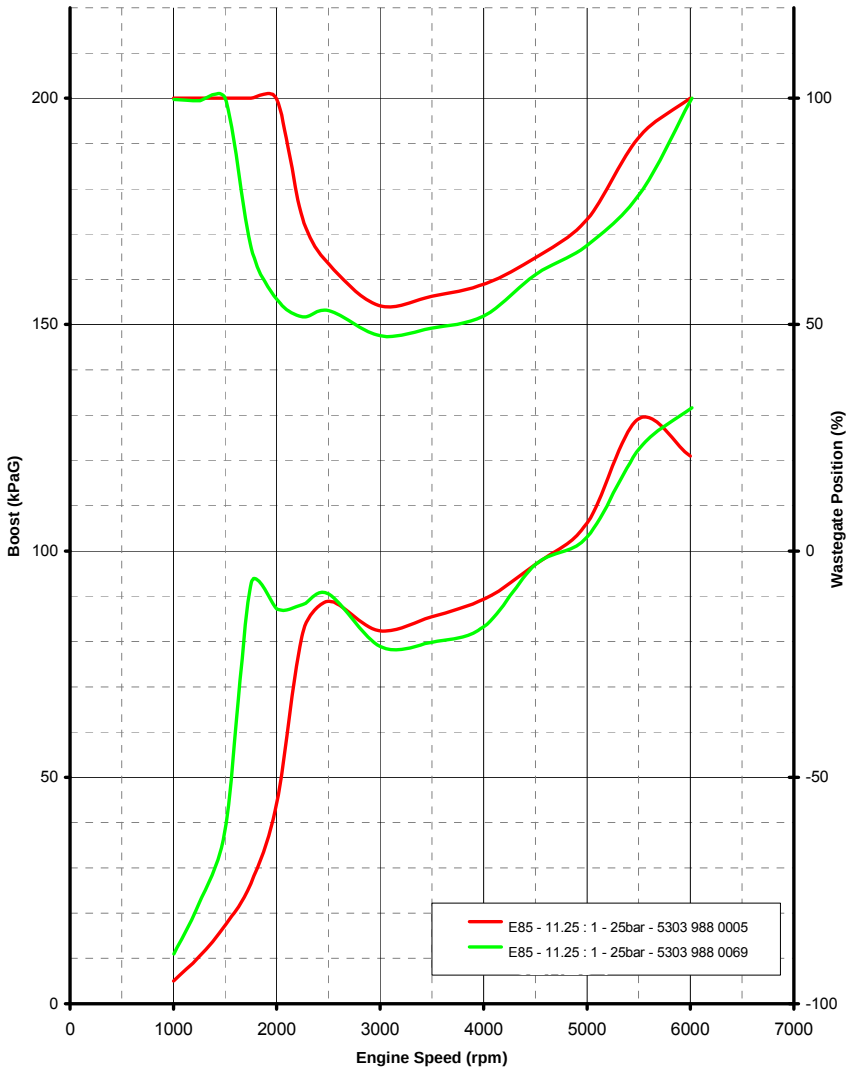

Figure 102:- Comparison of Boost and Wastegate Position With 0005 and 0069 Turbochargers DI3 Engine – Gasoline Fuel – 11.25 :1 Compression Ratio – 25bar Performance Level.

The improvement in low speed boost is due to differences in the compressors of the two turbochargers, the 5303 988 0069 can generate a greater pressure ratio across the compressor at low flow rates [19]. The wastegate is required to modulate the output of the 5303 988 0069 turbocharger at speeds in excess of 1500rpm so as not to exceed the 25bar BMEP performance objective, with the 5303 988 0005 the wastegate was not opened until engine speeds in excess of 2000rpm.

Improved low speed boost and similar high speed performance make the Borg Warner 5303 988 0069 turbochargers more suitable for use on the DI3 Engine, it does not however offer sufficient capacity to make the use of cooled EGR for combustion phasing improvements or exhaust gas temperature reduction possible.

Downspeeding

The full load testing conducted on the DI3 engine confirmed that downspeeding was an option that should be considered to improve fuel economy. As previously discussed, in downspeeding, a vehicle uses higher gear ratios, thus under drive cycle conditions the engine will run slower and at a higher load. Reducing engine speed to reduce friction losses and increasing engine load tends to reduce pumping losses. Thus fuel economy is improved.

The impact of downspeeding on fuel economy for the MAHLE DI3 engine is shown in Table 15.

Engine Configuration	Fuel	Downspeeding (%)	City Fuel Consumption (MPG)	Highway Fuel Consumption (MPG)	Combined Fuel Consumption (MPG)
2.2L Ecotec Direct	Gasoline (E0)	0	26.2	34.4	29.3
MAHLE DI3 9.25 : 1	Gasoline (E0)	0	29.8	35.0	31.9
		5	30.2	35.3	32.3
		10	30.6	35.6	32.7
		15	31.0	35.7	32.9
		20	31.2	35.9	33.2
	E85	0	21.8	25.5	23.3
		5	22.1	25.7	23.6
		10	22.5	26.0	23.9
		15	22.7	26.1	24.1
		20	23.0	26.2	24.3
MAHLE DI3 11.25 : 1	Gasoline (E0)	0	31.1	36.7	33.4
		5	31.6	37.1	33.8
		10	32.1	37.3	34.3
		15	32.6	37.6	34.7
		20	33.0	37.8	35.0
	E85	0	22.8	26.8	24.4
		5	23.1	27.1	24.8
		10	23.5	27.3	25.1
		15	23.8	27.5	25.3
		20	24.1	27.7	25.6

Table 15:- The Effect Of Downspeeding On Drive Cycle Fuel Economy.

As the percentage of downspeeding is increased the fuel consumption is improved for all configurations of the MAHLE DI3 engine.

Table 16 shows that if the 11.5 : 1 E85 DI3 engine were downspeeded by 20% the fuel economy penalty compared to the 2.2L Ecotec Direct running on gasoline is reduced to 12.8%. If the DI3 engine were run on gasoline it would use 19% less fuel than the Ecotec.

Engine Configuration	Fuel	Downspeeding (%)	City Fuel Economy Improvement Over 2.2L Ecotec Direct (%)	Highway Fuel Economy Improvement Over 2.2L Ecotec Direct (%)	Combined Fuel Economy Improvement Over 2.2L Ecotec Direct (%)
MAHLE DI3 9.25 : 1	Gasoline (E0)	0	13.7	1.8	8.8
		5	15.1	2.7	10.0
		10	16.8	3.4	11.3
		15	18.2	3.9	12.3
		20	19.2	4.3	13.0
	E85	0	-16.9	-25.8	-20.6
		5	-15.6	-25.2	-19.5
		10	-14.2	-24.5	-18.5
		15	-13.2	-24.1	-17.7
		20	-12.1	-23.8	-17.0
MAHLE DI3 11.25 : 1	Gasoline (E0)	0	18.9	6.6	13.8
		5	20.6	7.7	15.3
		10	22.7	8.4	16.8
		15	24.4	9.3	18.1
		20	26.1	9.8	19.3
	E85	0	-13.0	-22.2	-16.8
		5	-11.7	-21.3	-15.6
		10	-10.4	-20.6	-14.6
		15	-9.0	-20.2	-13.7
		20	-8.0	-19.5	-12.8

Table 16:- Drive Cycle Fuel Economy Comparison - Downspeeded DI3 Compared to Ecotec

Table 17 shows predicted performance of the Chevrolet HHR with both the Ecotec and 11.5 : 1 DI3 engine (Borg Warner 5303 988 0069) fitted. Vehicle performance when judged by common metrics is generally similar for both the Ecotec and the E85 fueled DI3 engines.

As the final drive ratio of the DI3 powered vehicle is decreased acceleration times generally slow. This is most noticeable for passing acceleration, 50 to 70mph in top gear. As the degree of downspeeding was increased the engine speed at 50mph fell to 1570rpm below the speed at which the turbocharger makes significant boost. For accelerations from rest the slowing of acceleration times is offset to a large degree by the reduced number of gear changes required with higher final drive ratios (for example with 0% downspeeding it is necessary to change gear during the 0 to 30mph acceleration, with 5% down speeding 30mph can be achieved in first gear).

The predicted accelerations of the DI3 engine when fueled with gasoline were slightly worse than when fueled by E85, due primarily to the loss of power associated with the spark retard necessary to avoid detonation with gasoline fuel.

In this application it might be appropriate to downspeed the DI3 engine by 15%. When fueled with E85 vehicle performance with the DI3 would exceed that offered by the gasoline fueled Ecotec, with the exception of the passing acceleration time (0.7 seconds slower). The gasoline fueled engine (with 15% downspeeding) would post acceleration times slightly worse than those offered by the Ecotec (again with the exception of the passing acceleration time, 1.1 seconds slower).

Engine Configuration	Fuel	Downspeeding (%)	Combined Fuel Consumption (MPG)	0 to 30mph Acceleration (seconds)	0 to 60mph Acceleration (seconds)	50 to 70mph Acceleration (seconds)	Standing 1/4 Mile (seconds / mph)	Maximum Speed (mph / gear)
2.2L Ecotec Direct	Gasoline (E0)	0	29.3	3.2	8.3	11.9	16.5 / 86.8	130 / 5
MAHLE DI3 11.25 : 1	Gasoline (E0)	0	33.4	3.4	8.6	10.1	16.7 / 86.6	132 / 5
		5	33.8	3.2	8.7	10.8	16.7 / 86.4	132 / 5
		10	34.3	3.2	8.7	11.7	16.7 / 86.7	132 / 5
		15	34.7	3.2	8.4	13.0	16.7 / 87.4	129 / 5
		20	35.0	3.3	8.4	14.8	16.7 / 87.2	131 / 4
	E85	0	24.4	3.3	8.3	10.1	16.4 / 89.1	141 / 5
		5	24.8	3.1	8.3	10.8	16.4 / 88.9	137 / 5
		10	25.1	3.1	8.3	11.6	16.4 / 89.2	133 / 5
		15	25.3	3.2	8.0	12.6	16.4 / 90.7	129 / 5
		20	25.6	3.3	8.1	14.0	16.5 / 89.6	134 / 4

Table 17:- The Effect of Downspeeding on Vehicle Performance.

If a fuel economy comparison is made with commercially available fuels, E10 and E73.7, the penalty of running the DI3 on E73.7 with 15% downspeeding is reduced to just 6% (combined) over the E10 Fueled Ecotec engine.

Task 4.4 Final Commercialization Analysis of Optimized E85 Engine.

'Conduct commercialization analysis on High Efficiency Clean Combustion E85 Optimized Engine concepts to determine the feasibility of introducing it into the market place.'

The team was unable to complete this task due to time and funding limitations.

6 Summary and Conclusions

The key project objective was to identify a means by which an engine that when fuelled with E85 would return similar volume based fuel economy to a conventional engine fuelled with gasoline in the same vehicle.

In addition to this the developed engine was to be a commercially viable package with the following characteristics:

- No degradation in legislated vehicle emissions when running on E85 when compared to a conventional engine running on gasoline.
- Run with all gasoline / ethanol fuels up to 85% ethanol.
- Show minimal performance degradation when fuelled with gasoline when compared to a conventional engine.
- Exploit any characteristics of E85 that are superior to gasoline.

The project's goal was to utilize technologies viewed as being capable of enhancing vehicle fuel economy in a way that exploits the properties of blended gasoline / ethanol fuels. The limit to the implementation of certain technologies employed was the requirement to run the developed powertrain on gasoline with minimal performance degradation. The addition of ethanol to gasoline fuels improves the fuels octane rating and increases the fuels evaporative cooling. Both of these fuel property enhancements make gasoline / ethanol blends more suitable than straight gasoline for use in downsized engines or engines with increased compression ratio. The use of downsizing and high compression ratios were fundamental to the fuel economy improvements targeted in this project.

The project was conducted in four phases.

Phase 1 - Proof of Concept.

Various simulation techniques were used to demonstrate the suitability of MAHLE's DI3 as a basis for the project.

Phase 2 – Exploratory Development.

Key project enablers (single cylinder engine, injectors, ionization based ignition system and MAHLE DI3 engine) were designed and procured.

Phase 3 – Advanced Development.

Rig and single cylinder engine tests were conducted to enable selection of the optimum fuel injector for the project. The Bosch HDEV5 was selected. Tests were also conducted to prove the suitability of the ionization based ignition system for determining combustion phasing, detonation and fuel composition on both the single cylinder and comparator engines. The ion based technology looked promising for detecting combustion phasing and detonation, however the suitability of ion sensing to precisely determine the alcohol content of fuel could not be demonstrated in this application. The comparator engine was baselined.

Phase 4 – Engineering Development.

The MAHLE DI3 engine performance was evaluated and optimized within the confines of the project. The effect of the technologies applied to the DI3 engine were analyzed.

The technologies applied to the DI3 engine were found to have the following effects:

Downsizing

Compared to the Ecotec engine, downsizing was seen to offer appreciable improvement in vehicle fuel economy while maintaining equivalent vehicle performance.

Variable Cam Timing

Variable cam timing allowed benefits in drive cycle fuel consumption to be realized. It was not necessary to compromise valve timing in the same way as would have been the case with a fixed cam system.

External EGR

Although internal EGR was modulated with variable cam timing, at high loads it was possible to improve fuel economy further by employing additional (external) EGR, even with the camshafts timed to give maximum overlap.

Cooled external EGR was targeted as a combustion system enhancement to allow optimized combustion phasing at high loads with gasoline fuel. Unfortunately, the turbo and EGR system configurations available with the DI3 as tested did not allow enough EGR to be introduced into the engine to significantly affect combustion phasing without degrading power output. Revisions to the EGR circuit or use of a different turbocharger may have allowed use of more EGR, but were not available within the timeframe required by this project.

Compression Ratio

Increased compression ratio was seen to give improvements in part load fuel economy. However increases in compression ratio were limited by the desire to minimize full load performance losses with gasoline fuel. Due to the amount of combustion retard necessary to avoid detonation with gasoline fuel and its effect on stability and power output, any increase in compression ratio above 11.25 : 1 would have caused the performance of the DI3 engine to degrade below that of the Ecotec. A hardware combination intended for use only with E85 fuel would have been able to incorporate a higher compression ratio, however the stated project goal of full fuel flexibility across all gasoline / ethanol blend combinations required a lower final compression ratio choice.

Downspeeding

As the degree of downspeeding was increased the drive cycle fuel economy was seen to improve and vehicle performance was seen to degrade. Up to 15% downspeeding vehicle performance with the DI3 engine was comparable with the non-downspeeded Ecotec in the target Chevrolet HHR.

The final optimized engine configuration was based on the MAHLE DI3 gasoline downsizing research engine. It was a turbocharged, intercooled, DI engine with dual independent cam phasing utilizing a compression ratio of 11.25 : 1 and would use a 15% reduction in final drive ratio in the target Chevrolet HHR.

The following comparisons may be made between the project's final optimized engine configuration and the comparator engine, a gasoline fuelled 2.2L Ecotec engine in the Chevrolet HHR. It should be noted that the 2.2L Ecotec Direct is more efficient than most current passenger vehicle engines, employing direct injection and a compression ratio of 12 : 1.

Fuel Economy

- Simulations suggest that in a Chevrolet HHR an optimized E85 fuelled DI3 engine with 15% reduction in final drive ratio would return a 13.7% drive cycle fuel economy penalty compared with a gasoline fuelled Ecotec Direct engine. If the same comparison were made with E73.7 and E10 fuels (more typical of what is commercially available) simulations suggest that the drive cycle fuel economy penalty would be reduced to 6%.
- All technologies applied to the DI3 engine to improve E85 drive cycle fuel economy helped gasoline fuel economy. The optimized project engine downspeeded by 15% when fuelled with gasoline would offer an 18.1% fuel saving over a gasoline fuelled Ecotec Direct engine in a Chevrolet HHR.
- Increasing the compression ratio of the DI3 engine from 9.25 : 1 to 11.25 : 1 improved brake thermal efficiency by around 4% for both fuels at drive cycle conditions.
- Drive cycle predictions showed that every 5% downspeeding would produce around a 1% improvement in vehicle fuel economy.
- The MAHLE DI3 engine was seen to deliver greater fuel economy benefits at light loads than at high loads relative to the comparator engine.

Emissions

- Engine out NOx emissions were lower for the DI3 running on E85 than for either the Ecotec Direct or the DI3 running on gasoline.
- Engine out HC and CO emissions were similar for the DI3 engine running on E85 or gasoline and the Ecotec Direct running on gasoline.
- Overall, measured feedgas emissions showed no requirement for aftertreatment other than with a standard three-way catalytic converter of similar specification to what is currently on the market.

Full Load

- The DI3 engine was able to make the peak power of the 2.2L Ecotec Direct at a lower engine speed, allowing downspeeding to be used as a technology to improve drive cycle fuel economy.
- The compression ratio of the DI3 engine was limited to 11.25 : 1 by combustion stability and torque degradation when running at full load on gasoline.
- Increasing the compression ratio from 9.25 : 1 to 11.25 : 1 on the gasoline fuelled DI3 engine necessitated the full load combustion phasing be retarded by 10^{o} to avoid detonation.
- No fuel enrichment was required to limit exhaust gas temperatures on the DI3 engine

with E85 fuel.

- It was not necessary to retard combustion phasing due to knock on the DI3 engine with E85 fuel at either of the compression ratios tested.
- The Borg Warner 5303 988 0069 turbocharger delivered significantly better low speed full load performance than the Borg Warner 5303 988 0005 turbocharger with no detrimental effect on either high speed full load or part load performance.

A multi phase program was undertaken with the stated goal of using advanced design and development tools to create a unique combination of existing technology to create a powertrain system specification that allowed minimal increase of volumetric fuel consumption when operating on E85 relative to gasoline. This project was able to define an engine specification envelope, develop specific hardware for the application, and then test that hardware in both single and multi-cylinder test engines to verify the ability of the specified powertrain to deliver reduced E85 fuel consumption. Finally, the results from the engine testing were input back into the vehicle drive cycle analysis tool to define a final vehicle level fuel economy result.

During the course of the project, it was identified that the technologies utilized to improve fuel economy on E85 also enabled improved fuel economy when operating on gasoline. However, the E85 fueled powertrain provided improved vehicle performance when compared to the gasoline fueled powertrain due to the improved high load performance of the E85 fuel. Relative to the baseline comparator engine and considering current market fuels, the volumetric fuel consumption penalty when running on E85 with the fully optimized project powertrain specification was 6%. This result shows that alternative fuels can be utilized in high percentages while maintaining or improving vehicle performance and with minimal or positive impact on total cost of ownership to the end consumer.

References

[1] A. Saitzkoff, R. Reinmann, and F. Mauss, (1997) *'In-Cylinder Pressure Measurements Using the Spark Plug as an Ionization Sensor'*, SAE 970857.

[2] L. Peron, A. Charlet, P. Higelin, B. Moreau, and J.F. Burq, (2000) *'Limitations of Ionization Current Sensors and Comparison with Cylinder Pressure Sensors'*, SAE 2000-01-2830.

[3] C. F. Daniels, G. G. Zhu, and J. Winkelman, (2003) *'Inaudible Knock and Partial Burn Detection Using In-Cylinder Ionization Signal'*, SAE 2003-01-3149.

[4] I. Haskara, G. G. Zhu, and J. Winkelman, (October 2004) *'IC Engine Retard Ignition Timing Limit Detection and Control Using In-Cylinder Ionization Signal'*, SAE Powertrain and Fluid Systems Conference, Tampa, Florida, USA.

[5] D. Lundstrom, and S. Schagerberg, (2001) '*Misfire Detection for Prechamber SI Engines using Ion-Sensing and Rotational Speed Measurements*', SAE Paper No. 2001-01-0993, SAE 2001 World Congress, March 5-8, 2001, Detroit, Michigan, USA.

[6] G. G. Zhu, I. Haskara, and J. Winkelman, (October 2004) *'MBT Timing Detection and its Closed-Loop Control Using In-Cylinder Ionization Signal'*, SAE Powertrain and Fluid Systems Conference, Tampa, Florida, USA.

[7] I. Haskara, G.G. Zhu, C. Daniels, and J. Winkelman, (October 2004) *'On Combustion Invariants for MBT Timing Estimation and Control'*, ASME Internal Combustion Engine Division Fall Conference, Long Beach, California, USA.

[8] G. G. Zhu, C. Daniels, and J. Winkelman, (October 2003) *'MBT Timing Detection and Its Closed-Loop Control Using In-Cylinder Pressure Signal'*, SAE 2003-01-3266, SAE Powertrain and Fluid Systems Conference & Exhibition, Pittsburgh, Pennsylvania, USA.

[9] I. Haskara, G. Zhu, C. Daniels, and J. Winkelman, (October 2005) '*Closed Loop Maximum Dilution Limit Control using In-Cylinder Ionization Signal'*, SAE 2005-01-3751, SAE Powertrain and Fluid Systems Conference & Exhibition, San Antonio, Texas, USA.

[10] Rassweiler, G. M., and Withrow, L., 1938, '*Motion pictures of engine flames correlated with pressure cards.*', SAE Transaction, 1938, 42, pp. 185–204.

[11] Mittal, M., Zhu, G., and Schock, H.J., 2009, '*Fast mass fraction burned calculation using net pressure method for real-time applications.*', Proc. IMechE, Part D: J. Automobile Engineering, 223(3), pp. 389-394.

[12] J. B. Heywood, Internal Combustion Engine Fundamentals, McGraw-Hill Book Company, 1988.

[13] F. M. Salih and G. E. Andrews, (October 1992) '*The Influence of Gasoline / Ethanol Blends on Emissions and Fuel Economy*', SAE 922378, SAE International Fuels and Lubricants Meeting and Exposition, San Francisco, California, USA.

[14] W. Dai, S. Cheemalamarri, E. Curtis, R. Boussarsar and R. Morton, (2003) '*Engine Cycle Simulation of Ethanol and Gasoline Blends*', SAE 2003-01-3093.

[15] American Society of Testing and Materials, '*ASTM D 5798 Standard Specification for Fuel Ethanol for Automotive Spark-Ignition Engines*'.

[16] Coordinating Research Council, (August 2006) '*SUMMARY OF THE STUDY OF E85 FUEL IN THE USA 2006*'.

[17] Coordinating Research Council, (May 2007) '*SUMMARY OF THE STUDY OF E85 FUEL IN THE USA - WINTER 2006-2007*'.

[18] MTZ Article, (December 2003) '*2,2 l ECOTEC DIRECT – The new All-Aluminium Engine with Gasoline Direct Injection for the Opel Signum*'.

[19] Borg Warner Internal Turbocharger Characterization Document.